Design of an anti-lock brake algorithm based on wheel load measurements

B. Hazen

Master of Science Thesis

TU Delft Delft University of Technology

Delft Center for Systems and Control

Design of an anti-lock brake algorithm based on wheel load measurements

Master of Science Thesis

For the degree of Master of Science in Systems and Control at Delft University of Technology

B. Hazen

September 5, 2016

Faculty of Mechanical, Maritime and Materials Engineering (3mE) · Delft University of Technology

Copyright © Delft Centre for Systems and Control (DCSC)
All rights reserved.

Abstract

Anti-lock Brake System (ABS) is an active safety system nowadays implemented in every new car and could prevent the wheels from locking during heavy braking. Steering becomes ineffective and the brake distance longer than necessary when the wheels are locked. ABS has reduced the amount of non-fatal crashes significantly, but there are still situations in which it can control worse than driver would himself. For example, when driving on low-friction roads.

The aim in this thesis is to develop a new ABS algorithm using potentially available information about wheel forces. Data of wheel forces is currently not measured in consumer cars, but SKF is developing load sensing bearings which could be feasible for such cars. The sensor output provides more directly relevant information than wheel deceleration data does. The latter is used in current ABS technology.

A novel ABS algorithm that uses both force and wheel slip measurements for control is designed. The algorithm is validated on a Simulink model consisting of Delft-Tyre, simplified actuator dynamics, (optional) sensor noise, and a quarter car model.

An Extended Kalman Filter (EKF) based on the Burckhardt model acts as reference for the control algorithm. The Burckhardt model is a computationally lightweight formula and allows the EKF to be used on-line against relatively little computational cost. Friction estimation is essential in the designed ABS algorithm, as it is dependant on the road surface which is not known a priori.

The designed algorithm is first assessed in a Simulink model on different road surfaces. Field tests are performed as well. They show that the combination of force and slip measurements is indeed promising. On-line estimates using the EKF are found sufficiently accurate to be used as main reference for the controller.

Table of Contents

List of Figures

List of Tables

Acknowledgements

I would like to thank my supervisor Ir. S.M.A.A. Kerst in special for his support. I am grateful for the time he weekly reserved for our meetings and for the insightful and inspiring discussions we had. Even though I knew he actually had things of higher priority on his mind, such as his own research project or self-built camper van, I always had his full attention. Dr. B. Shyrokau has also been of great help. Every time I asked for something, he did more than I had hoped for. He was specifically supportive when it came to building the simulation and has therefore become the King of Simulation in my eyes. The support of Prof. E.G.N. Holweg was also highly appreciated. His enthusiasm for the project was motivating.

Aside from my supervisors, there are a few more people I would like to thank: Piet Aarden, who always managed to distract me with his internet videos. Niels Marck, who always made time to listen to me and think about my questions. Arnela Masic, for her mental support, especially when working during the Summer holidays.

I know this is starting to sound as if I won an award, but I would like to conclude these acknowledgements with my gratitude to the three most important people I know: Anja Roelen, Rob Hazen, and Ruud Hazen. I barely experienced any stress in the past year. And though that is part of my personality, I have them to thank for it.

Delft, University of Technology B. Hazen
September 5, 2016

Chapter 1

Introduction

This thesis presents the development and implementation of a renewed Anti-lock Brake System (ABS) algorithm. In this first introductory chapter, the effects of safety systems over the past years are discussed. Then challenges in ABS control are denoted (section 1-2). Subsequently, objectives of this project are elaborated on. This chapter is concluded with a thesis outline in section 1-4.

1-1 Road safety

Road safety research has increased exponentially since the 1950s [1]. In 1990 a little over 250 articles about road safety were published, whereas in 2010 there were 2,000 publications (see fig. 1-1). The research has availed to a great reduction of road fatalities, as shown in fig. 1-2.

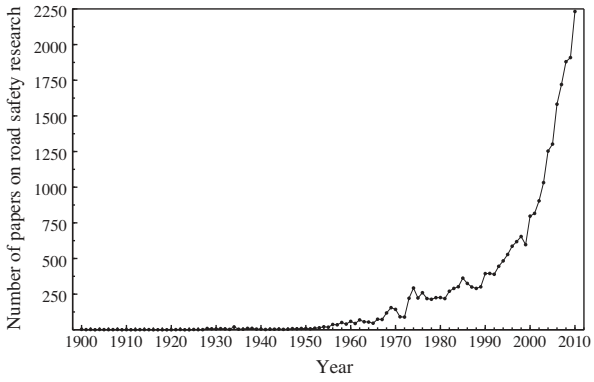

Figure 1-1: Yearly number of articles on road safety research from 1900 to 2010 [1]

The target of the European Commission was to reduce the number of annual road fatalities to 27,000 by the year 2010, and to 15,750 by 2020. The first goal was not reached, as the number

was at 31,500 then. For the second target, statistics show that the number of fatalities is going in the right direction to achieve it.

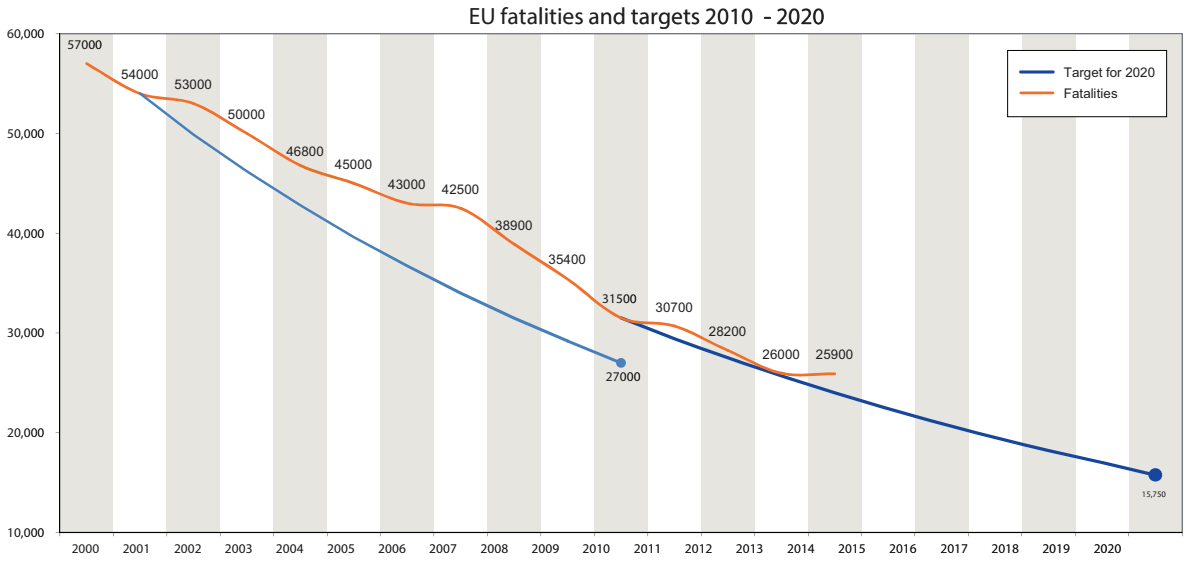

Figure 1-2: Evolution of EU fatalities 2000-2010 and targets for 2020 [2]

There are various ways to improve road safety such as placing street lighting, improving road quality, and installing road signs. The car itself is another factor which offers many ways to improve the safety of the driver or passengers. In general, it can be said that such safety systems are divided into active and passive systems. Passive safety systems reduce damage after an impact. Active safety systems are meant to prevent accidents and are, thus, active prior to the event of a potential crash.

Examples of passive safety systems are airbags, seat belts, and deformation zones. The development of passive safety is assumed to be near its limit [8]. ABS is an example of an active safety system. The initial goal of ABS was to maintain steerability during heavy braking. To achieve this, it prevents wheels from locking. Steering then remains possible, and the brake distance is often shortened as well. Nowadays, the system is fundamental in other safety systems as well, such as Braking Assist System (BAS), Electronic Stability Control (ESC), Cornering Brake Control (CBC), and Traction Control (TC).

As of 2004, car manufacturers in the Netherlands are obliged to implement an ABS. The first implementation of ABS in a production car dates back to 1978. It has since been developed to become of high importance in modern day car safety systems. Not only has the weight of the ABS been reduced by 85% since its first introduction by Bosch, the algorithms have been improved as well.

There have been various tests to the effectiveness of ABS [9, 10]. Though results from researches vary, most of them conclude that people have got no disbenefit because of it. An interesting finding is that ABS-equipped cars proportionally have fewer crashes with other vehicles, but a greater proportion of them run off-road. The latter shows a significant difference of 9% with respect to cars without ABS. These crashes occur even more when a vehicle drives on roads with low friction. An increase of 34% is observed in such situations. Long-term effects have been investigated as well and show that ABS has reduced the amount of non-fatal

crashes by 6% [11]. Furthermore, these cars crash 13% less frequently with pedestrians, bicyclist, or animals. When driving on low-friction roads, again, ABS-equipped cars perform worse than cars without the technology. It is, thus, clear that ABS can still be improved.

1-2 Challenges in ABS control

Current ABS is controlled based on wheel deceleration and slip. ABS performance of the current algorithm by Bosch already performs well. It is, however, an algorithm based on many heuristics, which makes it hard to tune. Considering there are still road surfaces and situations for which ABS could be improved, researchers have been trying to find a more mathematical approach to the algorithm. With a basis of the technology that is easier to interpret, it is expected that ABS could be more stable and robust on more slippery road surfaces. This mainly concerns wet, snowy, and icy roads.

Another challenge in the development of ABS is in the velocities at which the algorithm works. At lower velocity, it becomes increasingly hard to control as the wheels tend to lock more easily. Though the issue is not a primary focus of this thesis, it is a notable challenge (see section 1-3).

With the development of load sensing bearings by SKF, the first steps have been made into the direction of force measurements in consumer cars. Initially, the data is used to support deceleration data [12], but an algorithm that only uses force measurements has been tested as well [7]. An advantage of using force data over deceleration data is, for example, that force data provides direct information about tyre-road characteristics.

A more recently discovered challenge in ABS is to predict road surface characteristics. While braking, the estimation of these characteristics is necessary. It could allow the ABS to remain stable throughout the entire brake manoeuvre. Consequently, braking could become more efficient and robust with it. If the optimum is known with certainty even before it is passed, the brake torque could also be increased more rapidly.

Another challenge in ABS is providing lateral stability. Physically speaking, this requires the slip to be minimised. Figure 1-3 shows the relationship between normalised lateral force and slip. It visualises that the lateral force — which is required in order to make a turn — can only be maximised when the slip is minimised. The normalised longitudinal force versus this slip value shows a different relation (see fig. 1-4). So there are, in fact, two curves that should be taken into account. During this research, however, there is chosen to only focus on longitudinal motion.

1-3 Objectives

When ABS was developed initially, there were two main goals. The first of which is to maintain steerability throughout the brake manoeuvre. Steering is, however, not taken into account in this thesis to reduce the complexity of the problem.

The second goal of ABS is to minimise brake distance. Obviously, this could prevent an accident, or it would otherwise reduce the intensity of a crash. The brake distance is minimised

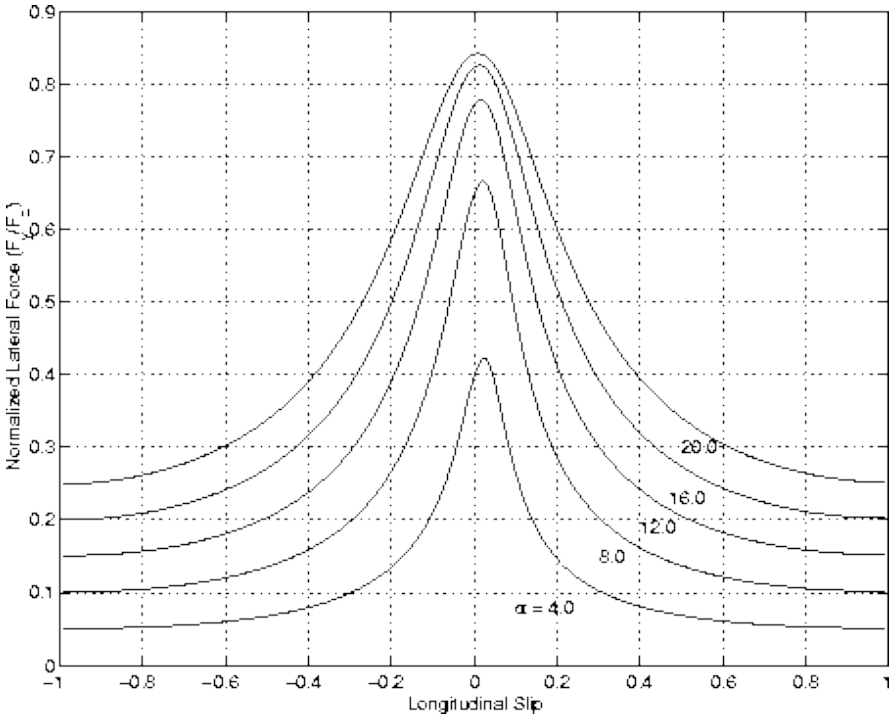

Figure 1-3: Normalised lateral force versus longitudinal slip [3]

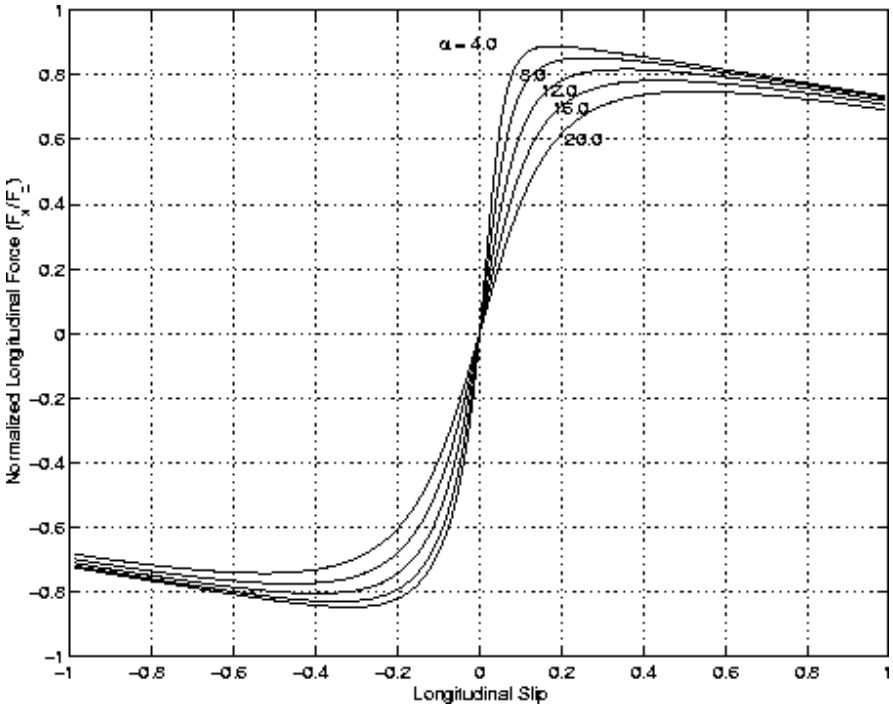

Figure 1-4: Normalised longitudinal force versus longitudinal slip [3]

by maximising the brake force, which is composed of a longitudinal and lateral force. For this maximisation, it is desired to find the highest possible friction coefficient. Equation (1-1) describes the relationship between the measured forces and the friction coefficient. For this research, it is assumed there is no a priori knowledge about the road surface. The maximum friction coefficient is thus unknown. Consequently, the corresponding optimal brake torque cannot be determined on beforehand. This information would not be available in practice either.

$$\mu = \frac{\sqrt{F_x^2 + F_y^2}}{F_z} \tag{1-1}$$

The goals of ABS are considered to set the goal of this research project. The main question that will be answered is as follows:

How can wheel force information contribute to an ABS algorithm?

To answer the question, several objectives have been set. These are listed below.

- *Analyse the physical behaviour of the vehicle.* An analysis should be performed to find general dynamical behaviour of a vehicle driving on a road. The only input to the system is the brake torque and its influence should be determined.
- *Set up a testing environment.* The testing environment can be used for initial testing of the designed controller.
- *Design a novel ABS algorithm.* Wheel force and slip are investigated to find how they could contribute to an improved ABS algorithm.
- *Investigate and evaluate the performance of the novel ABS.* Tests should be performed to confirm the validity of implementing the designed algorithm.

Now that the objectives are known, it must be mentioned that there are also boundaries set to reduce the complexity of the problem. The most important one is that braking shall occur in a straight line. Such a manoeuvre is more easily reproducible on a test track and is moreover simpler to model. The latter is important as it allows for simpler problem analysis. The assumption can be made as this will show the basic effect of the developed ABS algorithm. More simplifications and assumptions are mentioned throughout this report.

1-4 Thesis outline

This thesis consists of six chapters that lead to the answer to the research question. The first chapter was used as an introduction into the subject. Chapter 2 focuses on the fundamental equations representing the behaviour of the system.

In chapter 3 the problem of braking is discussed. The solution to this problem is to add a controller which regulates how strongly the brakes are applied. The chapter describes possible control methods and proposes a variant which is more thoroughly tested further on.

The functioning of the controller depends on reference points. The method used to determine these is described in chapter 4.

With the fundamental equations and all the requirements for a controller, simulations are performed and evaluated in chapter 5. The controller is assessed using multiple performance indicators.

Field tests have been performed to validate the possible contribution of force measurements to ABS. Chapter 6 elaborates on the found results.

The final chapter presents general conclusions about the project. Recommendations are also part of this chapter and should support future research in this field of study.

Chapter 2

Modelling

There are several reasons why there is chosen to initially design the ABS based on a model in Simulink. Testing an ABS algorithm in an actual car is time-intensive, whereas a simulation study could take a few seconds. It also allows for easier switching of circumstances. For example, if an ABS is to be tested on a wet road, the simulation can be adjusted by changing parameter values. Furthermore, performing identical experiments is of beneficial value to rule out the influence of specific parameters.

The complexity of a simulation model is often a trade-off between its accuracy and computational cost. It is furthermore important to note that the more dynamics a model takes into account, the harder it becomes to interpret its outcomes when looking for the influence of a specific change. This is why in this research project, there is chosen to build a relatively basic model of vehicle dynamics in Simulink such that a sufficient overview of the dynamics accounted for is maintained.

When it comes to modelling a brake manoeuvre, there are four major topics that should be taken into account. The first of which is how the vehicle as a whole is modelled. Relevant equations concerning wheel motion and its interaction with the road are covered in section 2-1. The secondly discussed component is the actuator (section 2-2). It is the only control input to the system. Its references are determined by the controller based on measured data. How this data is obtained is covered in section 2-3. The controller is elaborated on in chapter 3, but its place within the model is explained in section 2-4. A schematic overview of the model components is given in fig. 2-1.

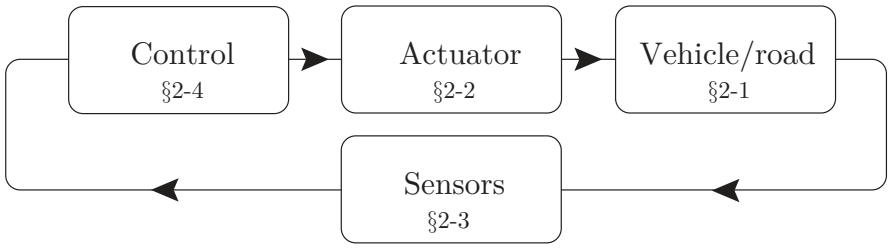

Figure 2-1: Schematic overview of the fundamentals model components

2-1 Vehicle and road

The vehicle model consists of four parts. The first topic is tyre-road contact and is be discussed in section 2-1-1. A general introduction is given to the relevant parameters for this research. In the following section equations of motion are covered (section 2-1-2). These equations still depend on how friction is defined, which is why this is covered in the next section. In section 2-1-4 tyre relaxation is introduced. This is another important effect which are taken into account during the simulation study. This section is concluded with an explanation of how these components are implemented in the definitive model.

2-1-1 Tyre-road contact

Contact between tyre and road plays a major role in dynamics of a vehicle. The interaction between tyre and road can be described by three forces and three moments as illustrated in fig. 2-2:

- F_x: Longitudinal force
- F_y: Lateral force
- F_z: Normal force
- M_x: Overturning moment
- M_y: Rolling resistance moment
- M_z: Self-aligning moment

The longitudinal force can be expressed as a function of the friction coefficient (μ_x) as is shown in eq. (2-1). To find the friction coefficient coefficient, more information is needed: normal load (F_z), longitudinal slip (λ), side-slip angle (α), and camber angle (γ). Each of which, except for the longitudinal slip, is indicated in fig. 2-2.

$$F_x = \mu_x(\lambda, \alpha, \gamma, F_z) \tag{2-1}$$

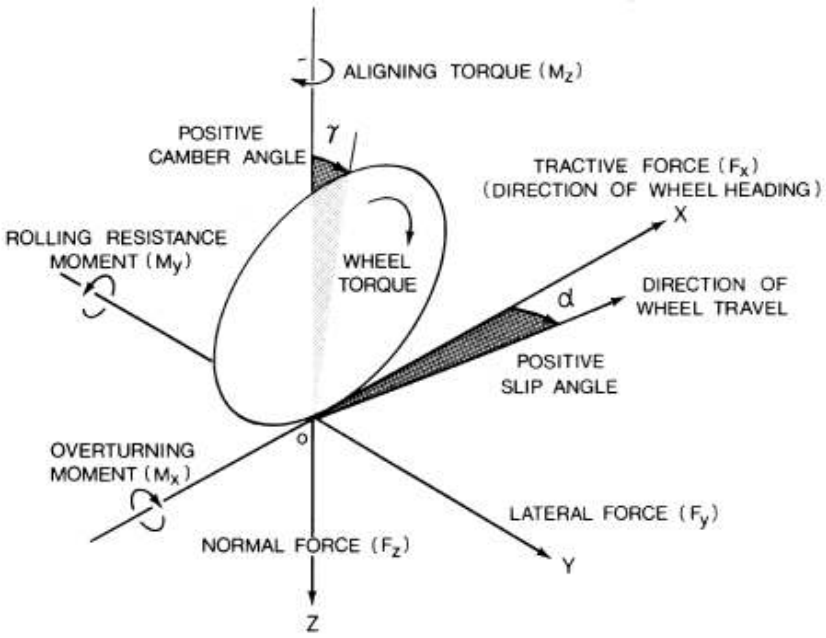

Figure 2-2: Relevant variables in the description of tyre-road contact. [4]

The longitudinal wheel slip can be determined by eq. (2-2), which is required for calculating F_x. When the wheel slip is mentioned throughout the rest of this thesis, the *longitudinal* one is always meant, unless specifically mentioned otherwise. The same goes for the friction coefficient. The wheel slip value is thus defined as the difference between vehicle velocity and wheel rotation speed as a fraction of the velocity of the car. Thus, $\lambda \in [0, 1]$. If the wheels are locked, ωr approaches zero, which means the wheel slip value approaches 1.

$$\lambda = \frac{v - \omega r}{\max(v, \omega r)} = \frac{v - \omega r}{v} \tag{2-2}$$

The parameters in this equation are defined as follows:

- v [m/s]: Vehicle velocity.
- ω [rad/s]: Angular velocity of the wheel.
- r [m]: Dynamic wheel radius. In some cases the tyre is assumed to be a rigid object with constant radius. However, in reality it is found that the radius depends on more parameters, such as the rotation frequency, the vertical load, and tyre inflation pressure.

Two assumptions are made to simplify the model with respect to ABS braking. This simplification is important to do the research, as the influence of changes becomes easier to deduce. Firstly, the side-slip angle (α) is set to zero, since no steering is applied. Secondly, the camber angle (γ) equals a constant, such as zero. Hence, friction is a function of normal load and longitudinal slip only.

Assuming friction is linearly dependant on the normal load, the formula can be rewritten to eq. (2-3). Because of the actual non-linearity, the equation do not hold unlimitedly. However, the loads during ABS braking are still low enough to use them. There is also an approximation of the relation between longitudinal friction coefficient and wheel slip for different side-slip angles, but this is an irrelevant topic for this research project, since no steering is applied.

The friction function can be defined in various ways. Section 2-1-3 goes into detail about the chosen friction model.

$$F_x = F_z \mu_x(\lambda) \tag{2-3}$$

2-1-2 Equations of motion

Wheel dynamics are described by the single-corner model, which is also known as the quarter car model. It is defined by eqs. (2-4) and (2-5) and can be physically explained to be only one front wheel and a quarter of the total mass of the car. It is explicitly noted this model concerns the front wheels, because braking them depends less on the rest of the vehicle dynamics. If the rear wheels are locked before the front ones are, yaw moment of the the vehicle has a destabilising effect. Since the current research project describes the fundamentals of an algorithm, rear wheels are not taken into account.

Alternative models are available as well, but the single-corner model is sufficient to show the basic workings of the algorithm. More sophisticated models mainly differ in determining the distribution of F_z among the tyres. It is not necessary to implement such a model to prove the benefits of the algorithm or performance. Especially since the eventually designed control algorithm does not combine information from different tyres to determine a control reference, the single-corner model suffices.

$$J\dot{\omega} = rF_x - T_b \tag{2-4}$$
$$m\dot{v} = -F_x = -F_z \mu_x(\lambda) \tag{2-5}$$

The symbols in this equations are defined as follows:

- T_b [Nm]: Brake torque.
- J [$\mathrm{kg \cdot m^2}$]: Inertia of the wheel.
- m [kg]: Mass of the quarter car.
- F_x [N]: Force of longitudinal tyre-road contact.

For the choice of this model, several assumptions are made. Important reasons are listed below.

- **Accurate information about F_z of each tyre is not required.** Despite F_z being an important factor for every separate tyre, a sophisticated simulation method that accurately determines the distribution of F_z across the tyres does not contain more relevant information for the design process.

- **Aerodynamics forces are not taken into account** as they are negligible during ABS braking. Not only are the forces and moments as exerted due to tyre-road friction significantly higher, neglecting aerodynamic forces also contributes to an easier identification of the influence of the algorithm.
- **No steering is applied,** which means $\alpha \approx 0$. This assumption allows for an easier identification and comparison of experiment results.

2-1-3 Friction

Equation (2-5) contains μ_x, which is yet to be determined. There are multiple methods available to calculate the friction coefficient. Different types of such models distinguish themselves mostly in the accuracy of tyre relaxation dynamics accounted for.

One of the most famous empirical models is the Magic Formula, developed by H.B. Pacejka in conjunction with Volvo [13]. Pacejka fitted measurement data to a model to obtain an accurate estimate of these forces [14]. The basic formula when only longitudinal motion is considered is shown below (see eq. (2-6)) [5].

$$F_{x0} = D_x \sin(C_x \arctan((1 - E)(B_x\lambda + \arctan(B_x\lambda)))) \tag{2-6}$$

Where:

$$\begin{aligned} \lambda &= \lambda + p_{H_{x_1}} + p_{H_{x_2}} df_z \\ D_x &= F_z(p_{D_{x1}} + p_{D_{x_2}} df_z)\Delta_{\mu x} \\ C_x &= p_{C_{x_1}} \\ E_x &= p_{E_{x_1}} + p_{E_{x_2}} df_z + p_{E_{x_3}} df_z^2 \\ K_x &= F_x(p_{K_{x_1}} + p_{K_{x_2}} df_z)\Delta_{K_x} \\ B_x &= K_x/(C_x D_x) \end{aligned} \tag{2-7}$$

In which λ is the longitudinal slip and $df_z = \dfrac{F_z - F_{z_0}}{F_{z_0}}$ with F_{z_0} the nominal load. Coefficients p are parameters used for curve fitting. $\Delta_{(\cdot)}$ are optional scaling parameters.

The original Magic Formula is more sophisticated than denoted in this report, because it can determine forces and moments in all directions as well. For this research project, however, only longitudinal forces are taken into account, leading to the choice of discussing eq. (2-6).

In the formula D is known as the peak factor. Figure 2-3 shows the influence of each of the parameters. It indicates D is the peak value of the friction function. Remaining parameters C, B and E are known as respectively the shape, stiffness and curvature factor.

The Magic Formula is clearly not based on the first principles. This does not prevent it from giving a highly accurate estimate of the actual friction. Over the years, the model has been modified several times to become the most successive tyre friction model. It is therefore also used in simulations performed for this thesis.

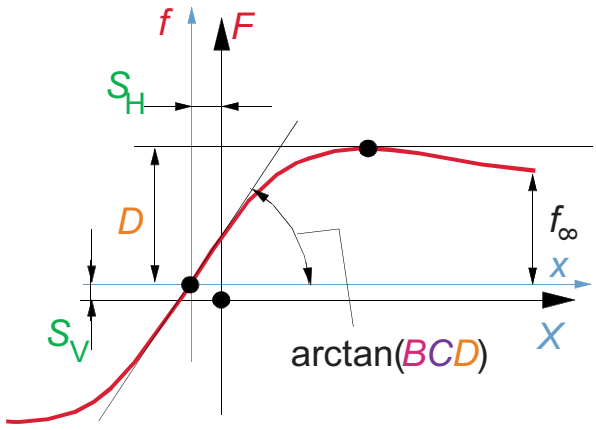

Figure 2-3: Parameter visualisation Magic Formula [5]

It can be said that the friction coefficient curve is approximately of the shape as shown in fig. 2-4. Without going too much into detail about controlling a brake manoeuvre, it is important to note the peak of the friction coefficient is at a unique slip value (λ^*). Different road types show variations in the steepness of the function on both the left and right side, but the one thing they have in common is that there is a single optimal friction coefficient, as indicated by the dashed line.

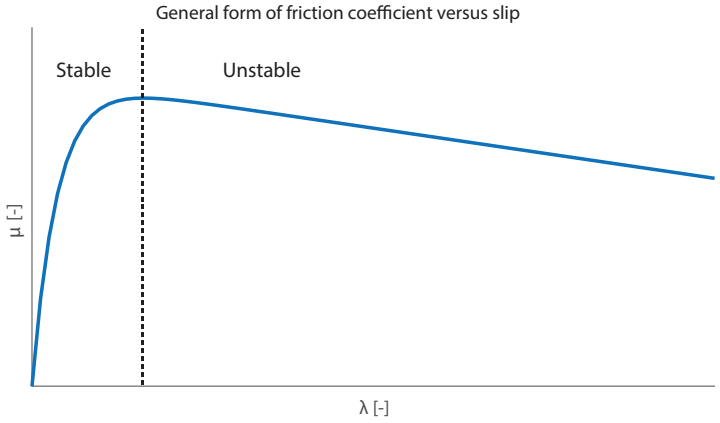

Figure 2-4: General shape of friction coefficient versus slip

A brief analysis on the effects of braking considering a general description of the friction coefficient curve as a function of the slip (see fig. 2-4) follows with two cases.

Case 1: brake torque too small to exceed the friction coefficient peak

When the longitudinal force increases, the friction coefficient does so as well. This ensures $\dot{v}$ and $\dot{\omega}$ remain stable (see eqs. (2-4) and (2-5)).

Case 2: brake torque is sufficiently high to exceed the friction coefficient peak

The second case is used to explain the effects of the unstable region. The unstable region is denoted in fig. 2-4. The peak can only be exceeded if the brake torque is greater than the maximum possible brake torque: $T_b > rF_z\mu_x^*$. Since on the right side of the curve the friction coefficient decreases with increasing slip, the system reacts differently. At this point $rF_x - T_b$ (and thus $\dot{\omega}$) becomes increasingly negative, because it causes a higher slip value while the effective friction force is inversely related to it. The described effect is the reason why the right side is referred to as the unstable region.

2-1-4 Tyre relaxation

Tyres exert a longitudinal force which depends on the road surface. With the description so far, these are the steady-state characteristics. In reality, this force is also strongly dependant on the tyre itself. Since the tyre is made out of flexible material, so-called tyre relaxation occurs.

A transfer function could be added to the model to add a delay to its results. Though this is a basic and inaccurate method, its level of realism is sufficient for initial testing of the designed ABS. The transfer function is described by eq. (2-8).

$$G(s) = \frac{v_\omega / S_{0l}}{s + v_\omega / S_{0l}} \tag{2-8}$$

With:

- v_ω [m/s]: Tyre linear velocity.
- s_{0l} [m]: Tyre relaxation length.

The tyre relaxation length depends on vertical load, slip, and inflation pressure. It expresses the length of the tyre which is required to restore a infinitesimal small element of the tyre to its stable position as of its road contact. This means that the relaxation length of a stiff tyre is lower.

The basic model (eq. (2-8)) was used during initial tuning and verification of the renewed ABS algorithm, but it was later replaced by the Magic Formula approach in the Delft-Tyre package by TASS international. The latter also includes more accurate tyre relaxation dynamics in the way it is eventually implemented. Tyre relaxation is a key element of whether and how an ABS algorithm works, because it disturbs the measurements of force in combination with slip. It is, thus, important to model it realistically.

2-1-5 Implementation

A braking vehicle is simulated using the quarter car model. The implementation of eqs. (2-4) and (2-5) in Simulink is straightforward and does not require further explanation.

When it comes to tyre-road contact, during the development of the algorithm, simple friction curves were used at first. Subsequently, the model was extended with a basic tyre relaxation model (eq. (2-8)). To obtain more realistic results, the Magic Formula was implemented in the simulation. The basics of this method are discussed in section 2-1-3.

TASS international has developed Delft-Tyre [15], which contains a set of tools to implement the tyre model. Since only longitudinal motion is considered, this block requires ω, v_x, and F_z as inputs. Parameters for the specific tyres that are used on a test track have been determined during previously performed experiments. The resulting data is combined into a single so-called tyre property file and can be imported in the Delft-Tyre model.

Even though it has been written that the simplicity of the model is of importance for interpretation of results, the Delft-Tyre model is used to obtain more realistic data. It is still desirable to exclude effects which are irrelevant to show the basic workings of the ABS algorithm. This is why symmetric tyre characteristics are assumed. Furthermore, the model is configured with smooth road contact using a single contact point. This setting is the most basic one the software offers. In further research, the effects of non-smooth road surfaces could be investigated. The model is set to include transient effects of tyre relaxation up to 10 Hz with a linear transient model. Lastly, only longitudinal forces are considered. For reproduction purposes, the above can be summarised into the code 3011, which can be used as a parameter of the Delft-Tyre model in Simulink.

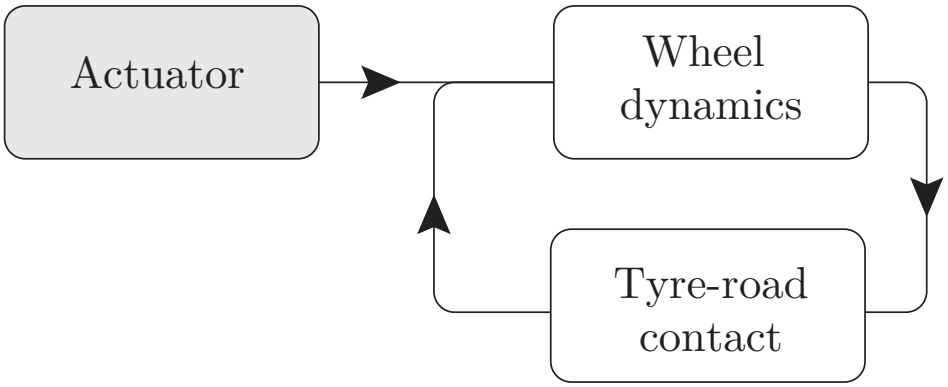

Figure 2-5: Fundamental scheme of *Vehicle* block. The *Actuator* block is not part of this, but it shown to visualise the location of its input.

2-2 Actuator

There is one more major aspect when it comes to ABS braking: actuator dynamics. Delays and non-linearities already occur due to tyre relaxation. Actuator dynamics also increase the complexity of the problem by adding another delay.

The BMW is equipped with Hydraulically Actuated Brakes (HAB) (see fig. 2-6). In terms of control, it is interesting to investigate how the force to the brake calliper is transmitted.

A reliable and efficient method for this is the hydraulic brake system. This technique allows for control and amplification of the applied force. When the driver presses the brake pedal, a certain pressure is built up in the hydraulic system. This is subsequently transmitted through the build valve to the brake cylinder. In the event of ABS braking, the marked section (see fig. 2-6) is enabled. A dump valve, which is connected as a feedback loop, can discharge pressure and is connected to a low pressure accumulator. Lastly, a pump is present. This pump can increase the pressure in the pipeline. There are three control actions the HAB can execute:

- **Increase brake pressure:** By closing the dump valve and opening the build valve, the pressure in the pipeline increases. The pump contributes to this higher pressure, and as the dump valve is closed, it can only increase. The maximum pressure is limited to Âğthe driver input.
- **Decrease brake pressure:** By closing the build valve and opening the dump valve, the pressure becomes less. Neither the pressure generated by the pump nor by the driver can now reach the brake cylinder, and pressure is lost through the dump valve.
- **Hold brake pressure:** When both valves are closed, the pressure in pipeline 2 remains the same as it is a completely closed circuit now.

The brake pressure is, obviously, not changed instantly. The build valve (as shown in fig. 2-6) has to rapidly increase or decrease brake pressure and is simplistically modelled by a transfer function as described by eq. (2-9). A delay is added as well to simulate the response time of the system. Experiments have shown this delay is approximately 9 ms for the brake system of the BMW, which is used for validation in this thesis.

$$F_{calliper}(s) = \frac{1}{1 + \frac{1}{70}s} e^{-0.009s} \tag{2-9}$$

Earlier field test results provide insight in the delay that is caused by the actuator. Looking at the data, it is possible to obtain plots such as fig. 2-7. This information is used to find that the transfer delay is approximately 9 ms.

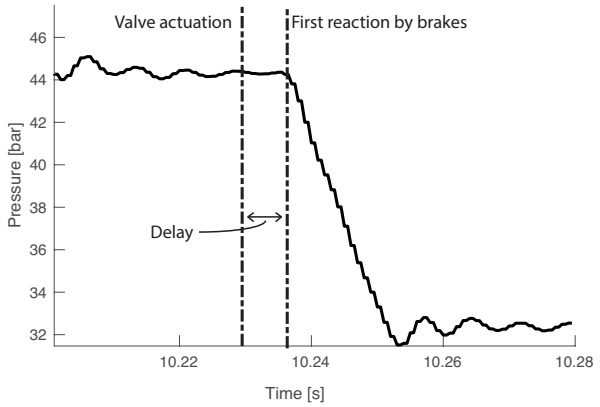

Figure 2-7: Actuator response during field test

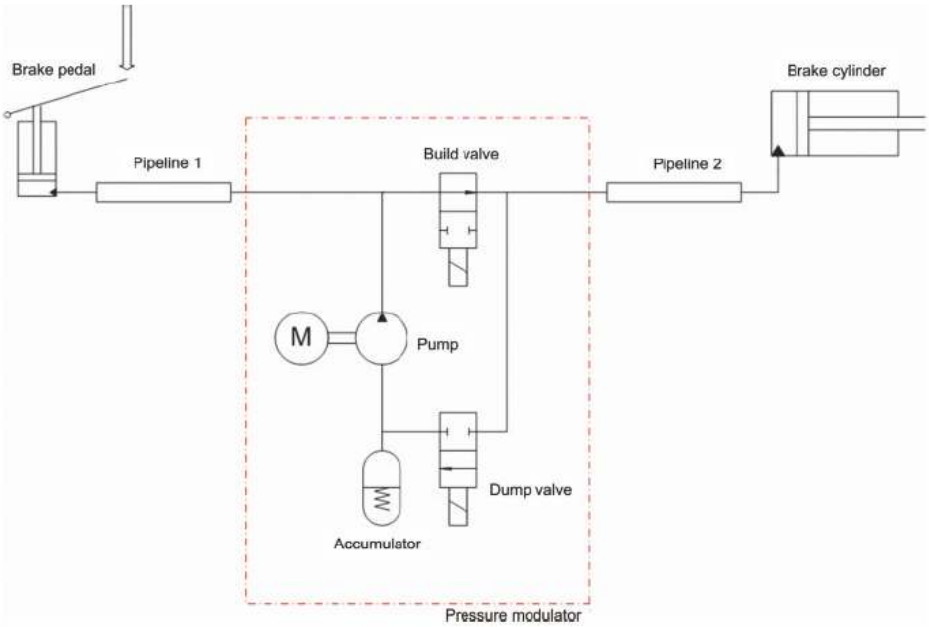

Figure 2-6: Hydraulically actuated braking system [6]

In this report, the brake torque is controlled. The assumption is made that there is a linear relation between the brake pad and dish. According to [16] the influence of hysteresis is less than 5%. For the sake of simplification this effect is therefore neglected. The resulting model for the actuator is thus a transfer delay of 9 ms plus a first-order transfer function (eq. (2-9)).

2-3 Sensors

A part of a more realistic control system is that its data feed does not deliver perfect information. This data inaccuracy has to be simulated. The *Sensor* block therefore contains models that add white Guassian noise to the signals. The noisy signal is hereafter lead through a butterworth filter. A smoother, yet noisy, and delayed signal is as such obtained. Figure 2-8 schematically shows the structure of this procedure.

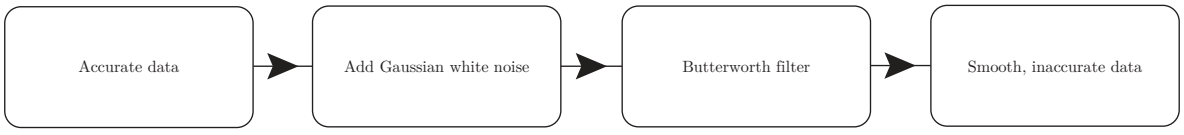

Figure 2-8: Fundamental scheme of the *Sensors* block

All parameters that are relevant to the controller are subject noise. The signals T_b, λ, F_x, and F_z are transformed into less accurate ones. In Simulink, the block *AWGN* offers the ability to add white Gaussian noise. The variance of the noise is generated using the ratio of signal power to noise power. The signal power is determined by squaring each RMS value of the signal. The signal to noise ratio is chosen to be 10 dB (1:3.2) for every signal. Data obtained with earlier experiments have been used to guess appropriate values.

Figure 2-9 shows an example of a brake manoeuvre with noisy data. The amount of noise present looks similar to the noise observed in experiments (for example fig. 4-5), but experimental data is required in the end to draw better conclusions.

Whether noise is included during experiments is mentioned. At first instance it is disabled to show whether the basic principle of the controller works. Later on, it should give a better indication of the robustness and viability of the algorithm.

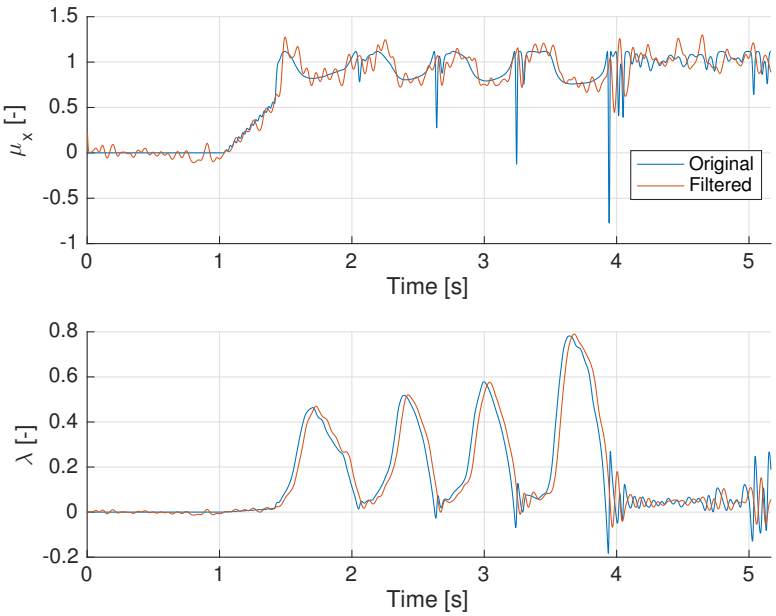

Figure 2-9: Comparison between actual values (indicated by *Original*) and the filtered signal

2-4 Control

The contents of the control block is elaborated on in chapter 3. Its place within the simulation is after the sensor block. The model is a closed-loop system, in which the controller uses sensor data to determine a reference signal for the actuator.

In this thesis the output reference signal is the requested brake torque. The actuator block is another controller that tries to track this signal. Though an actual actuator is more likely to track a brake pressure signal, this is not considered relevant for now.

2-5 Conclusions

There are multiple reasons why a model of a vehicle is built. It primarily takes less time than tests with an actual car, but a simulation is also an environment in which experiments can be performed under desired conditions. When a vehicle is modelled, the amount of dynamics must be considered. There is chosen to build a relatively basic model, such that a sufficient

overview of the dynamics accounted for is maintained. The general structure of the model is visualised in fig. 2-1.

Four major topics that are relevant to the simulation study have been discussed. The first subject is the wheel itself. This consists of the equations of motion of the wheel and a friction model. Equations of motion are straightforward, but of fundamental value within the vehicle model. Tyre-road contact can be modelled with several friction models. There has been chosen to use the Delft-Tyre package by TASS international, as this includes the Magic Formula and tyre relaxation dynamics. Especially the latter is of high influence and should carefully be taken into account when designing an ABS. Though the aim is to build a simplified model of relevant dynamics, this specific part is modelled more accurately because of its influence.

The remaining model components are modelled more simplistically. The actuator in the model consists of a transfer delay and an extra transfer function. These two should represent the response time of the actuator and the inertia of the brake fluid.

A next step in the development of the ABS as proposed in this thesis is how the controller responds to measurement noise. Sensor data is therefore perturbed using white Gaussian noise. Enabling this simulation feature should lead to more realistic results and it provides an indication of the robustness and viability of the controller.

The model, in short, consists of the following components:

- Quarter car dynamics without load transfer phenomena (section 2-1-2).
- Tyre-road contact is described by MF-Tyre (section 2-1-3).
- A transfer delay and transfer function represent the actuator (section 2-2).
- Sensor data is perturbed with white Gaussian noise (section 2-3).
- A controller (section 2-4).

Chapter 3

Controller design

When a driver heavily presses the brake pedal, the ABS should detect whether the driver would cause wheel lock with his input. If so, HAB allows for taking over control of the brake actuator (fig. 2-6). ABS should then release some of the brake pressure to prevent wheel lock.

With the use of a controller it is possible to apply the brake torque better than a driver would do himself. This chapter elaborates on the design of an ABS controller. Control variables will be discussed first in section 3-1. How these can be controlled is subsequently covered in section 3-2. Details of a basic force-based algorithm and the novel one follow in section 3-3. Its implementation will be explained in the following section. The chapter ends with conclusions.

3-1 Control variables

There are various control variables that are used in the design of an ABS. This section covers slip (λ) and force (F_x). The difference in control variables is covered first. Figure 3-1 shows a plot containing indicators for set-points. As aforementioned, for every tarmac there is a single optimal friction coefficient. To brake optimally on a surface, the system should be controlled in such a way that the maximum friction value is reached and retained.

The horizontal axis of the figure shows longitudinal slip; the vertical axis the friction coefficient. Control variables that correspond with the vertical axis are force and deceleration. In general, it can be stated that regulating for these in a continuous controller requires the set-point to be chosen well. The problem with this is that such values are non-unique: they could exist on both sides of the friction coefficient curve. A low one can be chosen to reach an equilibrium on any surface, but this could result in a too conservative, suboptimal design [6]. In general, controllers using multiple phases are used as will be explained in section 3-2.

3-1-1 Slip

Wheel slip is a variable for which always a single corresponding friction value can be found. Slip depends on both the velocity of the wheel and the chassis (eq. (2-2)). Though the wheel

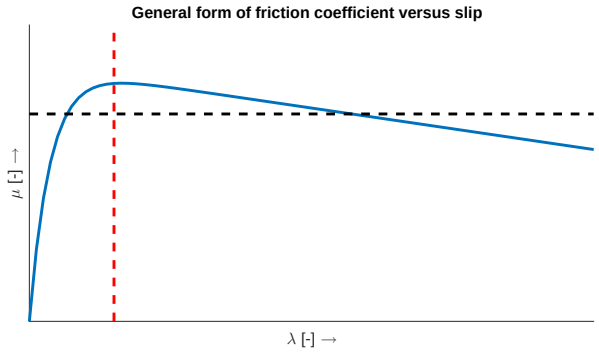

Figure 3-1: General shape of friction coefficient with indicators

rotational velocity can easily be measured using a magnetic encoder, it is challenging to determine the velocity of the chassis. Regular GPS could theoretically provide this required information, but its bandwidth is too small to be used for ABS purposes. There are also investigations in which the wheel slip is determined using acceleration [17], and this data might even be combined with GPS data. In this thesis, it is assumed slip data is available. During the field tests that are performed for this research, this data will be available as well.

Differentiating the equation to determine wheel slip to time results in eq. (3-1). Slip dynamics become infinitely fast for low velocities. By looking at the equations, it can be found that $\dot{\lambda}$ increases for lower values of v. This makes it harder to control the system. Brake torque should therefore be applied more gently or conservatively at lower velocities.

$$\dot{\lambda} = -\frac{r}{v}\dot{\omega} + \frac{\omega r}{v^2}\dot{v} \tag{3-1}$$

$$\omega = \frac{v}{r}(1-\lambda) \tag{3-2}$$

Given that the slip value controlled for lies in the stable region, a benefit of controlling using wheel slip data is that the brake torque converges to a fixed value. It is furthermore relatively easy to design a controller that reaches the reference value, even without a specified maximum in friction [18].

Looking back at fig. 3-1 it is clear every slip value corresponds with a single friction value. It is a variable that, in principle, can be robustly regulated. However, determining this optimum is problematic if only slip measurements are performed. Another downside of it is that when the slip optimum is low, the influence of noise increases.

3-1-2 Force

A relatively new technique to control the ABS is based on force measurements. Though the method is not necessarily new, load-sensing bearings could allow for the implementation in consumer cars in the near future, while other sensors with the same goal are too expensive. It is a product SKF has been developing for the past two decades. The following quote describes the benefits of determining forces with the use of bearings.

"The bearing deformation based approach has several advantages compared to the other approaches which makes commercial implementation more feasible. First of all, the bearing outer-ring, at which the measurement takes a place, is non-rotating significantly simplifying data acquisition. Besides that, in contrast to tires, the bearing usually serves the entire lifetime of the vehicle. On top of that, the bearing based approach is robust to tire and rim changes. Furthermore, as the bearing is placed between the brake mount and its point of application, bearing load measurement allows for the measurement of the brake tangential force. This force can be used to reconstruct the applied brake torque, which is a very useful control variable in vehicle dynamics control. Lastly, due to the low weight of the sensory parts only a minimal increase of unsprung mass will result, such that the dynamic behavior is practically unaltered." [19]

Force measurements can be obtained faster than wheel deceleration data. In an ABS algorithm that uses forces, the friction coefficient peak can be measured. If deceleration would be used to find this optimum, the brake torque should be known as well. This has a negative effect on the accuracy of this estimate. A force-based approach is therefore promising.

The algorithm as shown in [7] is based on how forces relate with the wheel slip derivative (see eq. (3-3)). The right-hand side of this equation determines the sign of $\dot{\lambda}$. The factor $-\frac{1}{m}\sum_{i=1}^{4} F_{x,i}$ is found using force measurements. It is furthermore known that the bounds of $\frac{\omega r_w}{v} \in [0, 1]$. The second term in the equation can thus be measured entirely.

$$\dot{\lambda} = -\frac{\omega r_w}{v^2}\frac{1}{m}\sum_{i=1}^{4}\left(-\frac{r_w}{J}(rF_{x,i} - T_b)\right) \tag{3-3}$$

With the analysis so far, it can be concluded that the sign of the slip derivative is determined by $T_b - rF_x$. Equations (3-4) and (3-5) express when it is certain that the wheel slip is increasing or decreasing.

$$T_b - rF_x < 0 \qquad \rightarrow \qquad \dot{\lambda} < 0 \tag{3-4}$$

$$T_b - rF_x > \frac{J}{r}\frac{1}{m}\sum_{i=1}^{4} F_{x,i} \qquad \rightarrow \qquad \dot{\lambda} > 0 \tag{3-5}$$

Note that there is an area for which it is unknown whether the slip increases or decreases. This is described by the following condition:

$$0 \geq T_b - rF_x \leq \frac{J}{r}\frac{1}{m}\sum_{i=1}^{4} F_{x,i}$$

Without these bounds, it would have been possible to determine $\dot{\lambda} = 0$. This would allow the maximum friction force to be calculated. Instead, checking for possible higher longitudinal force by changing the brake pressure is required. In section 3-2 the practical implementation of using the longitudinal force for control is discussed.

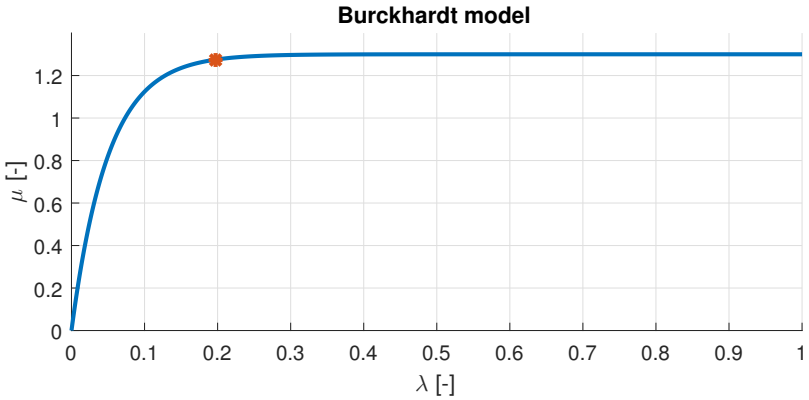

Figure 3-2: Friction coefficient curve without a peak

3-1-3 Combining force and slip

A control method based purely on slip lacks information about the optimum when no prior knowledge about the road surface is available. Especially for a real-life implementation, such data is crucial.

Would a control method be developed that solely uses longitudinal force data, it is required to encircle the friction coefficient peak to keep track of the optimum. Recall the friction coefficient curve. This curve provides insight in the applicability of a control methods. The slope on the right side of the curve is a lot less steep than on the left side. Furthermore, sensors return noisy data. As a consequence it is harder to measure a decrease of force a soon as the friction peak is passed to either side of the curve.

Combining information about both could be beneficial. The implementation of it in a controller is the main topic of this thesis. The combination lies within the link between longitudinal force and slip. An extreme example is if a friction coefficient curve would show no peak at all, such as in fig. 3-2, it is wishful to control for the red marker: keeping the slip low for controllability and the longitudinal force near-ideal.

Linking the two variables could prevent the control system from searching for a higher force value if the force barely decreases with respect to the maximum that was measured before. If the slip increases and the longitudinal force remains approximately the same, the slip value could trigger the algorithm to stop searching for a higher longitudinal force. In the next section it is discussed more thoroughly how this combination is practically implemented.

3-2 Control methods

Before discussing control methods, a statement relevant to this entire section is that when the dynamics of the wheel ($v \to 0$) become infinitely fast, any control method should be switched off or behave differently at lower velocities. In the current stage of the development, the main focus lies on when the vehicle velocity is greater than a certain minimum. At lower velocities, it takes more time to return from an unstable mode, so an option would be to perform control more conservatively.

Control variables have been discussed in the previous section. In the current section methods to control the system based on those variables are covered. In basic control problems, the PID controller is often used. Section 3-2-1 discusses its possible implementation in the problem faced in this project. The following subsection elaborates on the use of a multiple-phase controller. The latter explains the controller that is designed in this thesis.

3-2-1 PID control

The PID controls a system continuously, whereas the brake actuator is controlled discontinuously. Even without considering delays in response time caused by tyre and actuator dynamics, tuning a PID for the purpose of ABS is non-trivial. In the stable region of the friction curve, a PID could work fine. However, for stability, dynamics on this right side demand a controller that changes the brake torque more aggressively than when the brake torque is increased. A compromise must be made, because using a single PID controller with constant parameters would mean the time required for the system to return to a stable state is unnecessarily long.

The implementation of a PID controller is now discussed with the assumption that reliable information about slip and force is available. Since the slip value is unique, it is relatively simple to control for. Theoretically, this could be an efficient method for ABS braking. Practically, detecting the optimal slip value reliably is non-trivial.

The PID could also be used to control for a friction coefficient reference. A direct problem that must be tackled is the non-uniqueness of this value. Figure 3-1 showed that the same friction coefficient can be measured at two different slip values, where the first is on the stable side of the curve and the second on the unstable side. Therefore, implementing a PID controller that is solely based on a friction reference is not a practical solution. It is possible to find whether the friction coefficient peak was passed, and then use different control parameters for the PID. This is, however, similar to controlling in multiple phases, which will be discussed in the next section.

3-2-2 Multiple-phase control

This subsection elaborates on a controller that utilises phases. The main property of this method is that it can function in different ways per phase. The multiple-phased controller was also used by Bosch [20] and used deceleration as one of its control variables. Using this type of controller, it is relatively simple to make exceptions to the basic algorithm.

Theoretically, it is possible to measure the optimal brake force once and subsequently use this as a reference for the controller. However, in this thesis, it is assumed that during braking a changing road surface should not lead to inefficient control.

If one is to design a controller that is solely based on slip, it is possible to use one phase in which a high brake torque would lead to exceeding the friction coefficient peak, and one phase in which the brake torque is lowered to prevent wheel lock. Especially on the right side of the friction coefficient peak, the system could as such be tuned to decrease the brake torque more aggressively.

3-3 Control algorithms

Information about control variables and control algorithms in this section is combined to propose a novel ABS algorithm. It is believed that force-based control is a promising development in ABS. It provides direct information about friction, so it is expected that the optimum can be encircled more accurately. ABS based on deceleration is well-known among researchers as it is an important control variable in current cars, but algorithms based on force less so. For this reason, an example of a basic ABS based on force measurements is presented in the first subsection. The following subsection elaborates on the proposed control algorithm, which uses the former as a basis.

3-3-1 A basis for force-based control

An algorithm that encircles the friction coefficient peak is proposed in [7]. Each cycle, the maximum longitudinal force is determined, and the brakes are applied accordingly. Do note that the longitudinal force depends on the normal force as well. The algorithm works in two phases. Briefly, the first phase ensures the wheel slip is decreased by setting the brake torque to eq. (3-6). In this equation, $\Delta T_b^- \geq 0$, which is an offset parameter that should guarantee the wheel slip will decrease.

$$T_b^-(t) = r_w F_x(t) - \Delta T_b^- \tag{3-6}$$

During the second phase the wheel slip increases by braking more heavily. The brake torque in this phase is set to eq. (3-7) with offset parameter $\Delta T_b^+ \geq 0$.

$$T_b^+(t) = \frac{J}{r_w}\frac{1}{m}\sum_{i=1}^{4} F_{x,i}(t) + r_w \cdot \max(\hat{F}_{sp}, \hat{F}_{x,max}(t)) + \Delta T_b^+ \tag{3-7}$$

$$\hat{F}_{x,max}(t) = \max_{t_s \leq \tau \leq t}(F_x(\tau)) \tag{3-8}$$

In this equation $\hat{F}_{x,max}$ represents the maximum longitudinal force as found in the current phase (eq. (3-8)). In eq. (3-9), α_F is a scaling parameter and $\hat{F}_{x,max,prev}$ is the maximum longitudinal force in the previous phase. This parameter normally lies between 0.9 and 1.0, and is used to improve algorithm cycling.

$$\hat{F}_{sp} = \alpha_F \hat{F}_{x,max,prev}(t) \tag{3-9}$$

For both phases, there exists a trigger that will lead the system to the next state. It is described by eq. (3-10). This equation checks whether the currently measured F_x is lower than the measured maximum longitudinal force minus a specified offset.

$$F_x(t) < \hat{F}_{x,max}(t) - \Delta F_{x,tr} \tag{3-10}$$

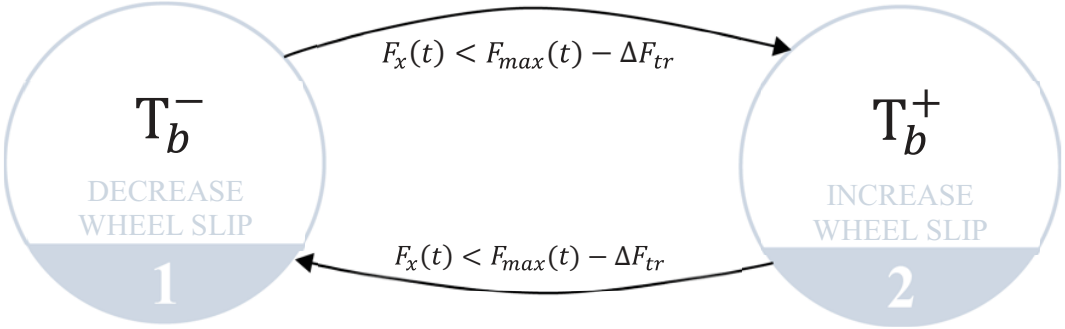

Figure 3-3: Force-based algorithm logic [7]

The $\Delta F_{x,tr}$ should be different when the system is in a state on the right side of the friction coefficient curve, because the friction coefficient decreases more slowly there than it increases on the left side. The algorithm logic is graphically shown in fig. 3-3.

3-3-2 Proposed controller

An improvement to the force-based algorithm is now proposed. It is important to note that longitudinal force depends on the normal load. Though load transfer phenomena are not considered in the simulations in this report, the algorithm is designed such that it can still work when they are. The friction coefficient gives more useful information about the maximum brake force if the normal load were to change as well. When the force-based controller is adjusted to one using the friction coefficient, the lower brake torque as described by eq. (3-6) remains the same. There is, however, a change in the brake torque for the second phase. Equation (3-7) is replaced by eq. (3-11). A difference is that the second factor is changed to an estimated optimal longitudinal force ($F_z(t)\hat{\mu}_x^*$). Tuning parameter α_μ describes the minimal brake torque at the start of phase 2.

$$T_b^+(t, t_{phs}) = \frac{J}{r_w}\frac{1}{m}\sum_{i=1}^{4} F_{x,i}(t) + (\alpha_\mu + \alpha_{T_{b,add}}(t_{phs}))r_w F_z(t)\hat{\mu}_x^* \tag{3-11}$$

Practically, unfortunately, there is also an uncertainty added when the algorithm uses the friction coefficient. Since neither the normal load, nor the longitudinal force are determined with full certainty, the measurement reliability of the friction coefficient is inherently lower than that of either of them.

The estimate of the optimal friction value is crucial for the algorithm to work. The optimal friction coefficient can theoretically be determined using the same method as was used to obtain $\hat{F}_{x,max}$. In section 4-2 an alternative method is explained. For the remainder of this section, it is assumed μ_x^* is known.

Another addition is the function $\alpha_{T_{b,add}}$. It is a function that should ensure the systems starts before the optimal friction coefficient and then gradually exceeds it. The idea behind this is to initially control for, say, 90% of the optimum and end at a value higher than 100%.

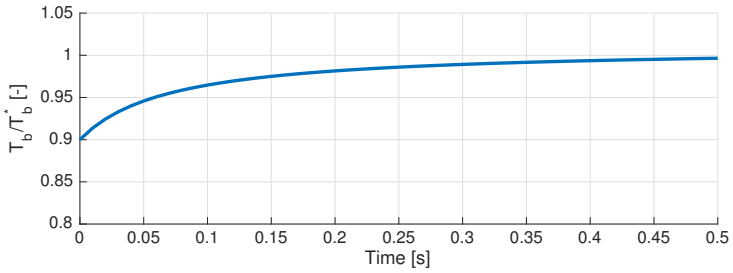

Figure 3-4: Control brake torque compared to estimated optimum over time

Equation (3-12) shows the equation that will be used in this research project. It is visualised in fig. 3-4.

$$\alpha_{T_{b,add}}(t_{phs}) = \alpha_{T_b}\left(1 - \frac{\alpha_{phs}}{t_{phs} + \alpha_{phs}}\right) \tag{3-12}$$

Using this method, the brake torque more gently increases as of the point where the system is stable. The used variables from the equation above are explained as follows:

- α_{phs} [-]: Scaling parameter for the influence of time.
- α_{T_b} [-]: Extra added fraction of $\hat{T}_b^*$ to exceed the friction optimum.
- t_{phs} [s]: Time since last phase update.

If tyre-road contact characteristics do not change too much, it is expected applying the brake torque according to eq. (3-12) would result in a relatively stable brake manoeuvre. When the vehicle velocity is lower than a certain value, exceeding the friction coefficient peak is more likely to lead to an unstable brake manoeuvre. This is why there is chosen to set $\alpha_{T_{b,add}} = 0$ when $v \leq v_{min}$.

Consider the case when the optimal friction coefficient is first found to be 0.20. While braking, the car goes from this slippery surface to a much rougher road on which a friction coefficient of 0.90 could be found. It would be best of the algorithm detects this change and increases the brake torque more rapidly. It is more important to find a higher friction coefficient when the found one is low. As such, the parameters of eq. (3-12) could be adjusted. α_{T_b} and α_{phs} could, for example, also become dependant on the magnitude of μ_x^*. This thesis does not focus on this specific scenario, but it does show mention this case as it should be taken into account for practical use of this method.

It was suggested to link a slip value to the measured friction. So instead of only looking for μ_x^*, its corresponding λ, which is denoted as λ^*, is now considered as well. If both optima are then available, the triggers of the force-based controller (eq. (3-10)) can be redesigned.

There are multiple options in designing a trigger that could be used. During the development of the algorithm, it is more insightful and clearer to keep the control variables separate and to regulate for them individually. It is then easier to deduce the cause of a phase switch.

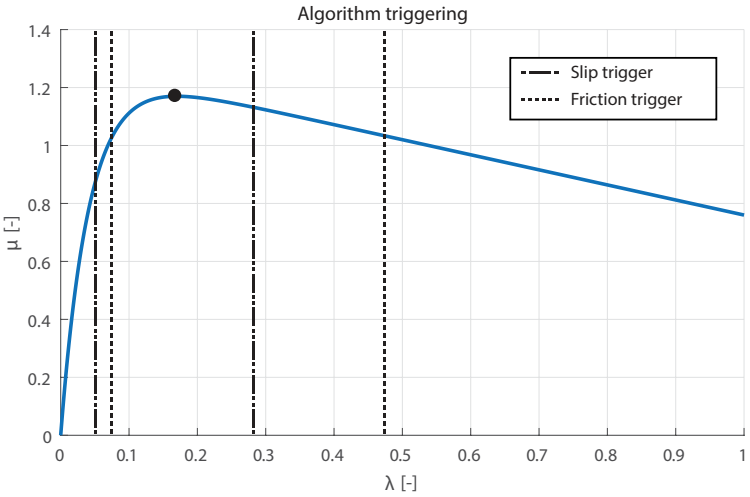

Figure 3-5: Algorithm triggering with slip and friction

Absolute deviations could be used in the triggers when written in separate ones per phase. On the left side of the curve eq. (3-13) is the suggested trigger. On the other side, eq. (3-14) is proposed.

$$\mu_x < \mu_x^* - \beta_{\mu_{x,tr,r}} \quad \text{OR} \quad \lambda > \lambda^* + \beta_{\lambda_{tr,r}} \tag{3-13}$$

$$\mu_x < \mu_x^* - \beta_{\mu_{x,tr,l}} \quad \text{OR} \quad \lambda < \lambda^* - \beta_{\lambda_{tr,l}} \tag{3-14}$$

To provide insight in phase switching using these equations, assume $\lambda^* = 0.17$ and $\mu^* = 1.17$, with $\beta_{\mu_{x,tr,r}} = \beta_{\mu_{x,tr,l}} = 0.15$ and $\beta_{\lambda_{tr,r}} = \beta_{\lambda_{tr,l}} = 0.10$. The algorithm would then trigger a next phase as shown by fig. 3-5. With these parameters, the friction value would trigger the next phase on the left side of the peak; the slip on the right side of the curve.

One could argue that the boundaries of either measurement value could be made smaller ruling out that a second parameter is necessary. If $\beta_{\mu_{x,tr,r}} = 0.05$, the algorithm would, theoretically, trigger at approximately the same point as the one based on slip. However, considering measurement inaccuracy and noise, phase switches might then occur at the wrong moments. Selecting values with a greater margin of error results in more reliable phase switching. A schematic overview of the phase determination is shown in fig. 3-6.

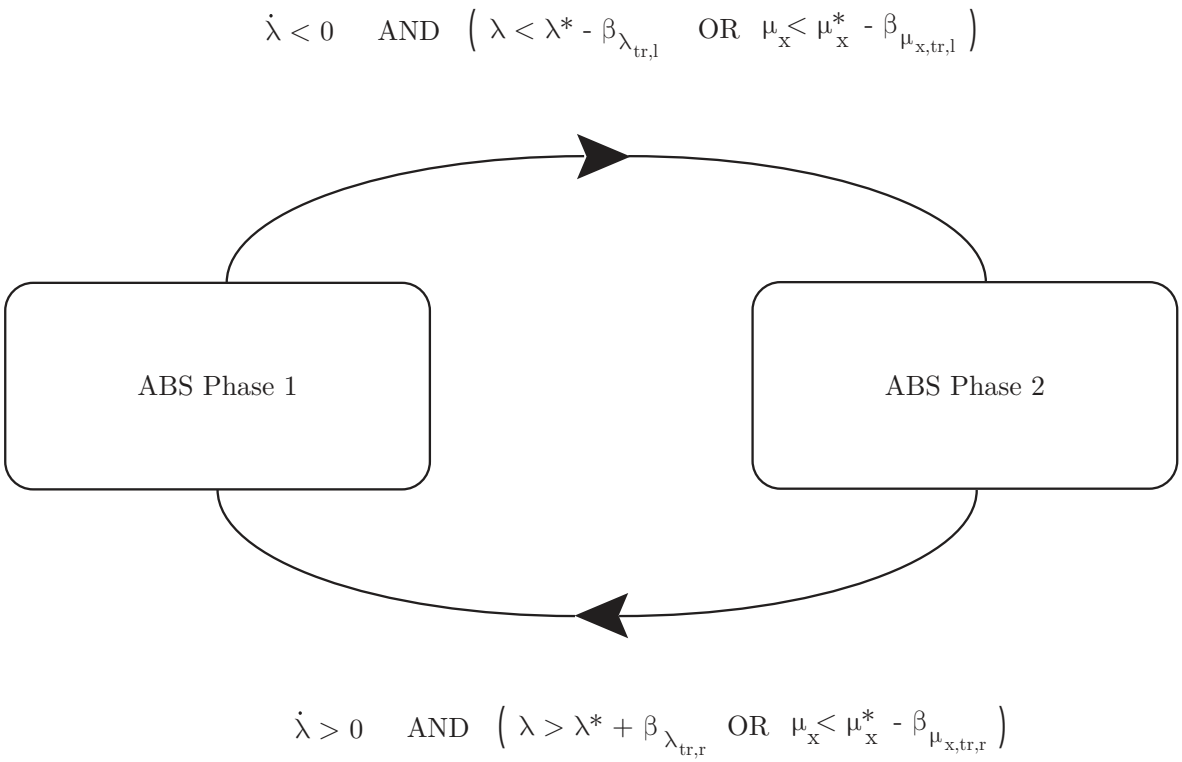

Figure 3-6: Phase switch algorithm

Cycling

With multiple-phase controllers in general the system state cycles around the friction coefficient peak, such that the optimum can be kept track of, and an appropriate brake torque can be controlled for. With the algorithm proposed in [7], each cycle is used to actually measure the maximum longitudinal force. It is required that the system passes the friction coefficient peak into the unstable region. As a result, the wheels could lock and the utilised friction coefficient decreases.

A system more preferable is one that controls for a force slightly under the maximum longitudinal force. It is troublesome to do so, since the road surface the car is driving on could change in terms of friction properties.

Case 1: Changing to a road surface while forcing the state to change
To give an example of the problems it can theoretically cause to control for a brake torque slightly under the optimum, assume the road surface actually changes. Furthermore, assume the car would drive on a cobblestone road in a state as indicated by *Current state* in fig. 3-7. If the brake torque would be kept constant, the brakes are applied with 95% efficiency. Keeping this constant when the road surface changes to dry asphalt, the system will stabilise on *New state*. As a consequence, the brake efficiency is now only 81%. Therefore, there must be found a criterion that triggers the algorithm to find the new optimum.

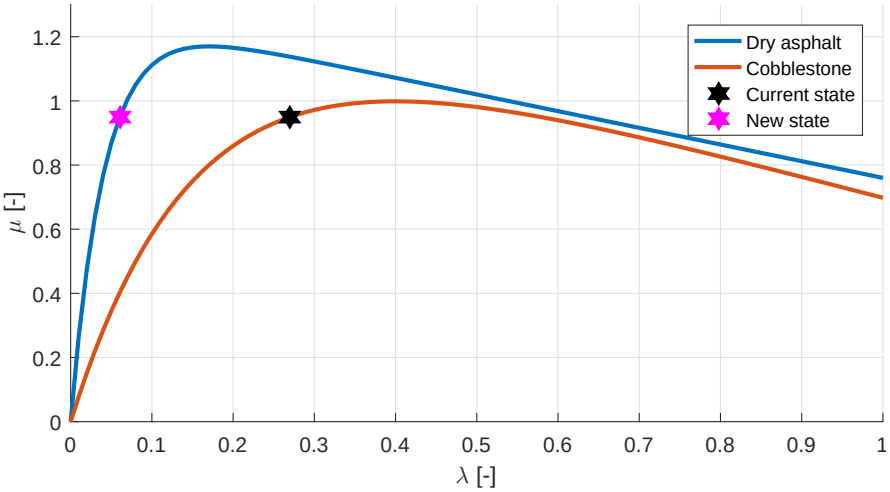

Figure 3-7: Example of two friction curves

It has been discussed that force and slip value are both tested separately to determine whether the algorithm should move to the next phase. In the current case, it becomes essential to link the two measurements. If a similar optimal friction coefficient is found for a significantly different slip value (fig. 3-7), it can be concluded that the previously determined optimum has become unreliable.

There is no need for an extra trigger in the algorithm. It will trigger a phase switch because of the force-based trigger first, as the state of the system will not move in a horizontal line from the black star to the magenta star. The slip initially remains the same, but the lower brake torque will lead the state of the system over the dry asphalt friction curve to the magenta star. In the meanwhile, sensors obtain new data that should give information about the new optima. As a consequence, when the *New state* is obtained, the algorithm has observed there could be braked more efficiently.

Case 2: Changing to a road surface with similar slope and the same state
Another case is if the friction coefficient optimum at some point is known with a 100% certainty. At this point, theoretically, the system could control for just below the optimum. In fig. 3-8 this point is indicated by a black marker. In case the car would drive on a road with friction characteristics as described by the curve *Road surface 1*, but then switches to *Road surface 2*, the car will continue to brake the same way it did before. It could, however, be braking 25% more efficiently. This is why it could remain important to check whether the peak is still at the measured or estimated point.

It must be noted that seeking for the highest friction coefficient is only beneficial if going into the unstable region does not decrease efficiency more than the potential benefit of finding a higher friction coefficient. Whether there is searched for a new optimum or not, either could thus be disadvantageous, depending on the situation.

Despite the possible advantage of controlling for a friction coefficient just below the optimum, it will be encircled with the algorithm as presented in this research project. There is decided to do so, as optimum estimation methods usually require the system to remain sufficiently excited. It is not within the scope of this thesis to develop such an algorithm.

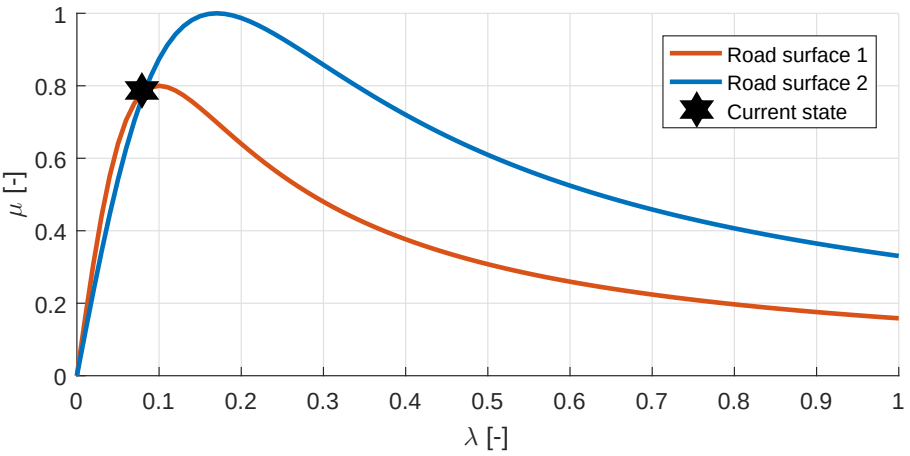

Figure 3-8: Example of two friction curves with a similar slope at the start

Phase updates

When switching from one phase to another, an increasing slip does not instantly start decreasing and vice versa. The slip and friction values will both go a bit further in the direction they were going just before the phase switch.

Consider the case when the control algorithm outputs that a switch from phase 2 to phase 1 is required. The car will still have an increasing slip value and, thus, a decreasing friction coefficient. If there is no check on whether the slip is actually decreasing, the force-based trigger could cause the algorithm to switch to phase 2 again while it is still on the unstable side of the curve.

A solution to this phase updating problem is to implement conditions that verify an increasing or decreasing wheel slip. These are given by eqs. (3-4) and (3-5).

3-4 Implementation

The control block contains the ABS algorithm. A multiple-phase controller is implemented, which was discussed in section 3-2-2. This controller internally consists of three steps (see fig. 3-9). In the first step, the optima of both friction and slip are determined. Chapter 4 goes into more detail about this process. At this point, it is assumed such an algorithm exists and returns valid data.

Measurements are compared to calculated optima, so the phase of the ABS can subsequently be determined. Phase switching occurs based on eqs. (3-13) and (3-14), which was visualised in fig. 3-6. To make sure the slip and friction values are actually moving in the desired direction, eqs. (3-4) and (3-5) were introduced.

Based on the acquired information about the optima and phase of the ABS, the reference brake torque is determined. Phase 1 leads to a brake torque as described by eq. (3-6), in phase 2 eq. (3-11) is used.

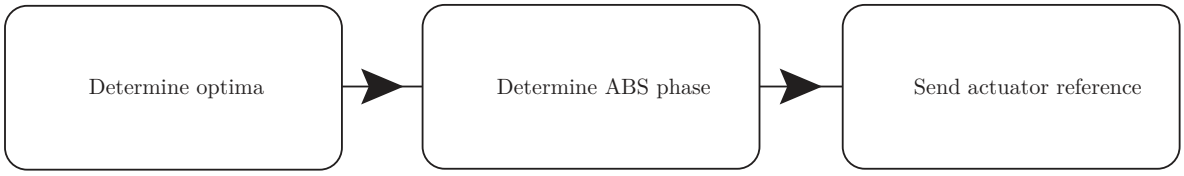

Figure 3-9: Fundamental scheme of the *Control* block

An exception that is made with respect to the algorithm as described in section 3-2-2 is a safety check which solely uses the wheel slip value. In the implemented algorithm, there is a boundary on the wheel slip of 0.4. As a consequence, the controller switches to phase 1 — with T_b^- — when $\lambda > 0.4$. Similarly, if the controller is already in phase 1, it must not switch to phase 2 for even the shortest period of time. As long as T_b^- is low enough, this extra rule should prevent wheel lock, and should not be required to be used. The rule is mainly introduced for safety when the algorithm is tested in a real car.

3-5 Conclusions

In ABS the friction force is maximised. A higher friction coefficient leads to a shorter brake distance. For different road surfaces, the optimal friction force is of different magnitude and reached at a different slip value.

Current ABS technology uses deceleration measurements. The actual longitudinal force can be determined only when the brake torque is known as well. Deceleration-based algorithms do not explicitly depend on friction coefficient data in order to function. Deceleration measurements provide sufficient, information to estimate whether the friction coefficient peak was passed. This is however troublesome on roads with less clear maximum.

With the introduction of load sensing bearings, it is believed ABS could become more reliable. Tyre forces can as such directly be determined, which means the friction coefficient becomes known as well. The same problem as with deceleration-based control still occurs, but should be smaller since the actual optimal friction coefficient peak is measured. A problem that remains is that the coefficient stays near its optimum with increasing slip on more slippery surfaces.

Though force measurements provide more direct information, its principle is close to deceleration-based algorithms. A key property is the non-uniqueness of their potentially reachable values. A friction coefficient of 0.8, for example, could lie in either the stable or unstable region of the friction curve. This is one of the reasons why in algorithms there is chosen to keep encircling the friction coefficient peak. Another reason is that the optimum controlled for remains up-to-date.

A slip-based algorithm could work, but two of its main problems are its measurement and its reference value. These are major drawbacks if a slip-based algorithms were to operate without any other measurements. Contrary to the previous control variables, slip values are unique. This property is key to simultaneously solving the problems of both type of control variables.

An ABS is proposed and summarised in fig. 3-6. A lower brake torque is applied in phase 1; a higher one in phase 2. The algorithm targets on encircling the friction coefficient peak. The proposed ABS checks whether either the current slip or force measurement is too far off from the optimum. In the first phase, there is chosen to apply a brake torque which is low enough to decrease the slip value (eq. (3-6)). The second phase consists of two factors, α_μ and $\alpha_{T_{b,add}}$ (eq. (3-11)). The first brings the system state near the optimum, yet still in the stable region. The second factor gradually increases the torque in order to exceed it.

Chapter 4

Friction estimation

The controller which was described in the previous chapter requires references of the optima of slip and friction. If measurements could be performed perfectly, the most straightforward method to determine these optima is to detect the maximum friction coefficient within a cycle and save the corresponding slip value. Practically, it is inaccurate to do so, because of measurement noise and because the system is only briefly in the optimal state.

First two friction models that could function within an estimator (section 4-1) are investigated. In the second section, the fundamentals of a friction estimation method is explained. It furthermore covers how the denoted friction models could practically be implemented in this estimator.

With a working estimator, its implementation in the simulation is discussed in section 4-3. Simulations are performed in the next section to show the validity of using this friction estimation method for the purpose of on-line road characterisation.

4-1 Friction models

The Magic Formula can be used to estimate road characteristics [21]. In this investigation, however, there is chosen to merely use it for simulation purposes. There is looked into two more models as they depend on fewer parameters. Consequently, they are computationally less costly, which benefits their potential on-line implementation. Moreover, tuning parameters of the friction estimator are easier to determine.

4-1-1 Burckhardt

A function that describes a relationship between slip and the friction coefficient was described by Burckhardt [22]. This method does not take tyre dynamics into account and is, thus, a static mapping. Technically, it can be said that the model assumes the tyre has an infinite

stiffness. The most-used formula describing the relationship is eq. (4-1). Figure 4-1 shows the curve for different surfaces according to the equation and experimental data.

$$\mu(\lambda, \vartheta) = \vartheta_1(1 - e^{-\lambda\vartheta_2}) - \lambda\vartheta_3 \tag{4-1}$$

As the ABS algorithm is be implemented in a real car as well, already available data recorded in April 2014 [7] for this particular vehicle are used. This data was obtained on dry asphalt using the car. A curve is found which better matches the situation that is experienced during experiments later on. The dashed line in fig. 4-1 shows the estimated curve that was obtained based on measurements. The friction coefficient lies a little higher than 1.0 and the optimal slip value is around 0.07. Even though the tests are performed on dry asphalt as well, the peak of the curve is lower and shifted about 0.10 to the left compared to the one that comes from the measurements by Burckhardt. This difference can be attributed to, for example, different tyre material properties or a different tyre tread.

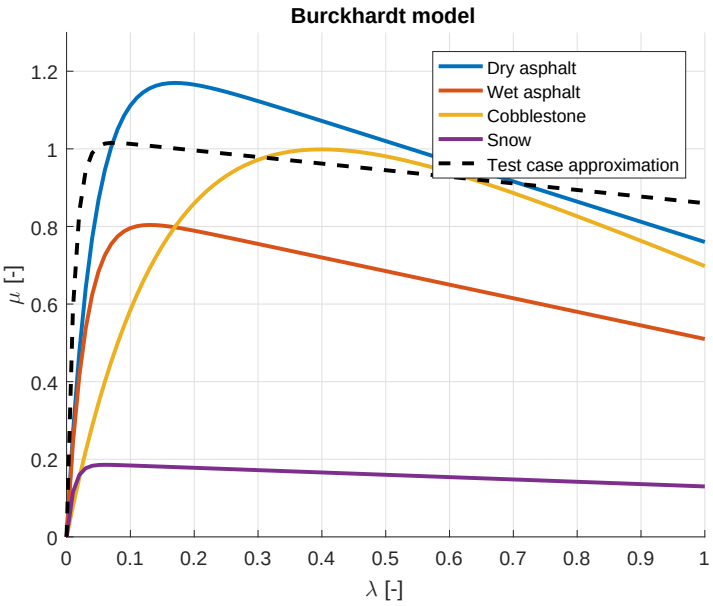

Figure 4-1: Burckhardt model

4-1-2 Simplified friction model

The Burckhardt model, as discussed previously, is based on three parameters. There is another relatively simple model, which requires even fewer. It was developed as an simple and insightful method to model friction. The function is not necessarily more realistic in terms of the whole curve, but is able to describe the curve up to the peak similarly well. Equation (4-2) shows this relation [23].

$$\mu(\lambda, \mu^*, \lambda^*) = \frac{2\mu^*\lambda}{\lambda^*\left(1 + \left(\frac{\lambda}{\lambda^*}\right)^2\right)} \tag{4-2}$$

Since this two-parameter model requires even fewer parameters than the Burckhardt model, but does seem to represent the initial slope well, it is an interesting one to take into account. Figure 4-2 shows a comparison between the discussed curves. The dashed lines show curves according to Burckhardt. The first property that is clearly different is the sharpness of the peak. In the model of Burckhardt, friction decreases quite linearly for these sets of parameters.

There is furthermore a notable difference between the steepness of the curve from zero wheel slip up to the optimum. The figure shows the slope of both models in that region differs, too. Burckhardt shows a steeper slope. The simulation study should give better insight in which of these can be used best.

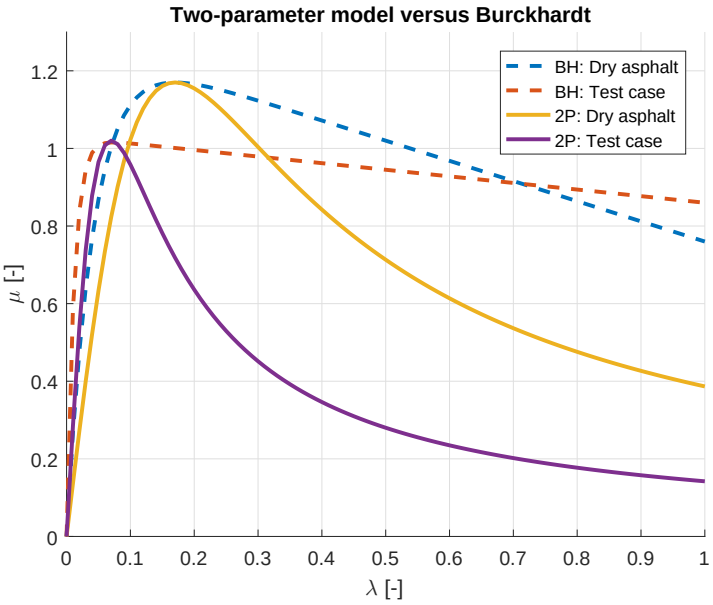

Figure 4-2: Model based on two parameters, where 2P is the two-parameter model and BH Burckhardt

4-2 The Extended Kalman Filter

There should be found a desired brake controller that maximises the longitudinal force. The sooner information about this optimum is available, the better. When the curve is known with sufficient certainty, the ABS could be able to control the brake torque to a near-optimal setting. It is unrealistic that the curve is known with full certainty at all times, but the idea of predicting road characteristics can still be useful. Using an Extended Kalman Filter (EKF), friction curve information can be estimated and its results can be used in the designed algorithm. The use of Kalman filtering is not new in vehicles, as it is currently often used to determine a state, such as the vehicle velocity [24] or tyre friction [25]. The approach in this thesis is different, because it is used as a method to determine the optimal slip value and friction coefficient.

The controller requires μ_x^* to be determined. The EKF can find this information more reliably than measuring optima by explicitly looking at the the maximum value during a phase. The signal contains noise and the EKF is able to filter it out by optimally fitting a curve to

measurements. The fundamentals of an EKF are explained in appendix A. This section focuses on the implementation of the discussed friction models within this method.

To implement the discussed friction models into EKF, first their derivatives with respect to their parameters must be determined. For the Burckhardt model, this comes down to eq. (4-3). In this equation the Jacobian of the Burckhardt model (h_{BH}) is denoted with a as defined in eq. (4-4).

$$H_{BH} = \frac{\partial h_{BH}}{\partial x} = \begin{bmatrix} 1 - \exp(-c_2\lambda) \\ c_1\lambda^* \exp(-c_2\lambda) \\ -\lambda \end{bmatrix} \tag{4-3}$$

$$a = \begin{bmatrix} c_1 \\ c_2 \\ c_3 \end{bmatrix} \tag{4-4}$$

The derivatives of the two-parameter model (h_{2P}) are found in eq. (4-5). For this model a is denoted by eq. (4-6).

$$H_{2P} = \frac{\partial h_{2P}}{\partial x} = \begin{bmatrix} 2\lambda\lambda^* \\ 2\lambda\mu_x^*(\lambda^2 - (\lambda^*)^2) \end{bmatrix} \frac{1}{\lambda^2 + (\lambda^*)^2} \tag{4-5}$$

$$a = \begin{bmatrix} \hat{\mu}_x^* \\ \hat{\lambda}^* \end{bmatrix} \tag{4-6}$$

Tyre friction estimation using an EKF can be implemented by executing the filter each measurement cycle. It is computationally lightweight to do so, because the largest matrix that has to be inverted is 3×3.

A problem that occurs with both friction curve estimation methods, is that the functions ($H_{(\cdot)}$) are not identical to the actual friction coefficient curve. Especially the model with two parameters, deviates significantly after the optimum. This does not have to be a problem, as most of the data points are collected on the left side of the friction coefficient peak. So if this part approximates the actual curve, it should be sufficient to find the optimal control parameters.

An effect that furthermore plays a role in the use of measurement data is tyre relaxation. If brake torque is changed, the effects of tyre relaxation cause the sensors to measure slip and force values which in reality do not fit in a static mapping. By changing the brake torque more slowly, these effects can be minimised.

The designed ABS algorithm keeps encircling the friction coefficient peak. Therefore, sufficiently varying measurement points are fed into the EKF. With this method, the friction estimator mainly focuses on fitting the curve to points that are most relevant for determining the optimum. If the ABS would control for a point just below the optimum of friction, this could become troublesome. There was tested to buffer older data points and feed them into the EKF, but this solution was found not viable (appendix B).

4-3 Implementation in the model

The model
The EKF is implemented with two methods and for two different curves. Both Burckhardt and the two-parameter model are used with and without the buffering method. In section 4-4 both models are compared extensively and the best one is chosen.

Input data
There are two measurement inputs to the EKF: the friction coefficient and wheel slip. Sensors mainly measure data near the peak, because it is encircled. If too little, or inaccurate data on the right side of the curve is measured, an curve without a peak could be estimated. Consequently, the estimate of the optima would become infinitely big. Two solutions have been implemented to prevent this problem.

Firstly, there are maxima set for both optima. The slip value cannot exceed 0.40 and the friction coefficient is 1.20 at maximum. However, still, it is preferable that neither of those values are reached. Especially when the actual optima are much lower.

The second solution for this is using pseudo-data. Every n measurements an extra data point at $\lambda = 1$ is fed into the EKF with $\mu_x = 0$. There is chosen to add one of those every 10 measurements. This greatly increases the chances that the curve shows a peak. Experiments have shown that the estimate is not influenced negatively.

Optimum determination
After calculations have been performed that determine the coefficients of the friction models, the optima of both friction and slip are searched for. In case of the two-parameter model, both optima are in the parameters. In case the curve of Burckhardt is used, another approach is required. Theoretically, it is easiest to find $\partial h/\partial\lambda < \varepsilon_\mu$, in which h is the friction curve, and ε_μ a positive value near zero. The latter is chosen conservatively to ensure the estimate is not in the unstable region. In the upcoming validation process, $\varepsilon_\mu = 0.015$, which was experimentally determined.

The practical implementation of finding the peak is slightly different. Instead of using the function `solve` in Simulink, the optimum is obtained through simply evaluating the friction function for multiple values of λ. The search is stopped when the stopping criterion as described by eq. (4-7) is met. The optimal slip value is determined up to a precision of 0.01. One could argue that this resolution is too low compared to a possible optimal slip value of 0.08. Since it is hard to control at higher precision, the proposed is still expected to be sufficient. An alternative for the `solve` function had to be found, because Simulink does not support it.

$$h(\lambda_k) - h(\lambda_{k-1}) < \varepsilon_\mu \tag{4-7}$$

Reliability
There is one more detail about the implementation of the EKF, namely when the reliability of the output is sufficient to be used as main control reference. Matrix P is again used for this. With a lower value of P, the model accuracy becomes more reliable. Every value on the diagonal of P represents one of the parameters in the model, which are of different scales.

This is why there is chosen to normalise the values on the diagonal of P with respect to each of the parameter values. As a result, the certainty of each of the parameters becomes clearer. This normalised P is denoted by P'.

Equation (4-8) is then used as a trigger to enable the EKF. Parameter β_P should be adjusted if measurement accuracy is not as high as in the regular simulation.

$$\frac{1}{3}(P'_{1,1} + P'_{2,2} + P'_{3,3}) < \beta_P \tag{4-8}$$

4-4 EKF validation

The EKF is of fundamental value in the ABS algorithm as designed in this thesis, because it should be the main reference for the phase triggers and brake torque. This section elaborates on the validity of using an EKF as a core component of an ABS algorithm.

It is first assumed the controller knows the optima of friction and slip perfectly well. The simulation uses $\mu_x^* = 1.12$ and $\lambda^* = 0.08$ for phase switching. The friction peak is encircled a few times throughout this brake manoeuvre. Two models were introduced that could be used to fit measurement data to. The EKF in both cases starts gathering data when the brake pedal is pressed and $\lambda \geq 0.02$. The latter is chosen, because lower values influence the filter negatively. This is caused by measurement inaccuracies which are relatively high there.

Figures presented in this section show a straight red line in the slip graph to show its optimal value. This is done so, as it is not as easily deducible from the plots to find this optimum compared to finding the optimal friction coefficient.

4-4-1 Model comparison

Two-parameter model

The two-parameter model is investigated first. The starting conditions of the filter are as defined in eqs. (4-9) to (4-13). The decision for these parameters is, obviously, arbitrary. However, in the determination of Q, there is chosen to use a 10 times lower noise covariance to find λ, because the slip measurements are of smaller magnitude.

$$P = I_2 \tag{4-9}$$
$$K = I_2 \tag{4-10}$$
$$R = 0.01 \tag{4-11}$$
$$Q = \begin{bmatrix} 1 & 0 \\ 0 & 0.1 \end{bmatrix} \cdot 10^{-7} \tag{4-12}$$
$$x_0 = \begin{bmatrix} 1.0 \\ 0.10 \end{bmatrix} \tag{4-13}$$

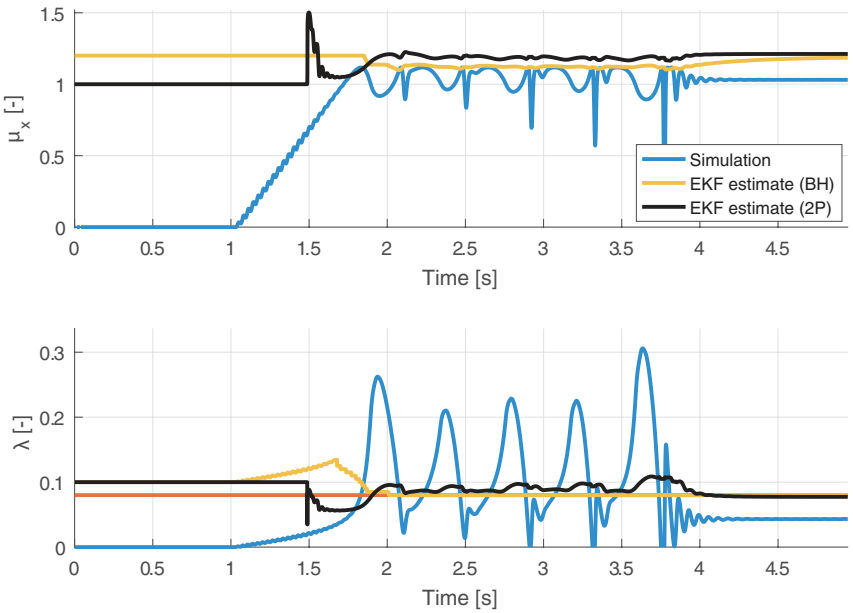

Figure 4-3: Using an EKF to fit both models to simulation data, where 2P is the two-parameter model and BH Burckhardt

Figure 4-3 shows the performance of the EKF when performed on-line for both models. The two-parameter model (2P) is considered first. The top graph clearly shows the initial conditions are maintained up to 1.5 seconds, because the slip does not reach a value higher than 0.02 until then. After this point, the model rapidly adjusts to obtain a more accurate estimate of the friction coefficient peak, but it is still off by 0.07 on average.

When $\hat{\lambda}^*$ is investigated, the filter starts with a very short drop at 1.5s. This is an effect caused by the way the brake actuator is simulated. There are two data points measured in this particular case, whereas the second point is a little lower than the first. The lack of data causes the filter to calculate a peak at that point. It is, however, quickly corrected when more data is put into the EKF.

The method finds the actual optimum accurately. The estimate does show bumps when the system returns to the stable region, but it only goes up to 0.10, and would mainly influence the trigger in phase 1. Force would expectedly be the main trigger in phase 1. A minor variation in $\hat{\lambda}^*$ is as such unlikely to cause false triggering in this mode. Lowering $Q_{2,2}$ leads to a much more stable value of $\hat{\lambda}^*$. The model is however required to adjust itself to another road surface if applicable, yet it should simultaneously be able to deal with noise.

Burckhardt model

The second model that was planned to be used for friction curve estimation was the one described by Burckhardt. Its parameters are not directly linked to the optima of friction and slip, so it is non-trivial to set equivalent initial conditions (eqs. (4-14) to (4-18)). It is assumed that the second parameter varies ten times as much compared to the first; the third

ten times less than the first. There is made use of standard Burckhardt parameters to draw this conclusion.

$$P = \begin{bmatrix} 1 & 0 & 0 \\ 0 & 10 & 0 \\ 0 & 0 & 0.1 \end{bmatrix} \tag{4-14}$$

$$K = I_3 \tag{4-15}$$

$$R = 0.01 \tag{4-16}$$

$$Q = \begin{bmatrix} 1 & 0 & 0 \\ 0 & 10 & 0 \\ 0 & 0 & 1 \end{bmatrix} \cdot 10^{-7} \tag{4-17}$$

$$x_0 = \begin{bmatrix} 1 \\ 20 \\ 0.1 \end{bmatrix} \tag{4-18}$$

Figure 4-3 shows the results for the Burckhardt model as well. The friction estimate is determined to be at 1.9 seconds and remains relatively constant as of that point. The estimate of friction shows that the EKF estimate increases initially. This thus does not cause any false triggering. The EKF finds a correct estimate when the system is at the friction coefficient peak, which is just in time. After this point, the estimate remains stable.

The value for $\hat{\lambda}^*$ shows similar characteristics. It manages to find the optimum well. False triggering based on slip also does not occur, because the optimum estimate is initially higher than the actual one. Lastly, the model shows a constant estimate once it has been found.

Looking at fig. 4-4, it becomes clear the estimation error using the formula by Burckhardt is smaller at all times for both friction and slip, except at the start. The latter is desired, as it prevents false triggering.

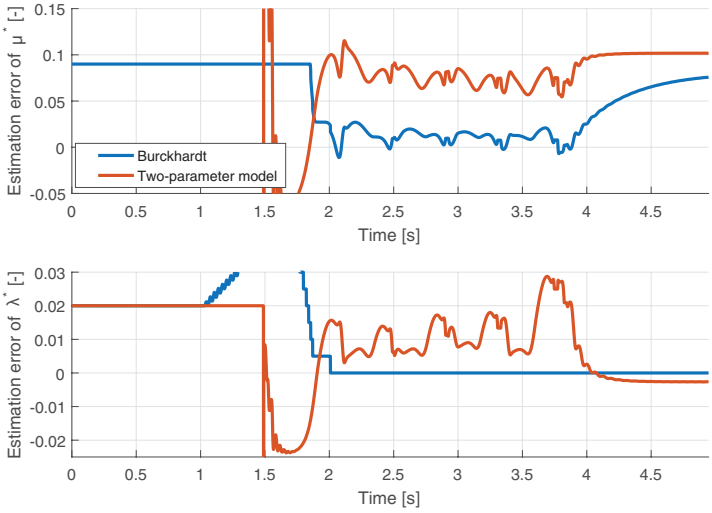

Figure 4-4: Estimation error comparison for two models

Using experimental data

There is also measurement data available from prior to the writing of this thesis. The data is recorded on April 2014 [7]. It is used to find the possible outcome of the EKF in field tests. Force measurements were performed using a VELOS measurement wheel. The performance results of the EKF are visualised in fig. 4-5.

With the two-parameter model, the same effect as before becomes visible, as it calculates that the peak is at a too low value of friction. Noise causes the model to fit the wrong peaks. This could lead to false triggering if the algorithm were to rely fully on the EKF. Aside from this problem, the filter also estimates a too high friction value.

The same problems then naturally occur when the optimal slip value is considered. It takes two cycles before the optimal slip is reasonably estimated, which is too long for an on-line implementation of the model. Preferably, the estimate is accurate before the friction peak is passed. It is furthermore found that the estimate is not as constant as desired.

Using the function by Burckhardt, more promising results are found. The optimal friction coefficient overall intersects with the peaks of the measurement values, which is good. At 9.2 seconds, there is a single measurement peak, but the filter does not directly adjust for it. This peak could be a measurement inaccuracy or the road surface could have been slightly different at that point. Either way, the peak does not influence the estimate significantly.

It is likely to be a measurement inaccuracy. The minimal influence of these few measurements is thus a good sign.

The slip estimate is accurately found, too. As of the moment the correct optimum is estimated, it remains nearly exactly at the same value. This is a desired result, because the road surface did not change during the test.

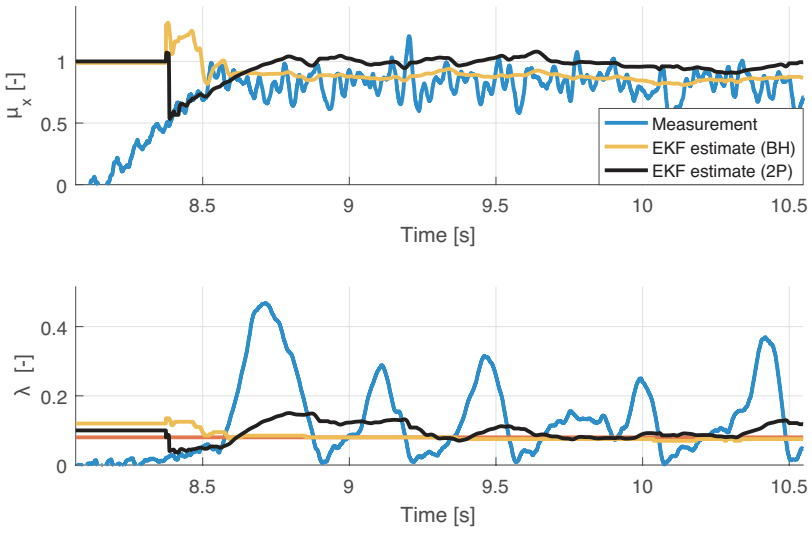

Figure 4-5: Using EKF to fit both models to experimental data recorded April 2014, where 2P is the two-parameter model and BH Burckhardt

Based on the results of simulation and, more importantly, of the experimental data, it is concluded that it is valid to use an EKF in an ABS. The data could serve as a reference for phase switching and can also be used to determine the required optimal brake torque. The form in which the EKF is be applied is based on the Burckhardt model. The two-parameter model is ruled out for the remainder of this thesis, as it performs worse on all currently investigated aspects.

4-4-2 Model performance

It was concluded that an EKF using the Burckhardt model could be a basis for an ABS. In this subsection more specific situations are tested for and there is also looked into the time required to find the optima. More information about how the simulations are performed can be found in chapter 5.

Varying optima

For different road surfaces the optima of friction and slip are different. There is now looked in the performance of the EKF when either of the optima changes.

In the first example, the model is tested with $\lambda^* = 0.15$ and $\mu_x^* = 1.12$. Looking at fig. 4-6, $\hat{\lambda}^*$ is clearly inaccurate and has negative consequences. Because the slip is estimated at 0.10, the controller is triggered to go to phase 1 before an accurate estimate of the friction coefficient peak is determined.

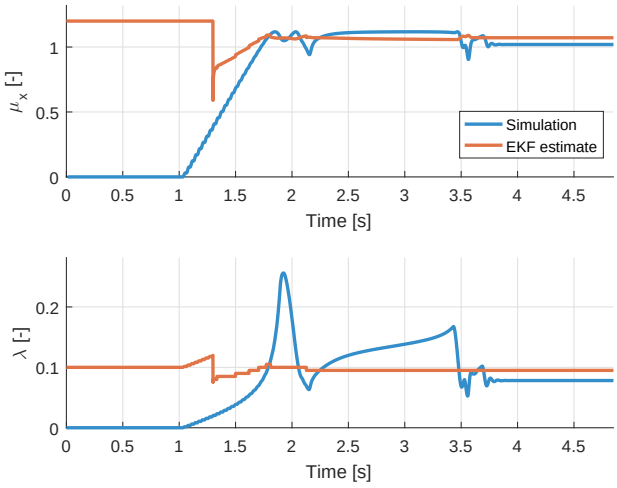

Figure 4-6: EKF results when $\lambda^* = 0.15$ and $\mu_x^* = 1.12$

Recall that the optimum is found through eq. (4-7) and that ε_μ was chosen conservatively. The value clearly has a negative effect on the estimate. If ε_μ is set to zero, the found estimate is exactly 0.15 and the problem as shown in fig. 4-6 would not have occurred. If the simulations of fig. 4-3 are redone with the new ε_μ, the slip estimate would become 0.10 instead of 0.08. That means the controller is triggered slightly faster to return to the unstable region, but it

is unlikely to lead to a problem. From this point onward, $\varepsilon_\mu = 0$, because it leads to more accurate estimates overall.

When varying the slip optimum to higher values such as 0.25, the EKF requires more time to find an accurate estimate. This is caused by the small variation in measured friction values. Consequently, the algorithm has troubles in determining the location of the peak. However, when the slip optimum is high, the accuracy of the estimate becomes less important, because the curve is more flat near its peak. There is thus a wider range of slip values that lead to a near-optimal friction coefficient.

The estimate of the optimal friction coefficient also shows notable behaviour. When μ_x^* is high, the estimate remains approximately the same and shows relatively small deviations throughout the brake manoeuvre. When it is lower, for example 0.60, the estimate is less constant. Even more so when the optimal slip value is 0.08 and tyre relaxation plays a bigger role. The estimate adjusts itself because of it and consequently varies between 0.55 and 0.65, which is a relatively big margin. If the optimal slip value is 0.15, the friction estimate only varies between 0.58 and 0.62.

Time required

Another interesting topic of the EKF is how fast it can estimate the friction curve. To determine when the EKF has sufficient certainty about the road conditions, a plot has been generated that shows normalised values of the diagonal of P (fig. 4-7). By normalised, it is meant that the regular error covariance is divided by its corresponding output value, so $P'_{i,i} = P_{i,i}/x_i$. The behaviour of the friction estimator is exactly as expected. The EKF is enabled at 1.5 seconds. The value of $P'_{1,1}$ is then the first to drop, because it is coupled to the first parameter of the Burckhardt model, which represents the initial slope. The second parameter determines the location of the peak. Indeed, the value of $P'_{2,2}$ decreases next. The last parameter corresponds with the slope after the peak and therefore $P'_{3,3}$ is also the last to decrease.

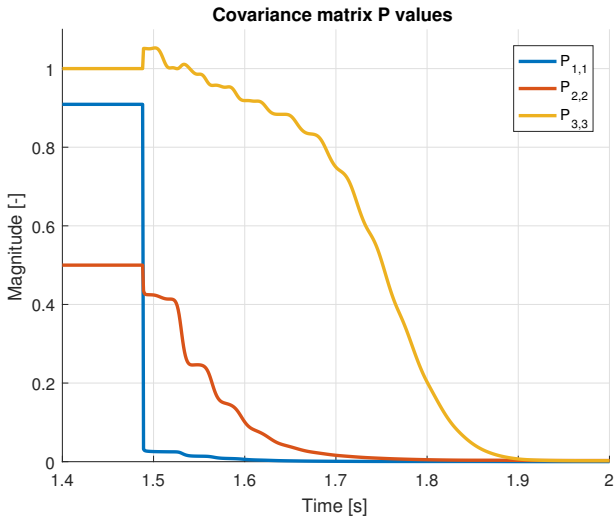

Figure 4-7: Normalised diagonal values of the error covariance matrix when simulating $\lambda^* = 0.08$ and $\mu_x^* = 1.12$

Based on the simulations that have been performed so far, the optima are found only just after the peak has been passed. Zooming in at fig. 4-7, it can be observed that the values on the diagonal of P remain relatively constant as of $t = 1.90$ seconds, which is 0.04 seconds after the peak is passed. Similar delays are found with other road conditions as well. The exact delay is not as important in this specific research project. It does show that a reliable estimate can be made within a short amount of time without the need of going through several cycles first. Looking back at fig. 4-5, it even looks as if the EKF manages to find the optimum even before the peak is passed. Corresponding values of P' are shown in fig. 4-8. From that figure it can be concluded that even though the optimum is found, there is insufficient certainty.

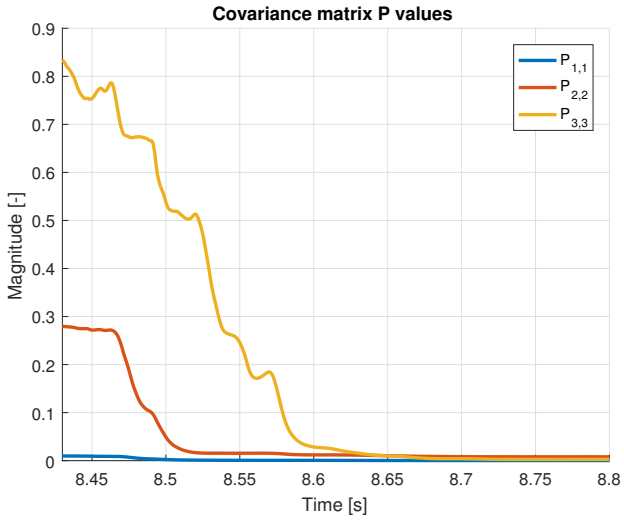

Figure 4-8: Normalised diagonal values of the error covariance matrix when using experimental data from April 2014

4-5 Conclusions

Two friction models have been discussed: Burckhardt and the two-parameter model. Aside from their mathematical expression, they are different in their curve characteristics as well. The two-parameter model has a steeper initial slope, and decreases more rapidly after the peak. It was expected that most of the data would be measured near the peak, so the representation afterwards would not become a problem.

The models are both implemented in an EKF. Each measurement of slip and friction is an input to the EKF and should lead to fitting parameters of both friction models. As such, it should become possible to either predict or more accurately estimate the friction curve, which is required by the designed controller.

Based on the validation study, it can be concluded that the Burckhardt model is overall better than the two-parameter model to implement in an EKF. This conclusion is based on the precision with which both optima are determined, but it is also visibly more constant and varies little when more data points are added.

It was also suggested to use a buffer, such that data points from the initial slope would not be neglected. However, the simulation study has shown that the EKF has sufficient information

when the optimum remains being encircled. Another addition to the EKF is the use of pseudo-data. Every 10 measurements a data point with $\lambda = 1$ and $\mu = 0$ is added to be sure a peak in the estimate is formed.

Experimental data showed even more clearly how the Burckhardt model performed best. The two-parameter model fits to small peaks caused by measurement inaccuracies, which leads to a too low friction coefficient estimate. Consequently, the ABS algorithm would control for values which lie before the actual optimum. The Burckhardt model, on the other hand, starts off by estimating the optima too high, but recovers as soon as the actual peak is near.

The chosen model shows it can find the optimum right after the friction coefficient is passed when using either simulation or experimental data. This conclusion is based on the fact that the values of P' barely decrease any more after that point. The accuracy of the estimate is also validated by looking at the error between the actual and estimated optima.

Chapter 5

Controller assessment in simulation

The fundamentals of ABS control have been discussed and a novel controller was proposed in chapter 3. The design will now be assessed in a number of steps. The first one is to develop a reference: a perfect brake manoeuvre. Though this would be an unrealistic target, it does show a theoretical limit to braking. To subsequently quantitatively express the quality of the controller, performance indicators are denoted in section 5-2.

The controller has so far solely been expressed as a function of a set of parameters, but values are yet to be assigned to them. Section 5-3 lists all required tuning variables with the values used in the validation process.

The simulation study plays the largest role in the testing process. It allows for easier switching of conditions than testing on an actual vehicle. Simulations are performed and their results are discussed in section 5-4.

5-1 The perfect brake manoeuvre

A brake manoeuvre is in this thesis considered perfect if the optimal brake torque is applied as quickly as possible, and, subsequently, retained until the vehicle stands completely still. For this, it is thus assumed the brakes cannot be applied instantly.

Assume braking starts at time instance t_i with a constant increase of brake pressure up to t_b. Then, this pressure is held until t_e. Figure 5-1 shows what this would look like. At F_x^*, the longitudinal force is at its maximum. In the next section, this ideal method of braking is utilised to compare the performance of the ABS algorithm.

There are practical limitations which prevent an algorithm to perform this well in regular driving conditions. The main causes are the uncertainty and variability of road surface characteristics.

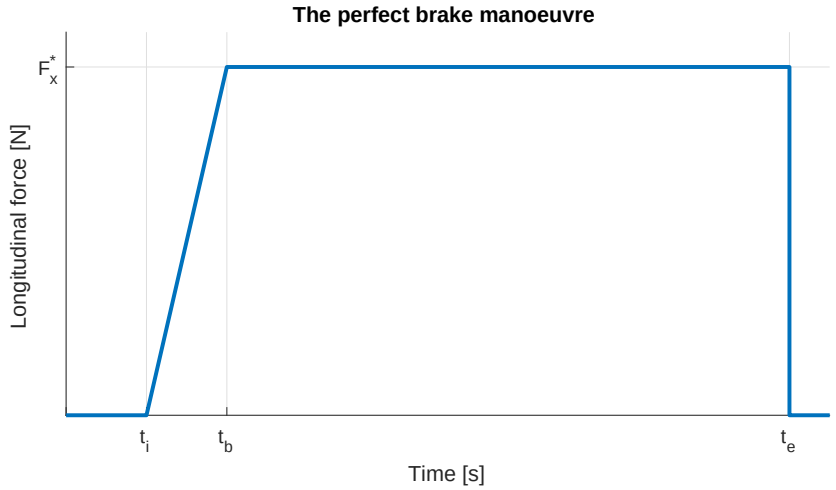

Figure 5-1: Perfect brake manoeuvre

5-2 Indicators

Performance indicators give an insight in how well an algorithm or its parameters perform compared to the ideal situation. Their relevance is elaborated on in this section. The computation of the discussed indicators is explained in appendix C.

- **Brake distance**
  The first indicator is trivial. One of the main goals of ABS is to minimise brake distance, so it is also a measure of performance.

- **Optimum deviation**
  The deviation of the optima of the friction coefficient and wheel slip indicate the controllability of the vehicle. The Root Mean Square Deviation (RMSD) provides useful information. It is a measure of the average absolute deviation of measurements with respect to the optimal situation.

  A value of zero would indicate a perfect brake manoeuvre is achieved. An ABS should thus minimise the RMSD.

- **Cycle frequency**
  The last indicator has to do with practical implementation. One could design an algorithm which encircles the friction coefficient peak with high frequency. Actuator dynamics, however, prevent such a fast method of control.

5-3 Control algorithm tuning

The implemented controller is two-phased. The tuning parameters have only been mentioned there, but their values have not yet been discussed. In table 5-1 all tuning parameters are given in an overview. A brief discussion about their values follows.

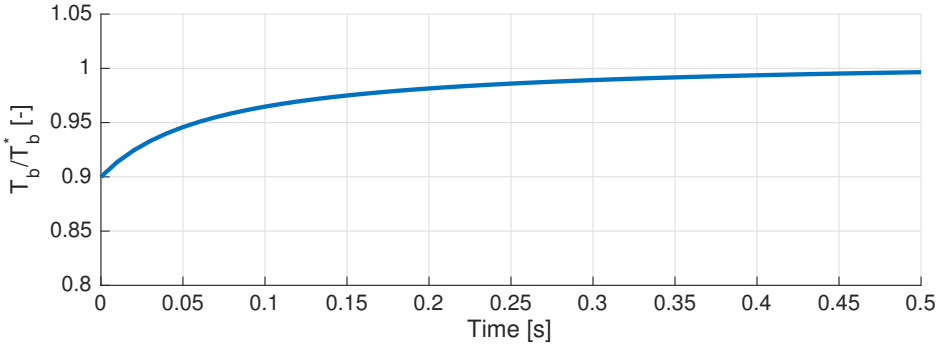

Figure 5-2: Control brake torque compared to estimated optimum over time

The first parameter that is discussed in α_μ, which was introduced in eq. (3-11). It is a safety margin to the estimate that makes sure the algorithm uses an optimal friction coefficient lower than the actual one. A value of 0.90 means there will be controlled for a friction coefficient which is 10% below the estimated optimum. In simulations, it has been observed that the estimated maximum friction coefficient is higher than the actual one most of the times. Consequently, there is chosen for a wide margin of 10%.

With $\alpha_{T_{b,add}}(t_{phs})$ a time-dependant relation for the brake torque was given to ensure a more gently increasing brake torque. Its parameters are, of course, arbitrary, and could be optimised in further research. At this point, it is chosen that $\alpha_{T_b} = 0.11$ and $\alpha_{phs} = 0.07$. This means that the brake torque is increased by 11%. The α_{phs} is a parameter of scale. With this information it is possible to generate fig. 5-2. It shows the increment of brake torque over time. Again, this is only a simple solution to the more fundamental idea of increasing brake torque more slowly over time. The model is not presented as an optimal method to do so. In the section 5-4-1, consequences of rapid changes in brake torque are visualised.

The next parameters that have to be defined are four maximum absolute ($\beta_{(\cdot)}$) deviations from the optima λ^* and μ_x^*. Their specific values are not discussed into too much detail, as their value is arbitrary and based on running simulations. It is, however, possible to give general statements about them.

The parameters are valued in such a way that the difference is measurable. If a friction curve has a small slope on the right side of the friction curve, choosing a small value for the maximum deviation of friction on this side would theoretically be a solution. In practice, measurement noise and inaccuracy disallow to use such small deviations, and the amount of cycles per second should not be too high either. Using data that has been obtained at Valkenburg in April 2014 [7], it seems valid to choose a difference of at least 0.10 with respect to the measured maximum.

Furthermore, the maximum deviations are chosen keeping in mind that the right side of the friction curve is unstable, and undesirable to be on. This is why the margin here is chosen as low as possible. On the left side of the curve, the friction coefficient drops quickly with respect to the slip value, so it is important to not choose too wide margins here either.

Lastly, the EKF has to be enabled according to eq. (4-8). Based on simulation and experimental data (see section 4-4-2), this value is arbitrarily chosen to become 0.20.

Table 5-1: Controller configuration parameters

Symbol	Value	Parameter description
ΔT_b^-	75 Nm	Brake torque lower than the current one (rF_x) for phase 1
v_{min}	16 m/s	Minimal velocity required to exceed the peak of friction.
α_μ	0.90	Safety margin to ensure a stable mode
α_{T_b}	0.11	Extra added fraction of $\hat{T}_b^*$ required to exceed the friction optimum
β_P	0.20	Maximum value of P' to enable the EKF
α_{phs}	0.07	Scaling factor influence of time on the applied brake torque
$\beta_{\mu_{x,l}}$	0.10	Maximum absolute deviation of μ_x from μ_x^* when in stable mode
$\beta_{\mu_{x,r}}$	0.17	Maximum absolute deviation of μ_x from μ_x^* when in unstable mode
$\beta_{\lambda,l}$	0.05	Maximum absolute deviation of λ from λ^* when in stable mode
$\beta_{\lambda,r}$	0.07	Maximum absolute deviation of λ from λ^* when in unstable mode

With parameters defined with the considerations above, it is expected that when the controller is in phase 1 — on the stable side of the curve — the algorithm is most-likely to switch based on force measurements. On this side, the friction coefficient decreases faster than the slip decreases.

5-4 Influences of tyre-road characteristics

The proposed controller is initially tested in a computer simulation. The influence of the maximum friction coefficient and its corresponding wheel slip are first elaborated on. The algorithm is then validated on a set of road surfaces in section 5-4-3. The effects of a road surface change are shown in section 5-4-4. The latter should show how the algorithm can adapt itself to a new situation. Specifically interesting in this part is the performance of the EKF.

5-4-1 Wheel slip

In the first considered case, the optimal friction coefficient is high at low slip. In this simulation $\mu_x^* = 1.12$, and $\lambda^* = 0.08$ are used. Figure 5-3 graphically shows how the controller influences the brake manoeuvre. The bottom graph shows the slip becomes increasingly higher with each cycle. The ABS is enabled at 1.8 seconds.

When a change of brake torque occurs, a quick drop becomes visible in the measurement of friction. An example is indicated by the 1. The drop is visible for multiple times, but only when there is switched to phase 2. At this point, tyre relaxation causes the measured slip value to become near zero, or even lower. This is the moment when the friction coefficient drops for a short amount of time.

The moment as indicated by 2 requires further explanation as well. The algorithm is expected to switch from phase 1 to phase 2, to pass the friction peak. However, it quickly switches an extra time between phases, before going into phase 2 for a longer duration. It is the cause of this switch and is graphically shown in fig. 5-4. Tyre relaxation is more of influence when the

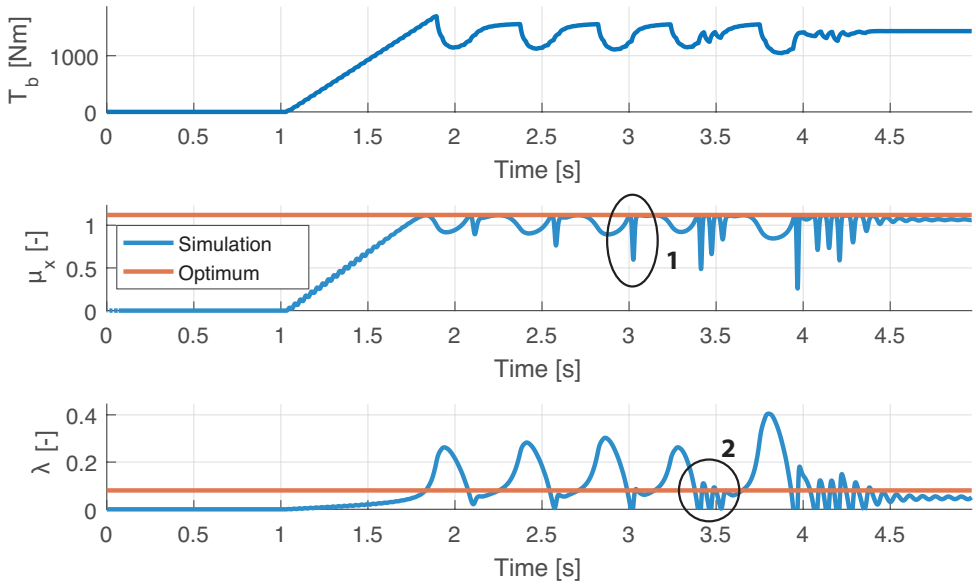

Figure 5-3: ABS performance with $\mu_x^* = 1.12$ and $\lambda^* = 0.08$, a priori knowledge, and no noise

initial slope of the friction curve is steep, because this means that a small variation in slip causes a relatively big change of longitudinal force. A fast variation in force leads to more elastic deformation of the tyre.

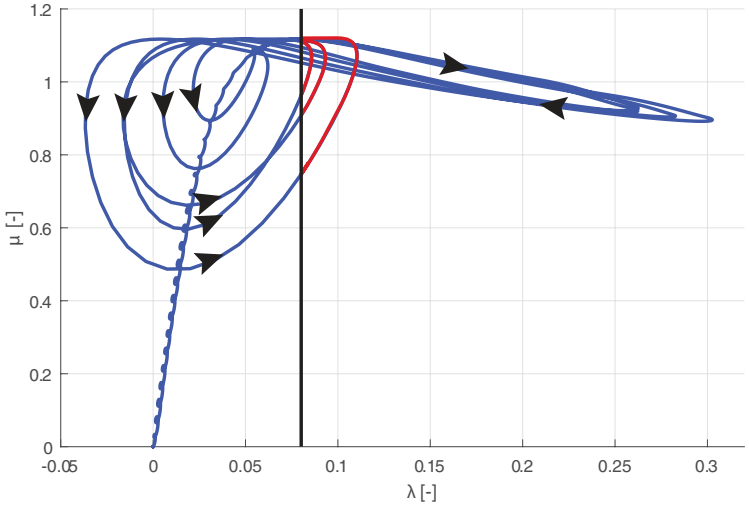

Figure 5-4: Reached friction curve values with $\mu_x^* = 1.12$ and $\lambda^* = 0.08$, a priori knowledge, and no noise

It is furthermore clearly visible that at lower velocities, controlling should be executed conservatively. Looking at 3.7 seconds, the slip value clearly has a higher overshoot, while the brake torque is not applied faster than in the preceding cycles.

To obtain more of an idea of the influence of the value of λ^*, one more comparison is made. Figure 5-5 shows the performance of the algorithm when the optimal friction coefficient is still 1.12. The cause of phase switches now exactly as expected. On the left side of the curve, the phase is updated because of a faster decreasing friction coefficient. While on the right side of the curve, there is switched based on the wheel slip value. The friction curve is scaled over the horizontal axis, so exceeding the peak into the stable region has a smaller impact on the utilised friction coefficient than was shown in the previous test.

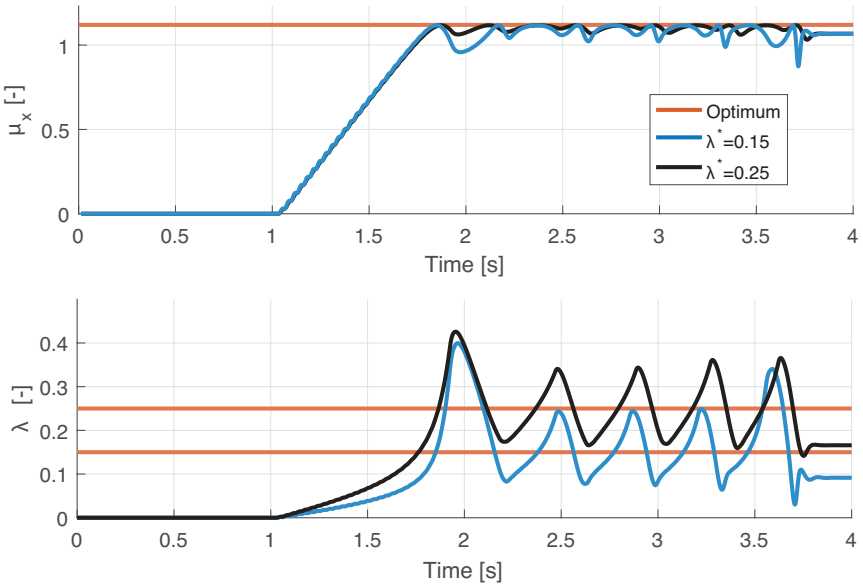

Figure 5-5: ABS performance with $\mu_x^* = 1.12$, $\lambda_1^* = 0.15$, and $\lambda_2^* = 0.25$, with a priori knowledge, and no noise

Tyre relaxation plays a smaller role for higher λ^*. When the system moves from the unstable region into the stable one, the overshoot due to tyre relaxation becomes smaller under these conditions. The EKF then receives data which comes closer to the static mapping by Burckhardt. This has a positive effect on its estimation.

5-4-2 Friction coefficient

When the brake manoeuvre is executed on a road with a lower optimal friction coefficient, the amount of required cycles increases. The frequency

The ABS is enabled earlier if the brake torque is increased at the same pace in every simulation. Figure 5-6 shows the first few cycles of brake manoeuvres where the road surface has different friction coefficient optima. The amount of cycles increases. The frequency of those remains approximately the same.

Another difference is the initial overshoot into the unstable region. It is approximately the same for lower values of μ_x, but is notably lower when the peak lies at 1.12. This can be explained by the friction coefficient dropping more in terms of its absolute value after the peak.

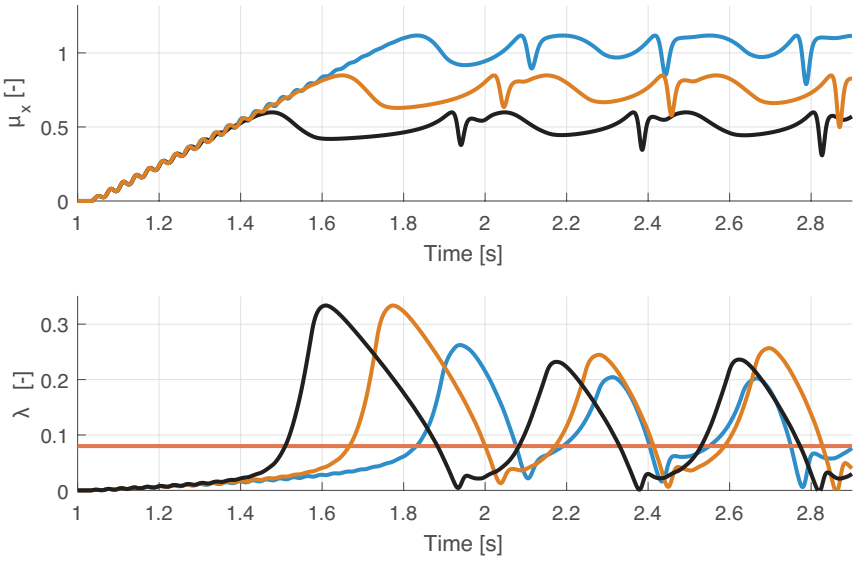

Figure 5-6: ABS performance for three values of μ_x and $\lambda^* = 0.08$, with a priori knowledge, and no noise

5-4-3 Assessment using performance indicators

The table in this subsection shows the results of the simulated. The brake algorithm is validated by varying the optima of wheel slip and friction.

The first two columns of the tables in this subsection show the maximum friction coefficient and its corresponding wheel slip value. When the EKF is disabled, these exact values are used as a reference to the phase switching algorithm. The first indicator is the brake distance. There are three numbers. The first, s^*, is the value which would be found when there is braked perfectly. The second, s_s, stands for the simulation output. These two are used to show the magnitude of the numbers on which the percentages apply. The last is used as a main reference as it shows the percentual difference between the former two columns. The second indicator is the RMSD values for both friction and slip. These are the measurements of friction and slip compared to their optimum as of the moment ABS is enabled. The last column is the number of cycles, which is the number of phase switches divided by two.

The first simulation results that are discussed are when there is no noise and the optima are known. The simulation output is compared to the denoted performance indicators and put into table 5-2.

The optimal slip value is of relatively low influence on the brake distance. A higher friction coefficient, leads to a shorter brake distance. The brake time was determined as well and table D-1

From the RMSD values which are listed in the table, a conclusion that can be drawn is that RMSD_λ value is slightly higher for higher values of λ^*. Such an optimum means that the curve is more flat near the peak, which means the friction coefficient changes less with varying slip. Consequently, the algorithm switches less frequently, causing larger cycles. Note that a road

surface for which it holds that $\mu_x^* = 1.12$ shows the opposite effect: the RMSD_λ decreases with increasing slip. Because a friction coefficient of 1.12 is high, the flattening effect which is used as an explanation does not apply in these specific situations. Furthermore, it is observed that tyre relaxation plays a bigger role when the friction coefficient is this high. Tyre relaxation obviously has a negative effect on minimising the RMSD value of slip.

When the optimal slip value decreases, RMSD_μ decreases. The influence of the optimal friction coefficient on this RMSD value cannot be determined with certainty, but is definitely smaller than that of the value of λ^*. Again, the explanation behind this is the flatness of the curve. When solely investigating longitudinal friction optimisation, only RMSD_μ is relevant and it can be concluded that the algorithm performs better when the optimal slip value is higher.

The cycling frequency is not significantly influenced by either μ_x^* or λ^*. At all times, the frequency remains near 0.7 cycles per second.

Table 5-2: Simulation results when optima are known

μ_x^*	λ^*	s^*	s_s	s_{diff}	RMSD_μ	RMSD_λ	Cycling frequency
1.12	0.08	88.1	94.2	**6.9%**	0.14	0.10	0.7
0.85	0.08	107.8	118.0	**9.5%**	0.13	0.09	0.7
0.60	0.08	144.3	161.8	**12.1%**	0.10	0.08	0.6
1.12	0.15	88.2	91.3	**3.5%**	0.06	0.08	0.7
0.85	0.15	107.9	112.6	**4.4%**	0.05	0.08	0.8
0.60	0.15	144.4	154.8	**7.2%**	0.06	0.09	0.8
1.12	0.25	88.4	90.2	**2.1%**	0.04	0.07	0.7
0.85	0.25	108.1	111.0	**2.7%**	0.03	0.10	0.8
0.60	0.25	144.5	151.9	**5.1%**	0.04	0.12	0.8

If the output of the EKF is used as a reference, similar results as before are obtained. On average the algorithm with EKF enabled requires the same time to brake. In some cases, the car stops even faster. This is not necessarily a good sign, because in these particular cases the optima are estimated too conservatively, causing the system to remain longer in its stable region. Remaining longer in this region is not necessarily a problem, but the fact that the system becomes more efficient when the estimate is not accurate enough is an unforeseen positive coincident.

The patterns between changing optima and their corresponding performance indicators that were described before, still hold with the EKF enabled. The fact that the results are very similar is a good sign. It indicates that extending ABS with an EKF is viable. Specific numbers for the performed simulations with EKF can be found in table D-2.

The effect of noise

By adding noise to the data, a better idea of the robustness of the algorithm is obtained. The same tests as before are executed again, but now with added sensor noise. With respect

to the previous tests, the first notable difference is an increase in time and distance required for every brake manoeuvre. Other than different absolute values, the same characteristics as observed before are still visible.

Large differences are mainly found when $\mu_x^* = 0.60$. The magnitude of the noise added to the signal at this point is relatively big. When the EKF is used to fit measurements to a curve, it tends to fit it more to measurement noise.

The EKF should also be able to cope with noise and manage to find an accurate estimate. All the simulations are run again, but now with the output of the EKF as a reference to the controller. The results are, again, similar to the ones found before. When comparing these results to the previous simulations with perfect estimation, the time difference on average is approximately the same.

The average cycling frequency has changed after the addition of noise. It is now 0.9 on average, independent of whether the EKF is used.

The quantitative outcomes of the noisy simulations can be found in appendix D. It contains tables of the model output with and without the EKF used as a main reference.

5-4-4 Changing road surface

A primary goal of the proposed ABS is that it is able to adapt itself to new circumstances. The EKF could serve for this purpose. Two tests will now be discussed to see how the controller performs when the road surface changes. In each test, there is switched to new conditions at time instance $t = 2.5$ seconds. Four more cases are omitted for the sake of brevity, but their results can be found in appendix E. The most realistic scenarios are discussed in the following cases.

Case 1: μ_x^* changes from 0.85 to 1.12, λ^* changes from 0.15 to 0.08

The change that occurs in this particular case is the same as switching from the dry asphalt road from experimental data of April 2014 [7] to a wet one according to Burckhardt. The risk in this specific case is that there is controlled for a suboptimal brake torque.

Similar patterns as were shown before when the optima were isolated are found (fig. 5-7). The friction coefficient estimate is corrected within a reasonable amount of time. The slip optimum changed as well, leading to a steeper initial slope of the friction coefficient curve.

The slip optimum is corrected only slowly. In this case it does become more accurate in the end. This can be explained by the simultaneously increasing friction coefficient. A peak will then more clearly form at this new slip optimum. With a bigger difference, the correcting factor of the EKF increases as well.

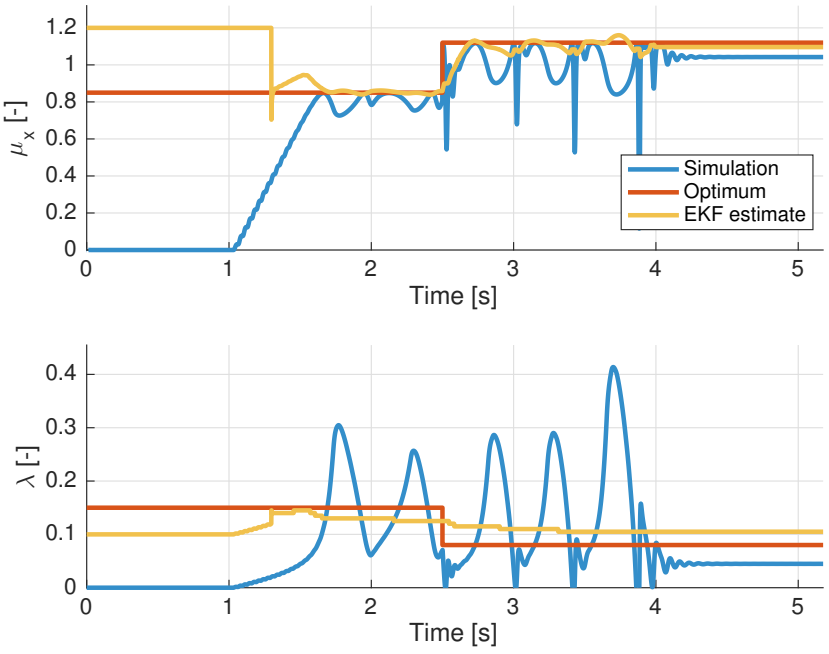

Figure 5-7: ABS results when the road surface changes: μ_x^* changes from 0.85 to 1.12, λ^* changes from 0.15 to 0.08

Case 2: μ_x^* changes from 1.12 to 0.85, λ^* changes from 0.08 to 0.15

The last considered case could cause wheel lock if the estimate of the optimal friction coefficient remains the same. The results as shown in fig. 5-8 show that the EKF manages to correct the friction optimum well. The slip optimum estimate, on the other hand, barely changes.

Though the slip optimum estimate is relatively inaccurate, the behaviour of the controller still leads to a stable brake manoeuvre. Not only is the ABS stable, but it also manages to control for a state close to the friction coefficient peak. The top plot shows the measured friction coefficient stays close to the EKF estimate and actual optimum.

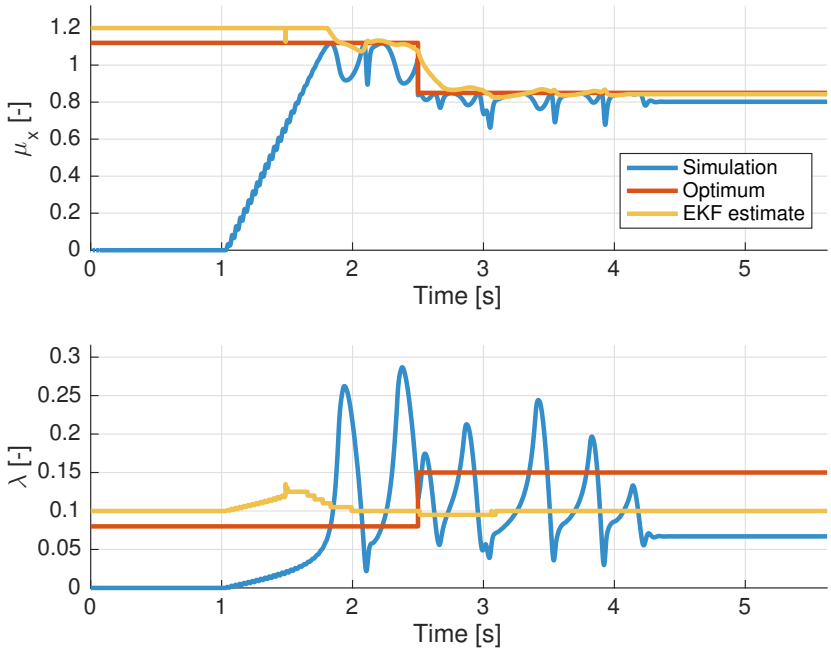

Figure 5-8: ABS results when the road surface changes: μ_x^* changes from 1.12 to 0.85, λ^* changes from 0.08 to 0.15

5-5 Conclusions

The first tests that were performed made use of a simulation model. All were compared to performance indicators of a perfect brake manoeuvre. These were: brake distance and time, optimum deviation, and the number of cycles.

Individual influence of the optima

The force and slip-based ABS was first researched in a simulation study. There was looked into how either of those optima influenced the performance of the controller with general statements. The corresponding conclusions concerning the wheel slip are as follows:

- Tyre-relaxation at low λ^* triggers the controller to switch phases based on slip instead of forces on the left side of the friction coefficient optimum.

- Tyre-relaxation may cause false triggering, but so far this has not led to unstable controller behaviour.
- The effects of tyre relaxation decrease with higher λ^*.
- At lower velocities $\dot{\lambda}$ becomes of such magnitudes that it is better to control conservatively.

Subsequently, the influence of the optimal friction value was investigated. The conclusions are listed below.

- The initial overshoot increases for lower values of μ_x^*.
- The magnitude of the friction coefficient barely influences the number of cycles per second.
- A road which is characterised by a lower optimal friction coefficient peak leads to a longer required brake distance and time.

Indication of the ABS and EKF performance
With more information about how the optima influenced the controller behaviour, various combinations of low and high optima of slip and friction coefficient were investigated. They were compared to the perfect brake manoeuvre as defined before. These tests were even more extensive, as the performance was also compared to situations with or without the EKF enabled, and with or without added sensor noise. Four series of simulations were therefore performed.

In the end, the following conclusions can be drawn:

- Lower λ^* cause a relatively longer brake distance with respect to perfect braking.
- Lower λ^* leads to a higher number of cycles.
- RMSD_μ decreases with higher λ^*.
- RMSD_λ initially slightly decreases with increasing λ^*, but shows an increase when λ^* has become 0.25.
- The number of cycles is independent of either μ_x^* or $\lambda*$, but does increase after the addition of noise.

Directly related to the EKF, the statements below can be made.

- For $\lambda^* = 0.08$, the EKF tends to estimate it higher.
- For $\lambda^* = 0.25$, the EKF tends to estimate it lower.
- The ABS, using the output of the EKF as a reference, on average does not perform notably worse in the performed simulations.

- RMSD_{μ} decreases for higher λ^*.
- RMSD_{λ} increases for higher λ^*.

By adding noise relative deviations from the optimal brake distance and the obtained are increased. However, the patterns that could be found in the previous experiments are still visible.

Changing road surface
The last series of simulations that were executed concerned the adaptability of the EKF. It was investigated how a road surface change influenced the controller references.

- The EKF barely corrects for an increase of slip optimum.
- The EKF slowly corrects for a decrease of the slip optimum.
- The EKF corrects a decrease of the optimal friction coefficient faster than an increase. Either way the correction is fast enough to keep a regular and stable braking pattern.
- If the optimal friction coefficient increases and slip optimum decreases or vice versa, the EKF corrects the estimates slightly faster than when only one optimum changes. These are also more realistic scenarios.

Chapter 6

Controller validation in field tests

The main target of the field tests is to show the potential benefits of force measurements for ABS braking. The goals of testing in a real vehicle are therefore, firstly, to show the benefits of phase triggering based on force and slip data. The second goal is to show the validity of using an EKF on-line to potentially use as control reference.

The experimental set-up is discussed first in section 6-1. Section 6-2 describes how the algorithm is implemented. The following two subsections elaborate on slip-based braking, and combined force and slip-based braking, respectively.

6-1 Experimental set-up

The experiments that have been performed took place at the former Valkenburg Naval Air Base in the Netherlands. The area was reserved for two days. Both of them were dry and sunny days. More specifically, it was 32 degrees Celsius on the first day and 24 on the second.

The area used for testing consists of a straight road with smooth bumps in it. When driving approximately 80 km/h, aggressive braking manoeuvre is initialised (see fig. 6-1a) to cause the algorithm to take over control.

A BMW 5 series built in 2009 is used for experimental validation (see fig. 6-1b). Several notes are made to provide an overview of the available technology in the vehicle:

- Custom hardware and a dSPACE environment enables the control of brake pressure of all wheels.
- A control panel in ControlDesk allows for adjusting constants in the uploaded Simulink model.
- A VELOS sensor fitted to the right front wheel determines both forces and moments in x, y, and z.

- A dual GPS sensor by Racelogic on the roof provides data of the vehicle velocity.
- Two action cameras are mounted to capture brake manoeuvres on video.

Vehicle velocity is required to determine the slip value. In regular consumer cars, a dual GPS sensor is not available, and even if they would, the sensor does not work in tunnels. In practice and in other investigations, alternative methods are used. An example of how this can be done is by the use of observers [17]. Their usability nor accuracy is a topic of investigation within this project.

During the experiments, only the front wheels were used for braking. Taking the rear wheels into account is a next step within ABS braking, because it requires to consider more dynamical behaviour. If the rear wheels lock, the yaw tends to increase, which then leads to an unstable brake manoeuvre.

(a) Wheel slip during brake test

(b) The car used for experimental validation

Figure 6-1: Photos during field tests

6-2 Implementation

This subsection describes the practical implementation of the model in the testing vehicle. Only the differences with respect to the model built for simulation purposes are discussed.

Brake torque
Equations (3-6) and (3-11) denoted the brake torques that would be used in both phases of the controller. These are dependant on force measurements. Though the car is equipped with a VELOS wheel, its output is not used as a reference for brake torque. The measurement values change too fast to reliably use within the reference of brake torque.

Instead of using a dynamical equation for the lower brake torque, a single static value was used, which is denoted in eq. (6-1). This value could be changed via ControlDesk during the testing procedure. When the road characteristics were known with higher certainty, the value of T_b^- could be increased to allow for faster encirclement of the friction coefficient peak.

The higher brake torque, which is used in phase 2, was determined with a time-dependant formula. The function as described by eq. (6-2) results in a stepwise increase of the brake torque starting from $T_{b,init}$. In this equation t_{phs} is a timer which is reset to zero when the

phase is updated. Parameter t_{step} is the duration before the next step in brake torque increase occurs. Lastly, $\Delta T_{b,step}$ is the magnitude of this change.

$$T_b^- = T_{b,init}^- \tag{6-1}$$

$$T_b^+(t_{phs}) = T_{b,init}^+ + \left\lfloor \frac{t_{phs}}{t_{step}} \right\rfloor \Delta T_{b,step} \tag{6-2}$$

The brake torque reference value was subsequently converted into the demanded brake pressure. A static relationship was experimentally found, which resulted in adding a gain of 1/30 after the brake torque reference.

EKF
During simulations, the EKF started gathering data as soon as the wheel slip exceeded a certain threshold of slip. The model is implemented differently in the car. The software also provides information about the user input. It was decided that the EKF would gather data while the user is still braking and reset as soon as the brake pedal is released. To obtain a specific value for this threshold, experiments were performed to determine the magnitude of noise. The minimal brake pressure to continue gathering data was as such determined at 10 bar. The predictor is also reset if $v < 2$ m/s.

6-3 Slip-based braking

To eventually test the full force and slip-based ABS algorithm, there is started with a basic ABS. A slip-based ABS algorithm is chosen for this, because it could easily and reliably be implemented in the test vehicle. Such a basic algorithm allowed for initial road surface characteristics analysis and it could, later on, already provide insight in when and whether the controller would trigger based on friction. Force measurements were thus excluded from the triggers. Before these experiments, an initial guess of the slip optimum is determined by increasing the brake pressure stepwise. In the discussion below, there is looked into the behaviour by the front right wheel, because it is the only one of which load data is captured.

To make sure the ABS would become active when the brake pedal is pressed hard, an extra trigger is added specifically for phase 0 — pre-ABS. If $\lambda > 0.10$, the ABS would be enabled and the system would send triggers according to a predetermined set of offsets from the optimum.

Figure 6-2 shows results of the front right wheel when the basic slip-based ABS is used with $v(0) = 23$ m/s. The ABS is clearly enabled at 13.0 seconds to decrease the brake pressure. This is exactly as programmed, as a trigger is set at $\lambda = 0.10$. A stepwise increment of brake torque is subsequently visible when there is switched from phase 1 to 2 at 14.2 seconds.

After phase 0, the controller is set to trigger at slip values of 0.02 and 0.13. The figure confirms that the slip value indeed decreases after 0.13 is passed. The last peak exceeds this value more, which is explained by the lower vehicle velocity and increased frequency of dynamics. A delay in the decrease of brake torque has a larger impact on the increase of wheel slip.

6-3-1 Friction estimation

The information acquired during the experiment allows for the determination of the slip and friction optima. Since the friction optimum is relatively slowly exceeded, the effects of tyre relaxation are reduced. The first method to find the optima is to approximate them visually using fig. 6-2. When the optimal value has exceeded the optimum, it should show signs of an exponential increase. As such the optimal slip value is estimated to be 0.08; the maximum friction coefficient 1.0.

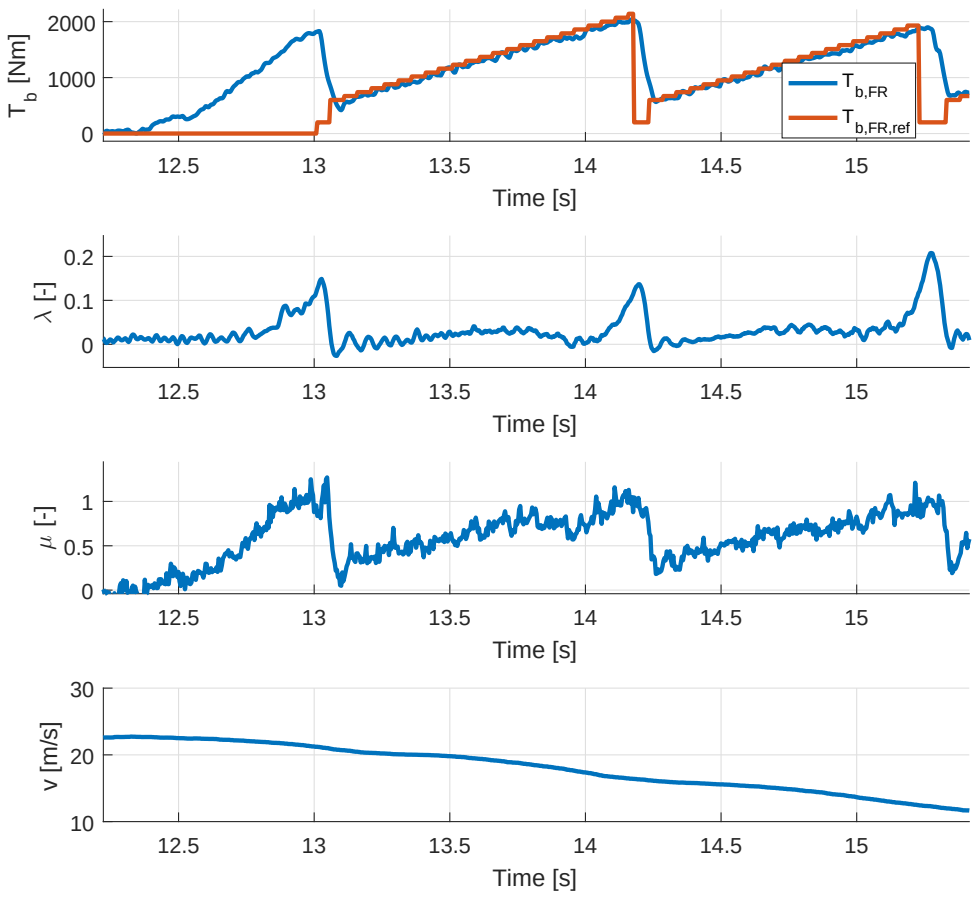

Figure 6-2: Experimentally tested slip-based ABS

The EKF should be able to determine these optima as well. In the previous section, it was denoted that the EKF would be enabled if the driver applies a brake pressure of at least 10 bar. Figure 6-3 shows the estimates as found by the EKF. In the top graph, the friction optimum initially drops, but it is corrected while more data is being gathered. If the proposed controller would trigger based on the EKF estimate, it would not falsely trigger, because it also checks the values on the diagonal of the normalised matrix P'. The threshold for this P' should be determined practically. Looking at the data, 0.1 is a valid boundary.

The slip optimum as found by the EKF is different from the visually determined optimum. It is hard to tell which is closest to the real one because of the measurement noise.

Looking at the value of P', notable behaviour occurs. The decrease of the values on the diagonal of P' is different compared to before. In the previous examples concerning the EKF, it was found that first $P'_{1,1}$ would decrease, then $P'_{2,2}$, and lastly $P'_{3,3}$. In this test, it can be seen that $P'_{2,2}$ is the last one to decrease. This implies that the location of the peak remains relatively uncertain for a longer period of time. It must be noted that if no pseudo-data is added ($\lambda = 1$ and $\mu_x = 0$), this does not happen.

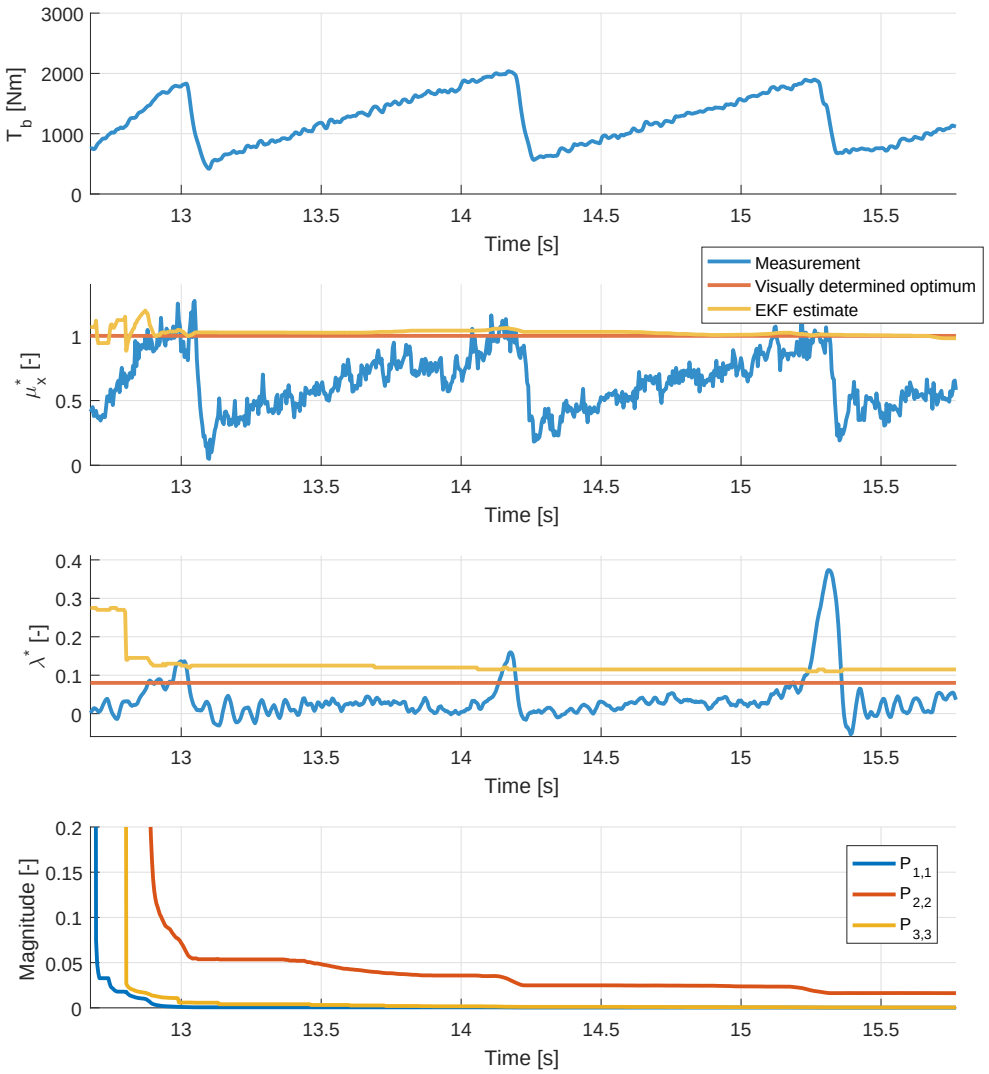

Figure 6-3: Experimentally tested slip-based ABS with EKF estimates

The measurements are now displayed differently. By plotting the friction coefficient as a function of slip, road surface characteristics should become visible in the form of a curve. The measurements are shown this way in fig. 6-4. Considering only these sensor data, it is not evident where the optima were.

Visually, one could say the optimal friction coefficient is approximately 1.0. The optimal slip value is harder to determine this way, because of the flatness of the curve. The EKF calculates an estimate as shown in the figure. Given the data, this appears to be a good fit. The initial slope could actually have been steeper, though. This would have led to an optimal slip value of for example 0.08. The combination of noisy data, a low optimal slip value, and a small decreasing slope after the optimum makes it particularly difficult to determine the ideal slip value with a small relative error. Still, absolutely speaking, the estimate in this experiment is only off by 0.04 at most. Looking at other data sets as well led to the conclusion that $\hat{\lambda}^*$ is about 0.10.

Observing fig. 6-3 more closely, the EKF even managed to find the optima before it was actually passed. However, it cannot be concluded that it can reliably do so before the system has been in the unstable region. The value of $P'_{2,2}$ is clearly still decreasing quite rapidly before 13.0 seconds. At this time instance, the optimum is briefly exceeded.

During the experiments and simulations, the slip estimate of the EKF is not once found lower than actual one. Keeping in mind that the proposed algorithm also takes the friction measurement into account, the problem becomes only small. On the stable side of the friction curve, the value of the friction coefficient is intended to trigger the algorithm. A lower estimate of slip could lead to triggering before the optimum is actually passed, whereas a higher one generally means the state of the system is slightly longer unstable. When determining $\beta_{\lambda,l}$, this can be taken into account to resolve the issue entirely.

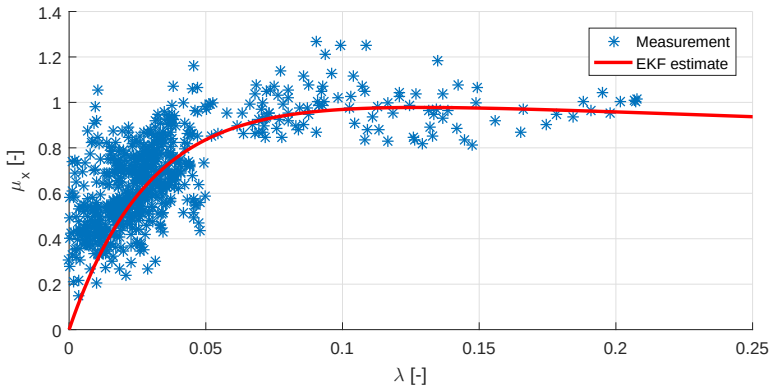

Figure 6-4: Friction and slip measurements slip-based ABS experiment

The effects of tyre relaxation are also hard to distinguish from the noise in fig. 6-4. Simulations showed that tyre relaxation caused the measurement of high friction values at low optimal slip, but this did not happen in the experiments performed with the car. Because it was quite warm outside, it was expected the tyres would show notable elastic behaviour. The absence of this can be explained by how T_b^+ is determined. Whereas in simulations the brake torque rapidly changed going from phase 1 to 2, in these experiments this occurred in about thrice the amount of time.

6-3-2 Slip and friction-based triggering

The phases in the slip-based ABS were only triggered based on the slip value. The next step is to trigger based on the friction coefficient as well. The same experiment as before is executed, but now there is looked into whether the controller would have triggered based on the measured friction coefficient. Do note that actual triggering using these data is not yet enabled.

In the bottom graph of fig. 6-5 the ABS phases are shown. The red vertical line indicates the friction conditions would have triggered a phase switch first. The black vertical line means the slip value is the first to meet its trigger conditions.

The same triggers as were used in the default simulation have been applied to this data as well. The results are exactly as expected: in phase 1, the algorithm first triggers to phase 2 based on the friction value. If the system is in phase 2, the slip value is the first trigger.

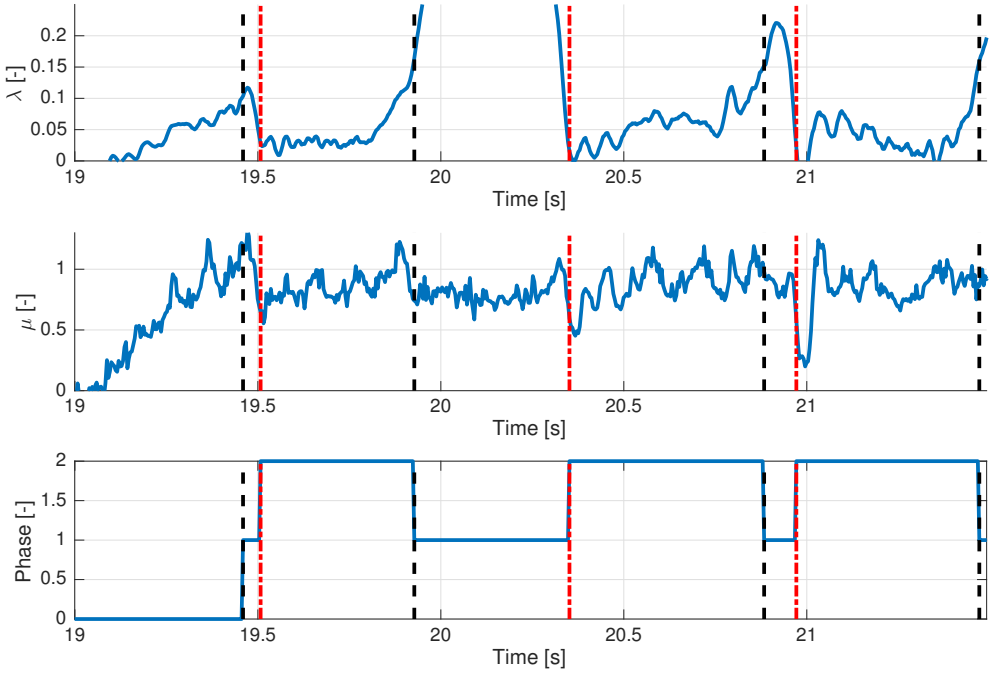

Figure 6-5: First phase switch trigger on slip-based ABS: red = friction, black = slip

6-4 Combined force and slip-based braking

The information obtained when slip-based braking is used provides insight in whether the force and slip-based braking algorithm could work in the test vehicle. The validity of using an EKF with the experimental set-up was discussed in section 6-3. One more experiment has been conducted and is meant to show the EKF output can be used as a main reference for the controller.

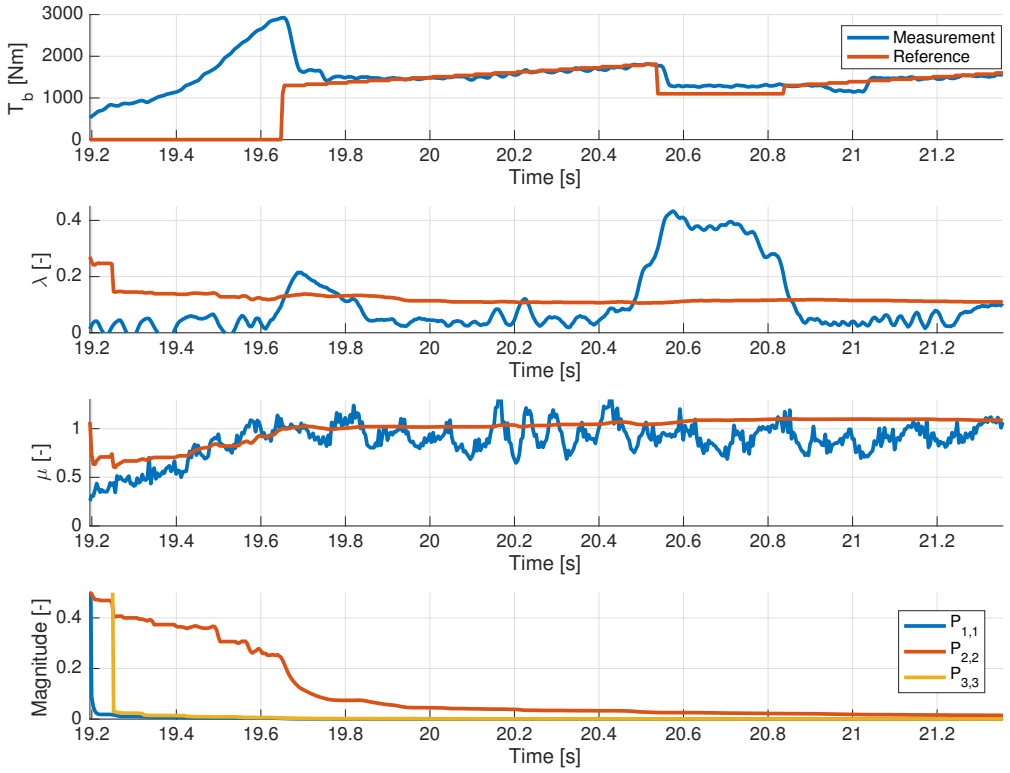

Figure 6-6: On-line estimates of the EKF

Figure 6-6 shows the estimates the EKF determined on-line. The predictor clearly managed to find optima that are close to the actual ones. The results are promising for the use of an EKF as an on-line reference. By enabling the predictor as a reference if $\bar{P}' < 0.1$, early phase triggering will not occur with the incorrect $\hat{\mu}_x^*$ when $t < 18.05$ seconds.

6-5 Conclusions

Experiments using a BMW 5 series are executed on two dry days at the former Valkenburg Naval Air Base. The vehicle is equipped with hardware and software that enables the control of brake pressure through ControlDesk. A VELOS wheel and dual GPS sensor provide information about forces and vehicle velocity, respectively.

Two ABS algorithms are implemented in the BMW: one slip-based and one that also takes the friction coefficient into account. Using only the first algorithm it is possible to gather important data about the road surface. An indication of the validity of using an EKF and a friction-based ABS is also made.

Optima of friction and slip are approximated both visually and through an EKF. It is found that $\hat{\mu}_x^* = 1.0$ and $\hat{\lambda}^* = 0.10$. The EKF manages to find this optimum even before it is actually reached, but it cannot be concluded that it can reliably do so before the system has been in the unstable region.

In the simulation study, this combination shows clear effects of tyre relaxation. During the practical experiments these are found either negligible or indistinguishable from noise. A probable cause for its minimal effect is the small change of brake torque when going from phase 1 to 2 with respect to the simulation study.

When slip is the only trigger to a next phase, it can be shown that measurements of the friction coefficient causes a trigger sooner when going to the stable side of the curve. Consequently, there is proceeded to implementing the controller using friction and slip.

The force and slip-based controller, indeed, triggers sooner on the stable side of the curve. Eventually, this means that the system can stay closer to the friction optimum when both measurement values can cause a trigger. The EKF is implemented as a last experiment. Though the predictor is not used as main reference for the controller, it does output on-line results of the EKF. The estimates it determines from the gathered data lead to the conclusion that using an EKF to use as control reference is viable for the tested road surface in a real car.

Chapter 7

Conclusions

This thesis presents the design of a novel ABS algorithm based on wheel force and slip data. Physical behaviour of the vehicle is analysed using a Simulink model, which consists of a quarter car model, Delft-Tyre, simplified actuator dynamics, and (optional) sensor noise. The simulation model is found sufficient for initial testing of dynamic vehicle behaviour, as relevant characteristics found in the simulation study are consistent with the ones found in field tests.

In the simulation, tyre-road contact is determined by the Delft-Tyre model, which takes tyre relaxation into account. To investigate tyre-road contact more generally, a simpler model is used. This is a function that expresses a relation between the friction coefficient and wheel slip. Its tuning parameters are based on data of wheel forces and slip. The resulting function can be visualised as an asymmetrical curve with a single peak. A steep slope on the stable (left) side and a smaller negative slope on the unstable (right) side characterise the curve. These properties lead to the hypothesis that passing the friction coefficient peak to the right side can be measured more reliably using wheel slip data than using wheel load measurements, and vice versa when determining whether the peak is passed to the left side.

The designed ABS algorithm results in encirclement of the friction coefficient peak. It is based on two phases: one ensures a decreasing wheel slip, another guarantees an increasing wheel slip. The control algorithm depends on references that describe the optimal friction coefficient and wheel slip. The maximum friction coefficient and its corresponding wheel slip value are considered the optima. Triggering occurs based on deviations of the measurement values with respect to these optima. The output of the controller, a brake torque reference, is based on this information, and prevents the wheels from locking.

Both the simulation study as well as field tests confirm that the combination of wheel force and slip data is of beneficial value to determine whether the friction coefficient peak is passed. Measurements containing noise still consistently lead to triggering in the hypothesised manner.

Results from the simulation study furthermore show that the cycling frequency with the designed ABS algorithm is independent of the tested road surfaces. The richness of the measurement data is therefore equal on these surfaces. When the optimal slip value on a road

surface is lower, this has a negative effect on the brake distance, and on the RMSD value of the friction coefficient compared to its maximum.

The necessary inputs for the control algorithm are the optima of the friction coefficient and wheel slip. The combination of wheel force and slip data allows for on-line friction estimation as well. An EKF is used for this purpose. The EKF uses the static mapping as described by Burckhardt to fit the measurement data to. Since this function is static, tyre relaxation dynamics negatively influence the friction estimator accuracy. The influence of this dynamic effect can be reduced by braking less aggressively. The effect is furthermore less significant when the maximum friction coefficient corresponds with a higher value of wheel slip. To retain a reliable estimate of the curve by the EKF, the system must be sufficiently excited. The system is sufficiently excited when data is measured on both sides of the peak.

The simulation study shows that using the friction estimator as reference for the designed controller does not result in significantly deviating performance of the designed ABS algorithm compared to when the optima are known a priori. This is a promising result for the practical application of the algorithm, since in reality the optima are not known a priori either.

The formula by Burckhardt is computationally lightweight, which allows the EKF to be tested on-line during field tests as well. Sufficiently accurate estimates to be used as reference for the designed ABS controller are determined while braking. Both in simulations and in field tests, the estimate of the friction coefficient is relatively more accurate than of that of the wheel slip. The wheel slip is generally approximated higher than the actual optimum. Its accuracy is however still sufficient to use for slip-based triggering on the right side of the friction coefficient curve peak. The estimation error is found 0.05 at most, which has minimal impact on the controller. It must be noted that the estimate of the wheel slip optimum is merely used for triggering, whereas, in simulations, the estimate of the maximum friction coefficient is also used to determine the brake torque.

It is found in the simulation study that there is a possibility no peak is formed in the estimated friction coefficient curve when insufficient data is measured on the right side of the peak. The addition of pseudo-data at $\lambda = 1$ with $\mu_x = 0$ ensures a peak forms in the estimated curve. By adding more pseudo-data, the estimate of the optimum of wheel slip decreases.

Simulations show that the EKF adjusts its estimated maximum friction coefficient when the road surface has changed from dry to wet asphalt or vice versa. It does so when the peak is passed once more. This is a promising result, as the time the friction estimator requires to adapt itself should be minimal. The friction estimator does not manage to adapt the wheel slip optimum to the new road surface.

Whether the friction estimator returns reliable data can be determined based on values of the normalised error covariance matrix. In the algorithm as presented in this thesis, the average of the values on the diagonal of this matrix has to be lower than a specified threshold. In simulation tests and during field tests, this condition is met right after exceeding the friction coefficient peak for the first time. This means that the peak must be exceeded.

A simulated road surface change shows the reliability condition is found only helpful for the initial estimate. The average of values on the diagonal of the normalised measurement covariance matrix does not exceed the threshold again when road characteristics have changed. Though the algorithm in simulation does show it adjusts the estimated friction coefficient peak, no notable sign of it is found in the values of the covariance matrix.

Recommendations

A proof of concept has been described so far. This thesis can function as a basis for future research within the topic of ABS. A set of recommendations is listed below.

- *Use load sensing bearings to determine forces.*
  Experiments executed in this thesis made use of a VELOS wheel, as force information is required. It is expected that load sensing bearings could provide more accurate results. Consequently, the friction coefficient peak could be encircled more tightly. Moreover, it is more realistic that these would be used in consumer cars in the future.

- *Improve how the reference brake torque is determined.*
  The formula for T_b^+ was determined with the idea of more slowly exceeding the friction coefficient peak. How its parameters or the equation as a whole should be to apply the optimal brake torque requires more research. A suggested method is to also take the determined road surface into account. For example, if it is detected that a car drives on a road with a maximum friction coefficient of 1.2 and there is no road on which a higher one could be achieved, there is no need to exceed this peak.

- *Optimise phase switching parameters.*
  This thesis did not focus on optimising the maximum deviations of λ and μ_x with respect to their optima. More experimental testing could provide more insight in how tightly the friction optimum can be encircled. Of course, this also depends on how accurate the measurements are.

- *Add extra safety measures to prevent false triggering based on measurement noise.*
  A safety check is already implemented in the current algorithm, as it checks whether the system is before or after the friction coefficient peak. However, consider the scenario in which the system has just gone into the stable region and measurement noise causes a force-based trigger. The brake pressure will increase again and the system will become unstable again. This is not necessarily a problem, but it would be safer for it to be in the stable region for longer.

- *Determine when the EKF output can be used as on-line reference.*
  For now, normalised values of the error covariance matrix have been used to determine whether the EKF output was reliable enough to be used as main reference for the controller. This has worked so far, but in future work a better test or a method to indicate a more optimal value of β_P could be found. A suggestion is to run another EKF which is reset every phase. If its results deviate too much from the one functioning as controller reference, it indicates the estimates have become unreliable. Alternatively, there could be looked at the values in P of this secondary EKF. If the decrease of those values is too slow, then this is also an indication of uncertainty.

- *Take tyre relaxation into account in the EKF.*
  The EKF is now based on the formula by Burckhardt, but it does not take tyre relaxation into account. If it would, then if the slip optimum is very low, the effect would not have a negative impact on the estimates.

- *Improve performance of the EKF when the optimal slip changes.*
  It was shown that the optimal wheel slip is barely corrected when the road surface changes. This is a problem which should be solved. As suggested before, an option is to run a secondary EKF which could reset the EKF which is used for the control references.

- *Experiment with the algorithm for road surfaces on roads with lower friction optima.*
  In the introduction of this thesis it was stated that especially on slippery roads, ABS could perform better. This research has been a step towards the direction of better detection of the friction coefficient peak and could serve as a basis for future work when there is tested on road surfaces on which current ABS actually performs worse than manual braking.

Appendices

Appendix A

EKF fundamentals

The regular Kalman filter is used to reconstruct the state of a state-space model [26]. This is, thus, only useful if the system is both linear and written into a state-space form. The EKF allows to estimate parameters of non-linear functions, such as tyre slip models. The equations for this estimate are as described by eqs. (A-1) to (A-3) [21]. Subscript k indicates the measurement index value.

$$x_{k+1} = f(a_k, u_k) + w_k \tag{A-1}$$
$$a_{k+1} = a_k + \xi_k \tag{A-2}$$
$$z_k = h(a_k) + v_k \tag{A-3}$$

In these equations, x is the state vector. The measurement is described by z_k. It equals a function h plus measurement noise (v_k). Variables w_k and ξ_k indicate noise as well. Lastly, a_k contains the parameters that are to be estimated. It is defined by the following equation:

$$a_{k+1} = a_k \tag{A-4}$$

Before describing the equation which finds the estimate. It is necessary to determine a measure of the quality of the estimate. It is denoted by P_k and is defined in eq. (A-5). In this version of the EKF, Q is added as well. It is known as the process noise covariance matrix.

$$P_{k+1} = P_k + Q \tag{A-5}$$

The error covariance matrix is used to determine the Kalman gain. The measurement update of the EKF are described by eqs. (A-6) to (A-8).

$$K_k = P_k H_k^T (H_k P_k H_k^T + R_k)^{-1} \tag{A-6}$$
$$\hat{a}_k = \hat{a}_k + K_k(z_k - h(\hat{a}_k)) \tag{A-7}$$
$$P_k = (I - K_k H_k) P_k \tag{A-8}$$

Equation (A-6) contains R, which is the measurement covariance matrix. This describes the certainty of each measured state value. Lastly, H is defined as in eq. (A-9). It denotes the derivative of the model to which the data is fitted with respect to its parameters.

$$H_k = \frac{\partial h(\hat{a}_k)}{\partial a} \tag{A-9}$$

Appendix B

EKF using a buffer

Looking at a brief, yet extreme example: only once is the friction coefficient peak exceeded and subsequently the algorithm controls for a near-optimal brake torque. It would, thus, assume the friction peak is known and constant during the rest of the brake manoeuvre. As a consequence, the EKF only receives data from only a small variety of data points, which makes it hard to fit it to a curve. The older the data are, the less relevant they become to the filter. Data from after the friction coefficient peak become of smaller influence, so the estimates of the optima worsen.

An alternative method to use the EKF would be to define a buffer matrix (eq. (B-1)), with λ_{buf} defined as eq. (B-2). Subscript i denotes the index of λ_{buf}, which the last measured μ_x corresponds with the most. In the equations below, a resolution of 0.0025 of the buffer is used as an example.

$$L_i = \begin{bmatrix} \lambda_{buf,1} & \mu_{x,1,1} & \mu_{x,1,2} & \cdots & \mu_{x,1,n} \\ \lambda_{buf,2} & \mu_{x,2,1} & & & \\ \lambda_{buf,3} & \mu_{x,3,1} & & \ddots & \\ \vdots & \vdots & & & \\ \lambda_{buf,i} & \mu_{x,k,1} & \mu_{x,k,2} & \cdots & \mu_{x,k,n} \end{bmatrix} \tag{B-1}$$

$$\lambda_{buf} = \begin{bmatrix} 0.0025 & 0.0050 & \cdots & 1.0000 \end{bmatrix}^T \tag{B-2}$$

If the lying vector $\mu_{x,k}$ is of size one ($n = 1$), it would mean every slip value corresponds with a single force value. Assuming $n > 1$, it becomes possible to filter the measurements of the friction (F_x/F_n) for the corresponding wheel slip, a more reliable value can thus be obtained. It is, for example, possible to average the force measurements that correspond with the same wheel slip value. If strongly deviating force measurements are found, the buffer should be reset. Figure B-1 shows actual measurement data recorded in 2014, and the buffered data that is subsequently averaged with a buffer size of 20. A much more smooth curve is obtained, and it looks reasonable that a curve can be fitted more accurately to such data.

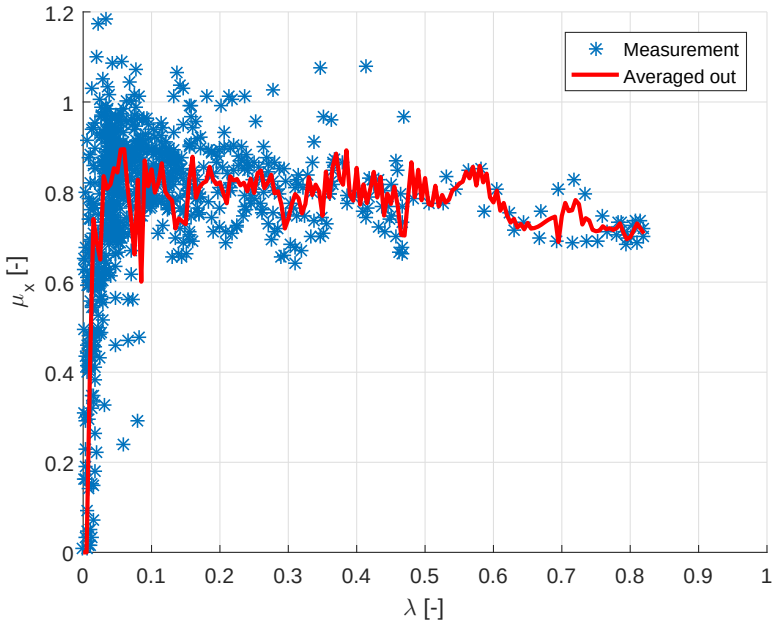

Figure B-1: Averaging of buffered data

The solution does bring along another problem with it. Whereas in the regular method the influence of older data points becomes smaller each iteration cycle, this one is focused on buffering relevant data and using them again. Older data only becomes non-influential when the buffer is fully refreshed.

Performance

The same simulation as in section 4-4-1 are performed, but now with the buffering method. A depth of 20 measurement points is used. The results are shown in fig. B-2. Using this method leads to a similar result as before looking at the filter using Burckhardt his formula. The estimate of the optimal friction is 0.07 lower than the actual one. The estimated optimal slip remains practically the same, because it is only 0.005 higher. As more measurement data is used, the resulting fit is quite constant.

If the ABS would control in such a way that the peak is only passed once, this method can use the older data to calculate a model. In such a scenario, it will prevent the filter from fitting data to a small variety of data points. However, if the road surface changes, the older data should be disregarded, as otherwise a new model is generated too slowly. It would be more practical if the EKF is simply disabled as soon as an ABS controller is designed such that it controls for a friction value just below the optimum.

Based on the results with the given dataset the method does not perform better than the standard implementation. At first it was expected that the regular EKF using the formula by Burckhardt without a buffer would perform worse over time, because measurements of the initial slope would become insignificant. Considering the estimates as shown in fig. B-2, it is assumed a buffer will not be needed with the regular algorithm. It is why there is chosen to use the EKF without a buffer in this thesis.

The other line in fig. B-2 shows the performance of the two-parameter model (2P). It is

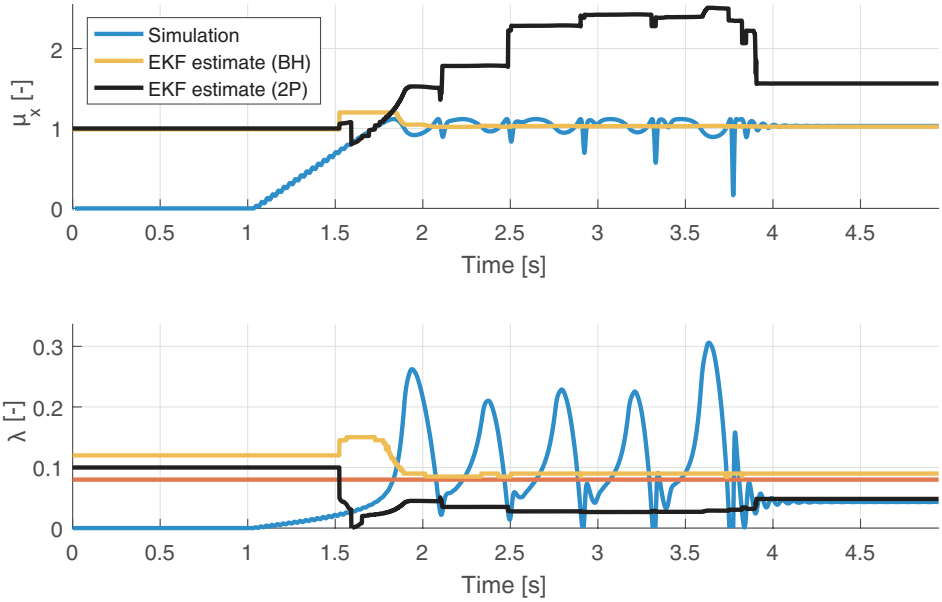

Figure B-2: Using EKF with a buffer to fit the Burckhardt (BH) and two-parameter (2P) models to simulation data

obviously worse than the regular implementation method. Data are put in from lower values of slip to higher ones. This means the latest data the filter has to process come from the right side of the curve. Since this side of the curve shows a significant difference with the actual curve (see fig. 4-2), the calculated optima are off by a great margin. This does not necessarily mean the two-parameter model cannot be used in practice.

Appendix C

Calculation of performance indicators

Brake distance and time

An approximation of the brake distance is based on the kinetic energy of the car (eq. (C-1)) and the work required for braking (eq. (C-2)). Based on these energy values, it is possible to find an estimate of the minimal brake distance required. It is assumed that the kinetic energy equals the work required for braking.

$$E_k = \frac{1}{2}mv^2(t) \tag{C-1}$$

$$W = \int_{s=0}^{s^*} F_x ds \tag{C-2}$$

$$s^* = \frac{E_k}{\bar{\mu}_x^* F_z(t)} \tag{C-3}$$

Do note $\bar{\mu}_x^*$ is written down instead of μ_x^*. This is the case, because the maximum longitudinal brake force cannot be reached instantly. Consequently, the average value of μ_x over this time is used in the calculation. It is non-trivial to find $\bar{\mu}_x^*$. Another comment to this computation is that the normal load is considered static, since load transfer phenomena are not taken into account. In practice, the normal load on the front tyres increases when braking, such that a higher longitudinal force can be exerted on the road surface.

It is insightful to formulate the problem in two parts. During the first part, the brake pressure is still being increased. During the second, the optimal brake pressure is applied. The total of both requires a brake distance of eq. (C-4).

$$s^* = s_i + s_o \tag{C-4}$$

For the equation above, s_i and s_o must be found. s_i represents the brake distance which is overcome whilst the brake pressure is still being increased. It is therefore equal to eq. (C-5). With the average friction coefficient defined by eq. (C-6). In eq. (C-5) $\bar{v}$ is defined by eq. (C-7).

$$s_i = \bar{\mu}_x^* F_z(t)\bar{v} \cdot (t_b - t_i) \tag{C-5}$$

$$\bar{\mu}_x^* = \frac{1}{2}\hat{\mu}_x^* F_z(t_b - t_i) \tag{C-6}$$

$$\bar{v} = \frac{v(0) + v(t_b)}{2} \tag{C-7}$$

Next, it is required to find s_o. This variable is the remaining minimal required distance to brake as of the moment the ABS is initiated (eq. (C-8)). In this equation t_e is the time the ABS test has ended. Practically, this would be when $v = 0$ m/s. In this report, there is chosen to apply the ABS down to $v = 16$ m/s, as highly dynamic behaviour occurs at very low velocities, and this is not a point of interest in this thesis.

$$s_o = \frac{\frac{1}{2}m(v^2(t_b) - v^2(t_e))}{\hat{\mu}_x^* F_z(t)} \tag{C-8}$$

The optimal brake time is found through eq. (C-10) with η^* defined in eq. (C-9). Its relevance is obvious, but it must be noted that neither this indicator or the brake distance can be the only indicators. They do not show that the goal of ABS to maintain steerability is achieved. Specifically for the simulation study, neither do they show sufficiently whether it is practically possible to implement such an algorithm.

$$\eta^* = \mu_x^* \frac{F_z(t)}{m} = \mu_x^* g \tag{C-9}$$

$$t^* = \underbrace{t_i - t_b}_{\text{Time to cover } s_i} + \underbrace{\frac{v(t_b) - v(t_e)}{\eta^*}}_{\text{Time to cover } s_o} \tag{C-10}$$

Optimum deviation
The RMSD is defined by eq. (C-11). In the equation, y indicates the measured value and y^* its optimum. There are n measurements.

$$\text{RMSD}(y, y^*) = \sqrt{\frac{1}{n}\sum_{k=1}^{n}(y_k - y^*)^2} \tag{C-11}$$

It must be emphasised that there are two optima (μ_x^* and λ^*) that must be taken into account. Though it is possible to combine both factors by normalising them to their optimum, there is chosen to keep both indicators separated. The main reason for this is that the relative deviation of the wheel slip is likely to be higher than that of the longitudinal force. Especially if the optimal wheel slip is 0.08, the RMSD value will lead to values of different scale.

Cycles
The number of cycles is determined by looking at the plotted figures and the number of phase switches.

Appendix D

Simulation results

Table D-1: Simulation results when optima are known

μ_x^*	λ^*	t^*	t_s	t_{diff}	s^*	s_s	s_{diff}	RMSD_μ	RMSD_λ	Cycling frequency
1.12	0.08	3.70	3.97	**7.3%**	88.1	94.2	**6.9%**	0.14	0.10	0.7
0.85	0.08	4.65	5.10	**9.6%**	107.8	118.0	**9.5%**	0.13	0.09	0.7
0.60	0.08	6.37	7.08	**11.2%**	144.3	161.8	**12.1%**	0.10	0.08	0.6
1.12	0.15	3.70	3.83	**3.5%**	88.2	91.3	**3.5%**	0.06	0.08	0.7
0.85	0.15	4.65	4.86	**4.5%**	107.9	112.6	**4.4%**	0.05	0.08	0.8
0.60	0.15	6.37	6.81	**6.9%**	144.4	154.8	**7.2%**	0.06	0.09	0.8
1.12	0.25	3.71	3.79	**2.2%**	88.4	90.2	**2.1%**	0.04	0.07	0.7
0.85	0.25	4.66	4.80	**3.0%**	108.1	111.0	**2.7%**	0.03	0.10	0.8
0.60	0.25	6.38	6.70	**5.1%**	144.5	151.9	**5.1%**	0.04	0.12	0.8

Table D-2: Simulation results when optima are found with the EKF enabled

μ_x^*	λ^*	t^*	t_s	t_{diff}	s^*	s_s	s_{diff}	RMSD_μ	RMSD_λ	Cycling frequency
1.12	0.08	3.70	3.97	**7.4%**	88.1	94.1	**6.8%**	0.13	0.09	0.7
0.85	0.08	4.65	5.10	**9.7%**	107.8	118.4	**9.8%**	0.12	0.09	0.7
0.60	0.08	6.37	7.27	**14.1%**	144.3	164.7	**14.1%**	0.10	0.08	0.6
1.12	0.15	3.70	3.83	**3.3%**	88.2	91.3	**3.6%**	0.06	0.08	0.7
0.85	0.15	4.65	4.86	**4.4%**	107.9	112.4	**4.2%**	0.05	0.07	0.7
0.60	0.15	6.37	6.78	**6.4%**	144.4	153.6	**6.4%**	0.05	0.08	0.6
1.12	0.25	3.71	3.79	**2.4%**	88.4	90.6	**2.5%**	0.04	0.10	0.7
0.85	0.25	4.66	4.78	**2.6%**	108.1	111.6	**3.3%**	0.04	0.11	0.8
0.60	0.25	6.37	6.59	**3.4%**	144.5	148.9	**3.0%**	0.03	0.13	0.7

Table D-3: Simulation results with noisy measurements when optima are known

μ_x^*	λ^*	t^*	t_s	t_{diff}	s^*	s_s	s_{diff}	RMSD_μ	RMSD_λ	Cycling frequency
1.12	0.08	3.63	4.11	**13.1%**	85.5	95.7	**11.9%**	0.21	0.25	0.9
0.85	0.08	4.62	5.46	**18.4%**	106.6	123.0	**15.4%**	0.21	0.29	0.9
0.60	0.08	6.35	8.27	**30.1%**	144.0	175.9	**22.1%**	0.19	0.27	0.8
1.12	0.15	3.62	3.82	**5.4%**	85.0	89.5	**5.2%**	0.12	0.10	0.9
0.85	0.15	4.62	5.07	**9.8%**	106.7	115.5	**8.3%**	0.14	0.19	0.9
0.60	0.15	6.36	7.05	**10.9%**	144.1	160.8	**11.6%**	0.10	0.13	0.9
1.12	0.25	3.62	3.75	**3.6%**	85.0	87.8	**3.3%**	0.09	0.11	0.9
0.85	0.25	4.62	4.81	**4.0%**	106.9	111.1	**3.9%**	0.08	0.11	0.9
0.60	0.25	6.36	6.75	**6.2%**	144.2	153.4	**6.4%**	0.08	0.14	1.0

Table D-4: Simulation results with noisy measurements when optima are found with the EKF

μ_x^*	λ^*	t^*	t_s	t_{diff}	s^*	s_s	s_{diff}	RMSD_μ	RMSD_λ	Cycling frequency
1.12	0.08	3.65	4.17	**14.0%**	86.4	98.0	**13.5%**	0.22	0.25	0.9
0.85	0.08	4.64	5.52	**19.0%**	107.4	128.6	**19.7%**	0.19	0.25	0.9
0.60	0.08	6.35	8.11	**27.6%**	144.0	180.5	**25.3%**	0.16	0.22	0.9
1.12	0.15	3.63	4.10	**12.8%**	85.6	93.7	**9.5%**	0.21	0.34	0.7
0.85	0.15	4.62	5.17	**12.0%**	106.7	116.6	**9.2%**	0.16	0.25	0.8
0.60	0.15	6.36	7.07	**11.3%**	144.1	161.0	**11.8%**	0.10	0.12	0.7
1.12	0.25	3.70	3.80	**2.9%**	88.1	90.8	**3.0%**	0.09	0.09	0.9
0.85	0.25	4.64	4.96	**6.7%**	107.7	112.7	**4.7%**	0.11	0.20	0.8
0.60	0.25	6.36	6.76	**6.3%**	144.2	151.9	**5.4%**	0.08	0.13	0.7

Appendix E

Adaptability of the EKF

E-1 Case 1: μ_x^* remains 1.12, λ^* changes from 0.08 to 0.15

The influence of a rising optimal slip value is investigated in this first case. The controller is first tested with the optima known at all times. During these tests, the system did not show a notable dynamic effect due to the change. Control behaviour changed, of course. But when looking at the two separate parts, their behaviour is not different from the ones described in section 5-4.

The effects of a road surface change when the EKF is used as sole reference of the optima are clearly visible in fig. E-1. Initially, the estimates of both optima are sufficiently accurate. At 2.5 seconds the EKF should detect that the relation between slip and the friction coefficient has changed.

The EKF does indeed detect a change, but changes the height of the estimated curve instead of the value of $\hat{\lambda}^*$. Consequently, the friction coefficient controlled for is suboptimal and the brake torque slowly rises between 2.5 and 3.5 seconds: up to the point where the estimated optimal friction coefficient is correct again.

Though a valid estimate of the optimal friction coefficient is eventually found, the slip optimum estimate remains 0.10 after switching. It takes too much time to recover from the estimation error of μ_x^* to exceed the peak again and to find a new value of $\hat{\lambda}^*$. It is not until 3.5 seconds before the slip estimate slightly increases again. Therefore, another test is performed with a road surface change at $t = 2$ s. It was expected that the optimal slip would correctly be adjusted for if the peak was exceeded at least once more, but the results are similar to the current case.

An explanation can be found in the values of P throughout the brake manoeuvre. The parameter does not increase even though the estimate becomes more uncertain. Plotting the values on the diagonal of the error covariance matrix results in a figure similar to fig. 4-8. As a consequence, the algorithm has more problems adjusting itself. A method to resolve this problem is to define a second error covariance matrix and reset it every phase. By looking

at the values of this parameter at the end of every phase, it can be observed how well the latest measurements fit to the estimated curve. A time limit will have to be set for this check as well. If the model fails the test, the P which is actually used in the EKF should then be reset. The predictor should then use measurements that have been obtained since the latest phase switch. Pseudo-data at $\lambda = 1$ with $\mu = 0$ should be added as well.

From this case, it can be concluded that the EKF experiences troubles when determining a new $\hat{\lambda}^*$ after it was changed to a higher value. An important question that has to be answered in order to find whether this is a problem is: is such a theoretical road change valid? From the curves Burckhardt used to fit data to, it looks more likely that a road surface change often leads to a change in both λ^* and μ_x^*.

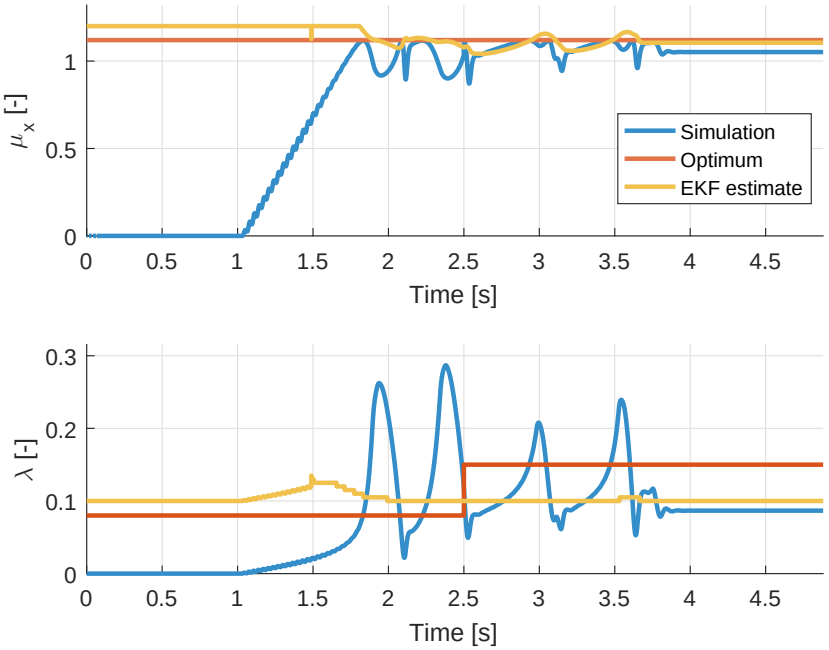

Figure E-1: ABS results when the road surface changes: μ_x^* remains 1.12, λ^* changes from 0.08 to 0.15

E-2 Case 2: μ_x^* remains 1.12, λ^* changes from 0.15 to 0.08

There is now looked into what happens if the optimal slip value changes to a lower value. Such a change in road characteristics could lead to the system suddenly being in an unstable state which was stable before. This would cause an increase in slip, leading to a switch to phase 1. However, until the slip estimate is accurate again, the controller will trigger too early.

Correcting the estimate takes relatively long for the EKF. Looking at the figure, it takes about a second before a value of 0.12 is reached, while it should be 0.08. Determining a slip optimum of 0.08 is always troublesome, because of the effects of tyre relaxation. Another simulation is therefore run with λ^* changing from 0.25 to 0.15, but the results are similar. The optimum estimate does show a correction, but only slowly. It must be noted that the correction is definitely better than presented in case 1, where the change of slip optimum had no influence on the estimated one at all.

From case 1 and 2 it is both concluded that the slip estimate either corrects slowly or not at all. An indicator should therefore tell whether the controller can still rely on the slip estimate. If not, either a new estimate has to be made or, in the worst case, the controller should not use its slip trigger. A new estimate can be found using the method as proposed in case 1.

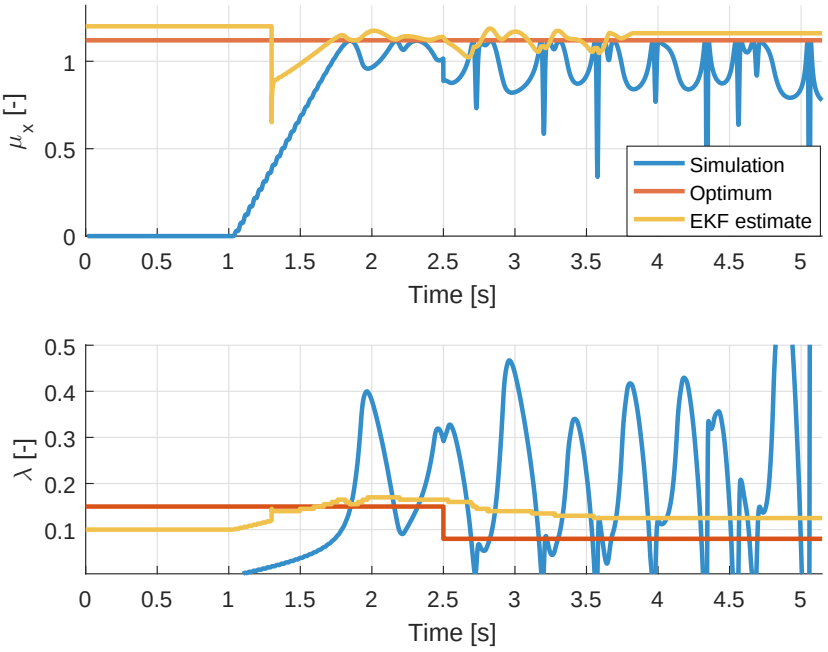

Figure E-2: ABS results when the road surface changes: μ_x^* remains 1.12, λ^* changes from 0.15 to 0.08

E-3 Case 3: μ_x^* changes from 1.12 to 0.85, λ^* remains 0.08

In case 3 and 4, the influence of a changing friction coefficient is investigated. It is relevant because if the predictor does not adjust its reference values to the controller, it could end up controlling for too high brake torques. If that would be the case, wheel lock will definitely occur, even when in phase 1.

Results of the simulation can be seen in fig. E-3. The optimum of friction is clearly corrected faster than the slip optimum was in the previous cases. It takes only 0.20 seconds to change the estimate from 1.12 to 0.85.

The moment the road surface is changed, the controller has just returned to its first phase, but is then directly triggered to go to phase 2 again. This a force-based trigger, because the estimate of the friction optimum drops quickly at 2.5 seconds. After this brief behaviour, the controller manages to return to a regular and stable pattern, with a new optimum reference.

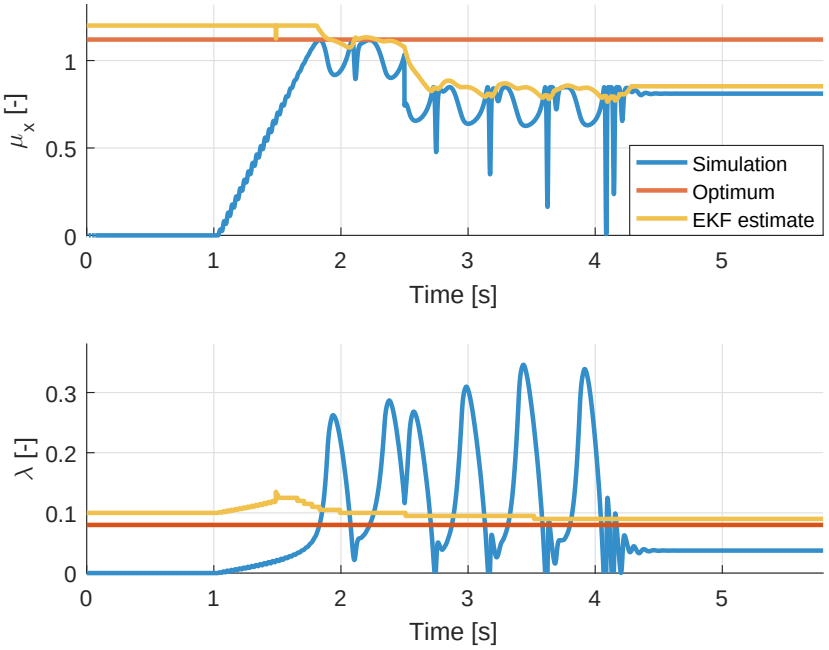

Figure E-3: ABS results when the road surface changes: μ_x^* changes from 1.12 to 0.85, λ^* remains 0.08

E-4 Case 4: μ_x^* changes from 0.85 to 1.12, λ^* remains 0.08

The fourth case is interesting because the algorithm is designed in such a way that it exceeds the estimated friction optimum relatively slowly and only by a predefined percentage. If the estimate is not or too slowly corrected, this leads to suboptimal braking.

Results from this case are surprisingly positive (see fig. E-4). At $t = 2.5$ seconds the controller is going to phase 2, which is perfect for this case. It indeed takes longer to exceed the friction coefficient peak and the optimum estimate is being corrected simultaneously. This is desired behaviour, because it means the peak will then eventually always exceeded.

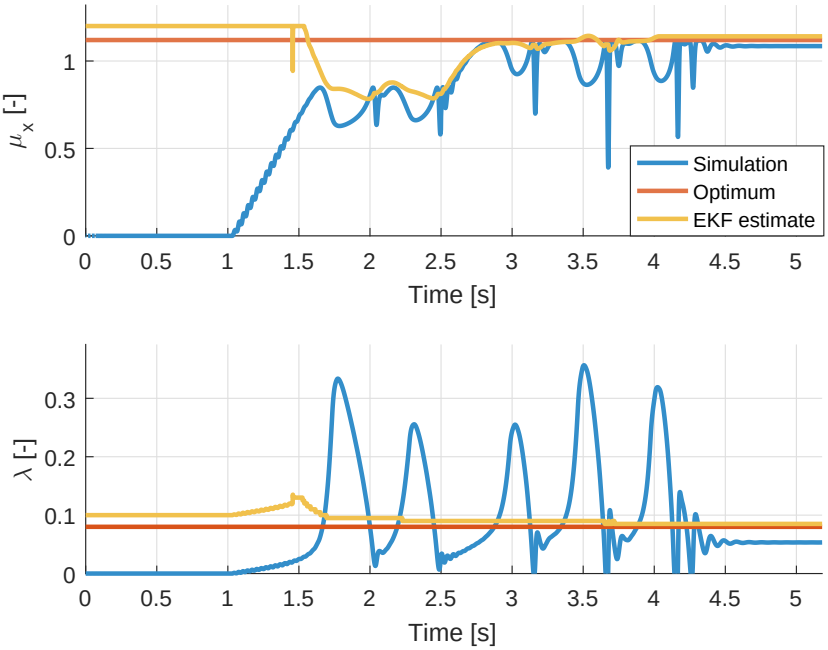

Figure E-4: ABS results when the road surface changes: μ_x^* changes from 0.85 to 1.12, λ^* remains 0.08

Bibliography

[1] M. P. Hagenzieker, J. J. Commandeur, and F. D. Bijleveld, "The history of road safety research: A quantitative approach," *Transportation research part F: traffic psychology and behaviour*, vol. 25, pp. 150–162, 2014.

[2] E. Commission, "Road safety evolution in the eu." http://ec.europa.eu/transport/road_safety/pdf/observatory/historical_evol.pdf, 1 2011. (Accessed on 04/19/2016).

[3] J. Taghia, "Vehicle simulation." http://www.javadtaghia.com/control-system-math/car-simulation, 09 2014. (Accessed on 06/02/2016).

[4] D. Tomasi, "Fitting of tire its experimental data." http://www.multibody.net/teaching/dissertations/2011-tomasi/, 10 2014. (Visited on 09/14/2015).

[5] A. Schmeitz, "MF-Tyre/MF-Swift." http://publications.tno.nl/publication/34606988/ORSVMS/schmeitz-2013-mftyre-presentatie.pdf, 2013. (Visited on 18/04/2016).

[6] S. M. Savaresi and M. Tanelli, *Active braking control systems design for vehicles*. Springer Science & Business Media, 2010.

[7] S. Kerst, B. Shyrokau, and E. Holweg, "Anti-lock braking control based on bearing load sensing," *ResearchGate*, 2015.

[8] J. Hultén, "Active safety introduction." Volvo Car Corporation presentation at CTH, 2006.

[9] J. Broughton and C. Baughan, "The effectiveness of antilock braking systems in reducing accidents in Great Britain," *Accident Analysis & Prevention*, vol. 34, no. 3, pp. 347–355, 2002.

[10] RACV, "Effectiveness of ABS and vehicle stability control systems," tech. rep., 2004. (Visited on 03/06/2016).

[11] C. J. Kahane and J. N. Dang, "The long-term effect of abs in passenger cars and ltvs," tech. rep., 2009.

[12] E. De Bruijn, M. Gerard, M. Corno, M. Verhaegen, and E. Holweg, "On the performance increase of wheel deceleration control through force sensing," 2010.

[13] L. Li, F.-Y. Wang, and Q. Zhou, "Integrated longitudinal and lateral tire/road friction modeling and monitoring for vehicle motion control," *IEEE Transactions on intelligent transportation systems*, vol. 7, no. 1, pp. 1–19, 2006.

[14] H. B. Pacejka and E. Bakker, "The magic formula tyre model," *Vehicle system dynamics*, vol. 21, no. S1, pp. 1–18, 1992.

[15] TNO, "Delft-tyre | www.tassinternational.com." https://www.tassinternational.com/delft-tyre, 2016. (Accessed on 04/18/2016).

[16] B. Shyrokau, D. Wang, K. Augsburg, and V. Ivanov, "Vehicle dynamics with brake hysteresis," *Proceedings of the Institution of Mechanical Engineers, Part D: Journal of automobile engineering*, p. 0954407012451961, 2012.

[17] D. Szöcs, A. Feneşan, and T. Pană, "Wheel slip measurement of an electric vehicle prototype using an accelerometer," *Conferinta Nationalaă de actionări Electrice, Editia XVI, Suceava*, 2012.

[18] M. Corno, M. Gerard, M. Verhaegen, and E. Holweg, "Hybrid ABS control using force measurement," *Control Systems Technology, IEEE Transactions on*, vol. 20, no. 5, pp. 1223–1235, 2012.

[19] S. Kerst, B. Shyrokau, and E. Holweg, "Reconstruction of wheel forces using an intelligent bearing," *SAE International Journal of Passenger Cars-Electronic and Electrical Systems*, vol. 9, no. 2016-01-0092, pp. 196–203, 2016.

[20] A. Handbook, "Robert bosch gmbh," *SAE,*, 1996.

[21] J. Van Ginkel, "Estimating the tire-road friction coefficient based on tire force measurements." http://repository.tudelft.nl/assets/uuid:3d5ee83c-a35e-4141-8408-ab3916ca1c8a/Thesis_Johannes_van_Ginkel.pdf, 2014.

[22] M. Burckhardt, "Fahrwerktechnik: Radschlupf-regelsysteme," *Vogel-Verlag, Germany*, p. 16, 1993.

[23] R. Rudd, "Estimating the mu slip curve via extended kalman filtering," *Math J*, vol. 11, pp. 91–106, 2006.

[24] D. Kun, L. Kaijun, and X. Qunsheng, "Application of unscented Kalman filter for the state estimation of anti-lock braking system," in *Vehicular Electronics and Safety, 2006. ICVES 2006. IEEE International Conference on*, pp. 130–133, IEEE, 2006.

[25] B. Samadi, R. Kazemi, K. Y. Nikravesh, and M. Kabganian, "Real-time estimation of vehicle state and tire-road friction forces," in *American Control Conference, 2001. Proceedings of the 2001*, vol. 5, pp. 3318–3323, IEEE, 2001.

[26] M. Verhaegen and V. Verdult, *Filtering and system identification: a least squares approach*. Cambridge university press, 2007.

Glossary

List of Acronyms

ABS	Anti-lock Brake System
BAS	Braking Assist System
CBC	Cornering Brake Control
EKF	Extended Kalman Filter
ESC	Electronic Stability Control
HAB	Hydraulically Actuated Brakes
PID	Proportional Integral Derivative
RMSD	Root Mean Square Deviation
RMS	Root Mean Square
TC	Traction Control

List of Symbols

α_μ	Tuning parameter for minimal brake torque in phase 2
α_F	Forgetting factor
α_{phs}	Scaling parameter for the influence of time
α_{T_b}	Extra added fraction of $\hat{T}_b^*$
λ	Wheel slip
μ_x	Longitudinal friction coefficient
t_{phs}	Time since last phase update
v_ω	Tyre linear velocity

ω	Angular velocity
F_x	Longitudinal force
F_y	Lateral force
F_z	Normal force
J	Inertia of the wheel
m	Mass
M_x	Overturning moment
M_y	Rolling resistance moment
M_z	Aligning moment
r	Dynamic wheel radius
s_{0l}	Tyre-relaxation length
T_b	Brake torque
v	Vehicle velocity

Index